



1992

# Metamorphic petrology and gravity studies of the Archean English River subprovince, western Superior Province, Manitoba and Ontario, Canada

Moira E. Campion  
*University of North Dakota*

Follow this and additional works at: <https://commons.und.edu/theses>

 Part of the [Geology Commons](#)

---

## Recommended Citation

Campion, Moira E., "Metamorphic petrology and gravity studies of the Archean English River subprovince, western Superior Province, Manitoba and Ontario, Canada" (1992). *Theses and Dissertations*. 48.  
<https://commons.und.edu/theses/48>

This Thesis is brought to you for free and open access by the Theses, Dissertations, and Senior Projects at UND Scholarly Commons. It has been accepted for inclusion in Theses and Dissertations by an authorized administrator of UND Scholarly Commons. For more information, please contact [zeinebyousif@library.und.edu](mailto:zeinebyousif@library.und.edu).

METAMORPHIC PETROLOGY AND GRAVITY STUDIES  
OF THE ARCHEAN ENGLISH RIVER SUBPROVINCE,  
WESTERN SUPERIOR PROVINCE,  
MANITOBA AND ONTARIO, CANADA

by  
Moirra E. Campion

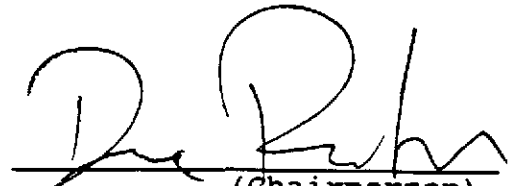
Bachelor of Science, University of Minnesota-Duluth, 1984

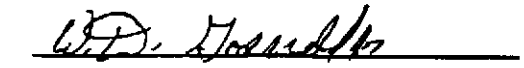
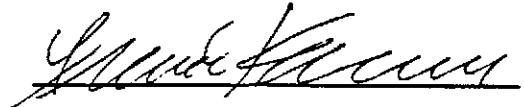
A Thesis  
Submitted to the Graduate Faculty  
of the  
University of North Dakota  
in partial fulfillment of the requirements  
for the degree of  
Master of Science

Grand Forks, North Dakota

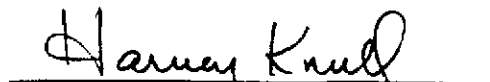
July  
1992

This thesis submitted by Moira E. Campion in partial fulfillment of the requirements for the Degree of Master of Science from the University of North Dakota has been read by the Faculty Advisory Committee under whom the work has been done, and is hereby approved.

  
(Chairperson)

This thesis meets the standards for appearance and conforms to the style and format requirements of the Graduate School of the University of North Dakota, and is hereby approved.

  
Dean of Graduate School  
7-20-92

Permission

Title: Metamorphic Petrology and Gravity Studies of the Archean English River Subprovince, Western Superior Province, Manitoba and Ontario, Canada

Department: Geology and Geological Engineering

Degree: Master of Science

In presenting this thesis in partial fulfillment of the requirements for a graduate degree from the University of North Dakota, I agree that the library of this University shall make it freely available for inspection. I further agree that permission for extensive copying for scholarly purposes may be granted by the professor who supervised my thesis work, or in his absence, by the chairperson of the department or the Dean of the Graduate School. It is also understood that any copying or publication or other use of this thesis or part thereof for financial gain shall not be allowed without my written permission. It is also understood that due recognition shall be given to me and the University of North Dakota in any scholarly use which may be made of any material in my thesis.

Signature *Maura Campion*

Date *July 16, 1992*

## TABLE OF CONTENTS

|   |      |
|---|------|
| LIST OF ILLUSTRATIONS . . . . .                       | vi   |
| LIST OF TABLES . . . . .                              | viii |
| ACKNOWLEDGEMENTS . . . . .                            | ix   |
| ABSTRACT . . . . .                                    | x    |
| INTRODUCTION . . . . .                                | 1    |
| METAMORPHIC PETROLOGY AND GEOTHERMOBAROMETRY. . . . . | 21   |
| Methods . . . . .                                     | 21   |
| Rock Descriptions . . . . .                           | 27   |
| Isograds and Phase Equilibra. . . . .                 | 31   |
| Results of Geothermometry . . . . .                   | 48   |
| Results of Geobarometry . . . . .                     | 55   |
| Summary and Discussion of Metamorphism. . . . .       | 60   |
| GRAVITY GEOPHYSICS AND MODELLING . . . . .            | 64   |
| Methods . . . . .                                     | 64   |
| Results . . . . .                                     | 73   |
| Northwest Profile - Manitoba . . . . .                | 73   |
| Southwest Profile - Manitoba . . . . .                | 81   |
| South Profile - Manitoba . . . . .                    | 82   |
| Northeast Profile - Manitoba . . . . .                | 88   |
| Southeast Profile - Manitoba . . . . .                | 92   |
| Ontario Profile - Ontario . . . . .                   | 96   |
| Summary and Discussion of Models. . . . .             | 100  |
| DISCUSSION. . . . .                                   | 105  |
| CONCLUSIONS AND RECOMMENDATIONS . . . . .             | 118  |
| APPENDICES . . . . .                                  | 123  |
| A: Thin Section Mineralogy . . . . .                  | 124  |

|  |      |
|--|------|
| B: Microprobe Analyses . . . . .           | .129 |
| I. Garnet. . . . .                         | .131 |
| II. Biotite . . . . .                      | .140 |
| III. Cordierite . . . . .                  | .149 |
| IV. Plagioclase . . . . .                  | .152 |
| C: Gravity Results . . . . .               | .156 |
| I. Northwest Profile - Manitoba . . . . .  | .158 |
| II. Southwest Profile - Manitoba . . . . . | .161 |
| III. South Profile - Manitoba . . . . .    | .164 |
| IV. Northeast Profile - Manitoba . . . . . | .167 |
| V. Southeast Profile - Manitoba . . . . .  | .171 |
| VI. Ontario Profile . . . . .              | .174 |
| REFERENCES . . . . .                       | .180 |

## LIST OF ILLUSTRATIONS

### Figures

1. Superior Province of Canadian Shield, with inset showing subprovinces of western Ontario and Manitoba. . . . .2
2. Geographic location map including Lac Seul and gravity study area. . . . .4
- 3A. Geologic map of a portion of the western Superior Province. . . . .6
- 3B. Legend for geologic map presented in Figure 3. . . . .8
4. Geographic location map of petrology study area, Lac Seul, Ontario. . . . .13
5. Location map of study areas for Henke (1984), Baumann (1985), Chipera (1985), Roob (1987) and Campion. . .15
6. Bouguer Gravity map of a portion of Superior Province. . . . .18
7. Eastern sample location map for Campion field area. .22
8. Western sample location map for Campion field area. .24
- 9A. Isograd location map of Lac Seul Study area. . . . .32
- 9B. Distribution of sample locations used to plot isograds. . . . .34
10. Orthopyroxene occurrences in the Lac Seul study area. 37
11. Mineralogical phase equilibria. . . . .39
12. Hand contoured isotherms in Lac Seul study area. . . 53
13. Hand contoured isobars in Lac Seul study area. . . . 58
14. Location map of modelled gravity profiles area in Manitoba and Ontario. . . . .65
15. Bouguer gravity profiles collected during this study from Highways 11, 304, 314 and 315, Manitoba. . . . 74
16. Bouguer gravity profile collected on Highway 105, Ontario . . . . .76
17. Observed and calculated profiles with modelled polygons--Northwest profile, Manitoba. . . . .79

|     |   |      |
|-----|---|------|
| 18. | Observed and calculated profiles with modelled polygons--Southwest profile, Manitoba. . . . . | .83  |
| 19. | Observed and calculated profiles with modelled polygons--South profile, Manitoba. . . . .     | .86  |
| 20. | Observed and calculated profiles with modelled polygons--Northeast profile, Manitoba. . . . . | .90  |
| 21. | Observed and calculated profiles with modelled polygons--Southeast profile, Manitoba. . . . . | .94  |
| 22. | Observed and calculated profiles with modelled polygons--Ontario. . . . .                     | .98  |
| 23. | Proposed tectonic evolution of ERSP and adjacent subprovinces. . . . .                        | .116 |



LIST OF TABLES

Table

|  |     |
|--|-----|
| 1. Relevant reactions--temperature/pressure conditions of formation. . . . .         | .42 |
| 2. Garnet-Biotite equilibria . . . . .   | .49 |
| 3. Calculated Perchuk and Lavrent'eva thermometry results for Henke's data . . . . . | .51 |
| 4. Garnet-Plagioclase-Sillimanite-Quartz geobarometry results. . . . .               | .56 |
| 5A. Rock units used in Manitoba gravity models. . . . .                              | .71 |
| 5B. Rock units used in Ontario gravity models . . . . .                              | .72 |

## ACKNOWLEDGEMENTS

Dr. Dexter Perkins supplied direction and useful critical evaluation throughout the project. Dr. Will Gosnold provided much guidance and technical review of the gravity survey and modelling. Dr. Frank Karner contributed valuable insight into the overall objective and accomplishments of this study. The entire thesis committee expedited review of draft documents to enable me to meet deadlines and I am grateful to all of them.

Financial support from Sigma Gamma Epsilon and the University of North Dakota Graduate School, and logistical support provided by Don Janes of the Ontario Geological Survey, helped to defray the cost of fieldwork. Dr. Richard LeFever contributed important administrative support. Thanks are due to Gloria Pederson for assisting in meeting the various deadlines and registration procedures.

My family is appreciated for patience and tolerance throughout this period. Jean Hoff provided considerable emotional and technical support. My husband, Paul Bulger, assisted with fieldwork for both parts of this project, as well as additional technical help, without his support through this I may not have been able to persevere.

## ABSTRACT

The tectonic development of the English River Subprovince (ERSP) of the Superior Province in Ontario and Manitoba, as with other Archean medium-high grade metasedimentary/gneiss terranes, is an area of active research. Geochemical and geophysical data were collected during this study to determine the metamorphic conditions of formation, and the relationship between surface and subsurface geology. The results of metamorphic studies by Henke (1984), Baumann (1985), Chipera (1985) and Roob (1987) were also integrated with those of this study. The temperatures and pressures of formation, as well as detailed gravity characteristics, constrain the postulated tectonic model for the ERSP.

Chemical data were obtained from the metasedimentary samples collected in the Lac Seul area, using an electron probe micro-analyzer for geothermobarometric calculations. The temperatures and pressures of formation were estimated using garnet-biotite geothermometers and garnet-cordierite-plagioclase-quartz geobarometers. Pressure, temperature, isograd and granulite occurrence maps were produced, which included results from all UND workers in the Lac Seul area.

Gravity data were collected along Highways 11, 304, 314 and 315 in Manitoba, and reduced to a Bouguer anomaly. The data were divided into five profiles. These profiles, in addition to one profile based on previously existing

Bouguer data in Ontario, were modelled using a two-dimensional gravity modelling program. The models were developed with a primary focus on the surficial geology.

No new isograds or mineral assemblages were identified in the Lac Seul area during this study. The index minerals found are garnet, biotite, cordierite, sillimanite and orthopyroxene. The temperatures results ranged from 577 to 751 °C. The highest temperatures were found in the northeast and the lowest in the southwest. Isotherms display a pattern of domes and basins. Pressure results ranged from 2.7 to 5.7 kb, with the highest values in the northeast and lowest in the west. The pressure and temperature values of this study were intermediate compared to the range found by other UND workers.

The gravity models display calculated profiles which closely resemble the observed anomalies. Modelling results indicate that the abundant granitoids at the surface are also pervasive at depth. There is also strong evidence that dense, mafic bodies exist at depth and may be a result of crustal underplating.

Determination of the tectonic regime operating during formation of the ERSP and adjacent subprovinces is hampered by the abundant granitoid intrusions. A potential sequence of accretionary tectonic events, distinguishing the northern and southern domains of the ERSP as individual subprovinces, is presented.

## INTRODUCTION

The English River Subprovince (ERSP) is an east-west trending Archean medium-high grade migmatized metasedimentary gneiss terrane. The ERSP is part of the western Superior Province of the Canadian Shield, and is located in Ontario and Manitoba (Fig. 1). A long standing problem in Archean geology is understanding the mechanisms which result in the juxtaposition of high grade gneiss terranes with low grade metavolcanic-metasedimentary terranes (Breaks et al., 1978). The ERSP provides a typical example of an Archean high-grade gneiss terrane. It is flanked to the north and south by the low-grade Uchi and Wabigoon Subprovinces, respectively. Detailed study of this area may assist in understanding the geological processes that operated to produce such a juxtaposition. This project contributes detailed geophysical and geochemical studies to supplement available information in the ERSP. This contribution will assist in producing a well constrained model for the tectonic development of the ERSP and adjacent subprovinces.

A geographic location map, a detailed geologic map and corresponding legend for a portion of the western Superior Province in the vicinity of ERSP are presented in Figures 2, 3A and 3B, respectively. Two separate domains comprise the ERSP--the northern metasedimentary domain (also referred to as the Ear Falls-Manigotagan Gneiss Belt,

Figure 1. Superior Province of Canadian Shield, with inset showing subprovinces of western Ontario and Manitoba. Figure displays east-west trending alternating metasedimentary gneiss subprovinces and greenstone-tonalite subprovinces.

(Part A obtained from Ayres and Thurston, 1985)

(Part B modified from Beakhouse, 1985)

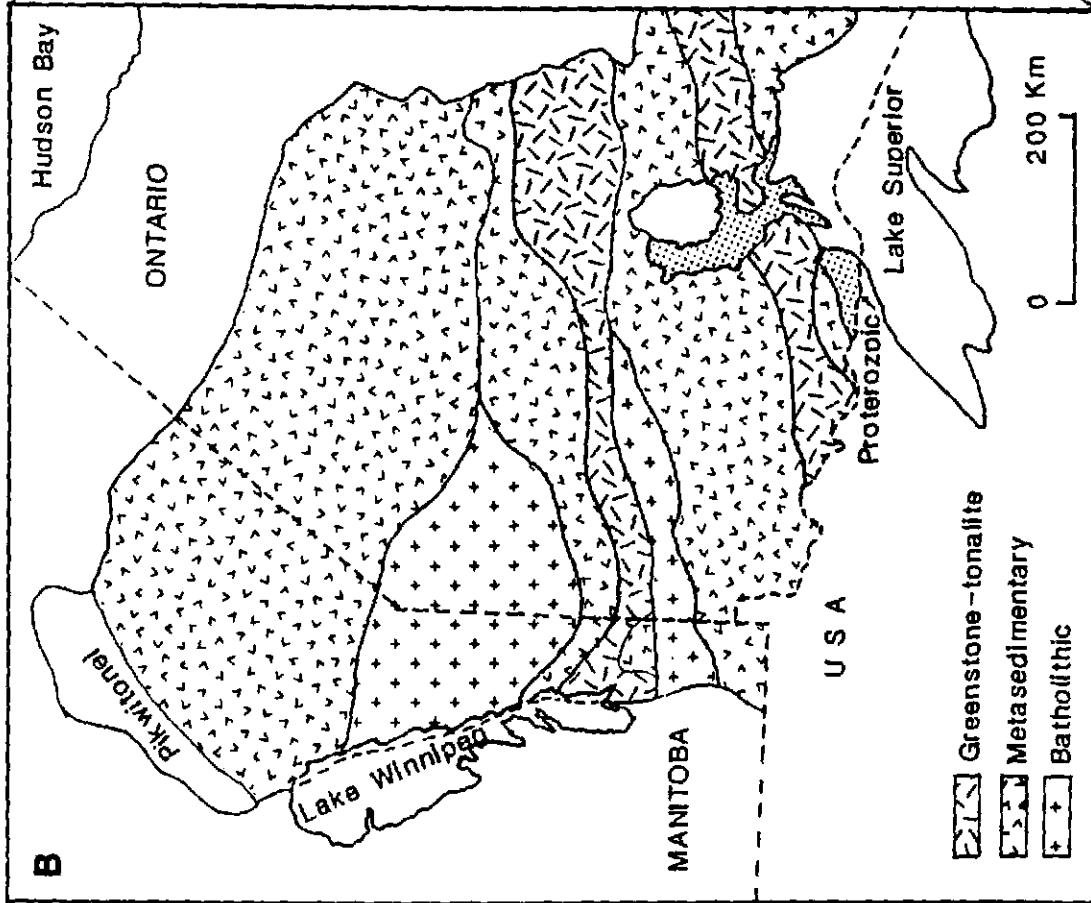
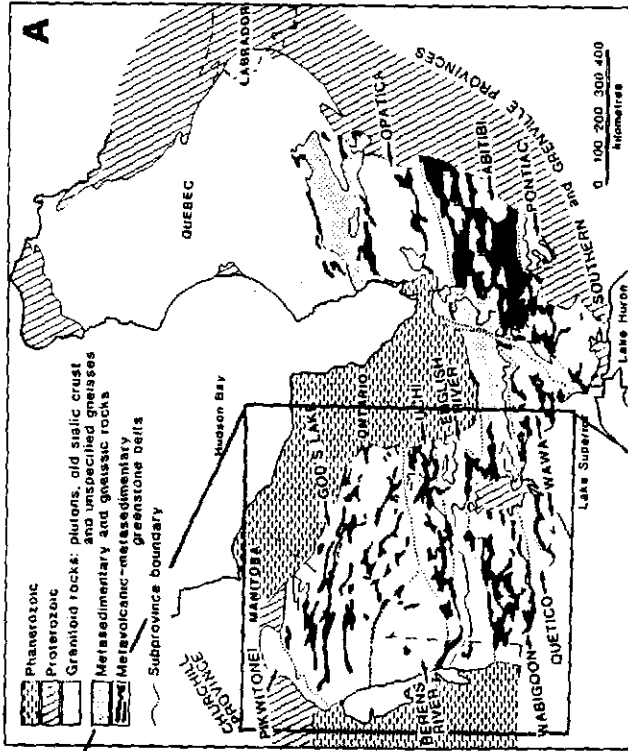


Figure 2. Geographic location map including Lac Seul and gravity study area. Map displays highways, towns and Lac Seul for reference.



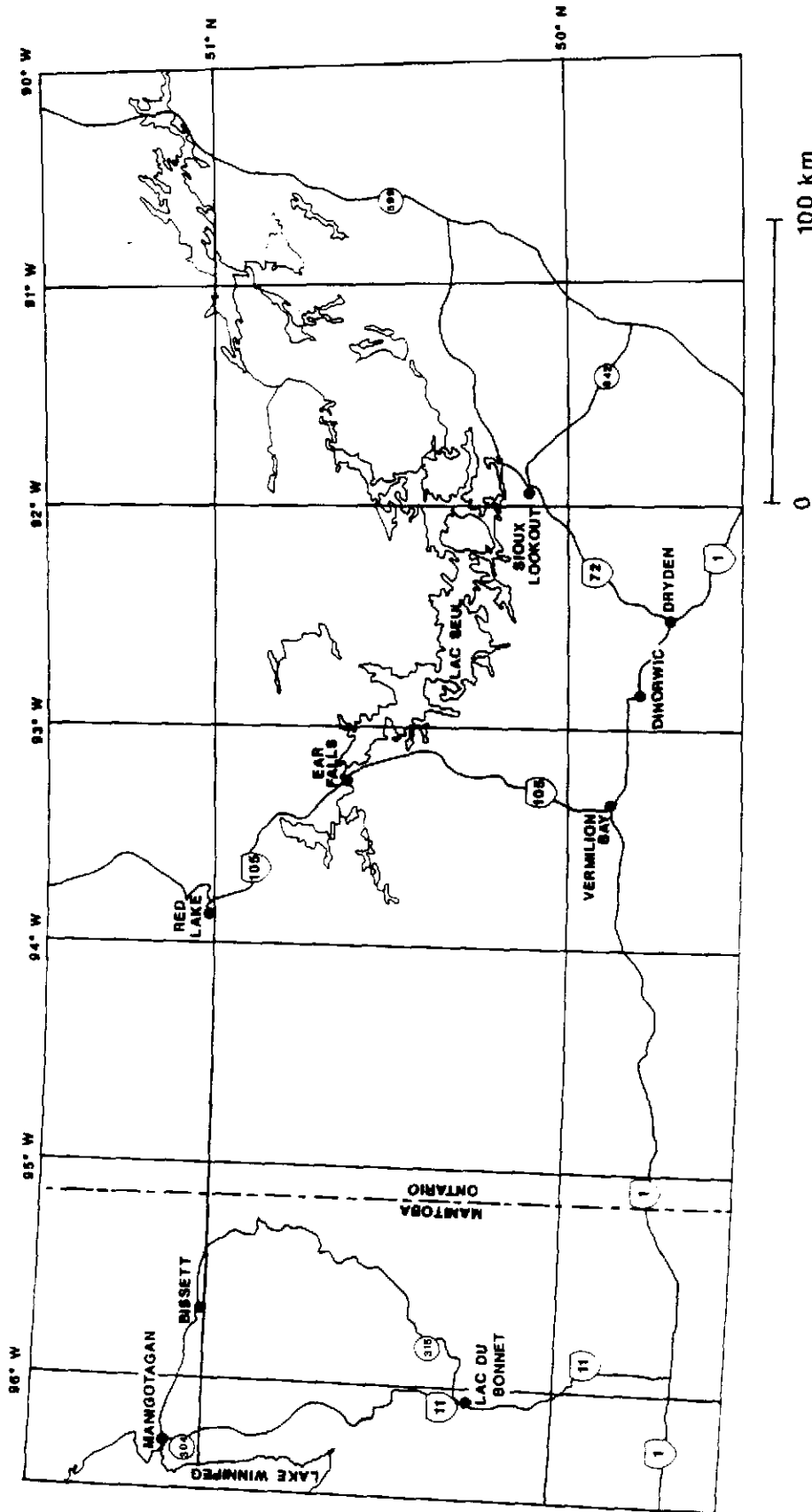


Figure 3A. Geologic map of a portion of the western Superior Province. The geology is compiled from several sources: Breaks, et al., (1978), Manitoba Mineral Resources Branch (1979), Ontario Geological Survey (1980), and Beakhouse (1985).

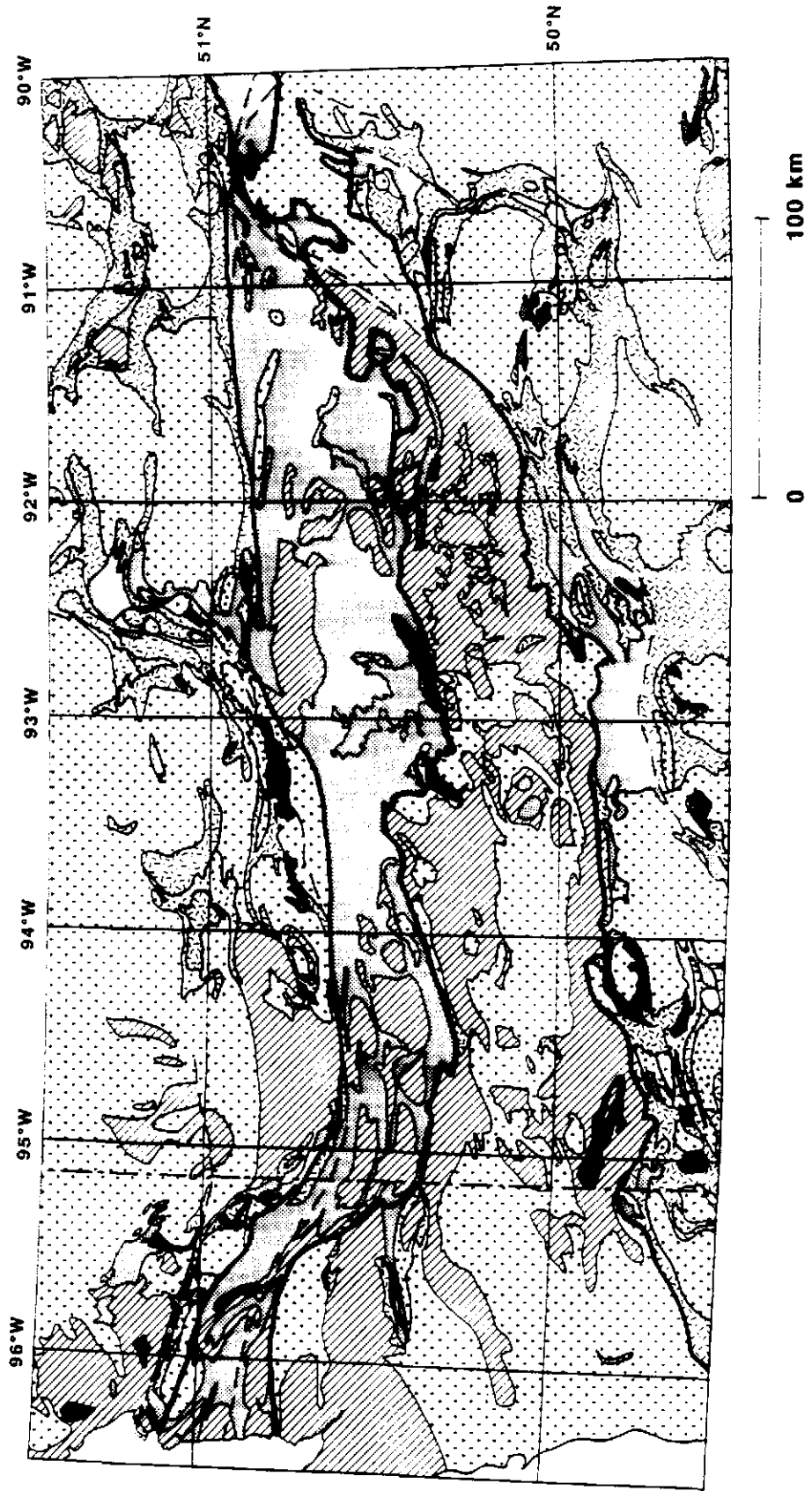
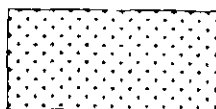
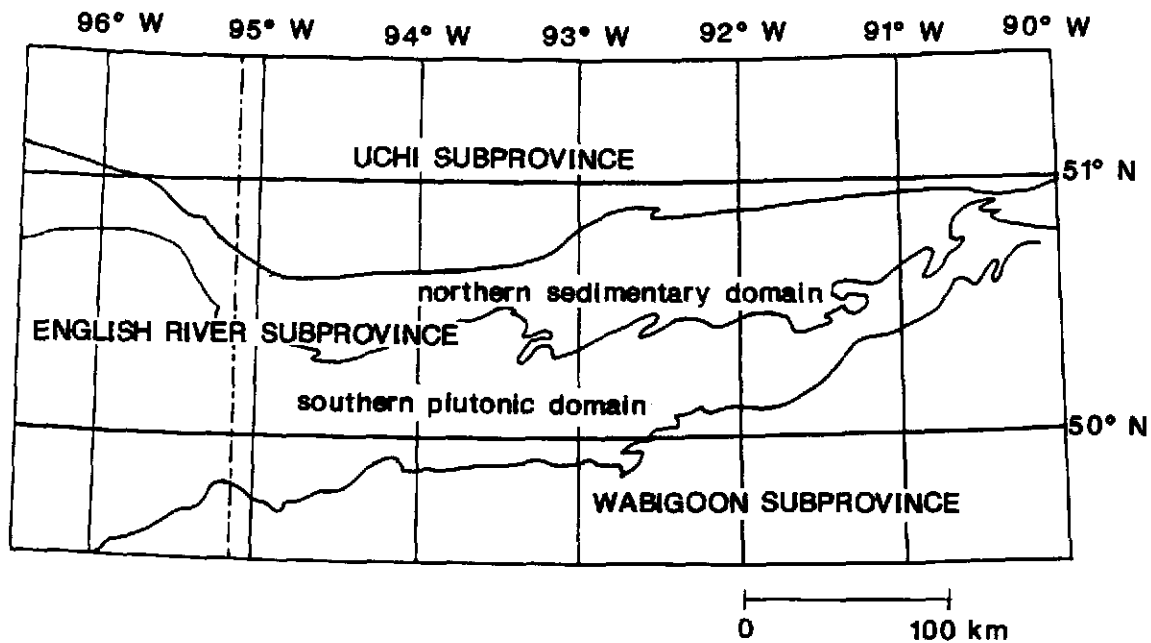
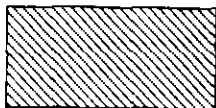


Figure 3B. Legend for geologic map presented in  
Figure 3A.



Granitic rocks, syenite, pegmatite, unsubdivided migmatite.



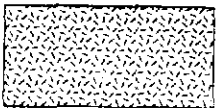
Tonalite, minor granodiorite, granite and related gneiss, minor metasedimentary and metavolcanic migmatite.



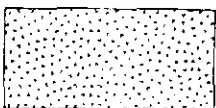
Gabbro, diorite, norite, pyroxenite, peridotite, dunite, serpentinite.



Metasedimentary gneiss, sandstone, mudstone, conglomerate, marble, chert, iron formation, and related migmatite.



Basaltic and andesitic flows, tuffs and breccias, minor sedimentary and mafic intrusive rocks; ultramafic rocks.



Rhyolitic, dacitic, and andesitic flows, tuffs and breccias.

especially in Manitoba) and the southern plutonic domain (known also as the Winnipeg River Belt) (Beakhouse, 1977; Breaks and Bond, 1977). Card (1990) refers to the southern plutonic domain of the ERSP as the Winnipeg River Subprovince. To be consistent with other UND workers, the term southern plutonic domain of the ERSP will be used throughout the descriptive portion of this thesis.

Included within the ERSP are also two small greenstone units, the Bird River and the Separation Lake Greenstone Belts. These are located between the northern and southern domains of the ERSP (McRitchie and Weber, 1971). Both of these greenstone belts are located near the Ontario/Manitoba border. The Bird River Greenstone Belt is in Manitoba and the Separation Lake Greenstone Belt, a much smaller body, is in Ontario. These greenstone units are considered to be related, and are probably erosional remnants of a formerly contiguous unit (Beakhouse, 1985). This adds further support to the distinction of the southern plutonic domain of the ERSP as a separate block.

The age relations of the ERSP, and adjacent subprovinces are thoroughly summarized in Card, 1990 and Ayres and Thurston, 1985. The only age dates reported for the northern domain ERSP is for two late-stage pegmatites dated at 2681 Ma and 2652 Ma (Krogh et al., 1976), and deformation and metamorphism at 2680 Ma (Card, 1990). Several age dates have been collected in southern domain

ERSP, here gneisses with dates ranging from 3170-2700 Ma are some of the oldest rocks found in any of the above mentioned subprovinces. Plutonic rocks and metamorphic events in the southern domain ERSP range in age from 2760 to 2660 Ma (Corfu, 1988; Beakhouse et al., 1988). The Uchi Subprovince has two igneous episodes occurring between 2.8 and 3.0 Ga and 2.75 and 2.73 Ga (Nunes and Thurston, 1980) with both volcanic and plutonic rocks in these suites. Card (1990) and Corfu and Andrews (1987) report younger plutonics in the Uchi Subprovince, with age dates of 2730 and 2680 Ma. The Wabigoon subprovince is reported to contain supra-crustals and plutonics ranging in age from 2747 to 2669 Ma (Davis and others, 1982; Anglin and Franklin, 1989), an occurrence of an older gneiss dated at 3.1-2.9 Ga (Davis, et al., 1988) and ductile deformation occurring at 2700-2710 Ma.

Previous work in the ERSP and adjacent subprovinces by Harris (1976), Harris and Goodwin (1976), Beakhouse (1977), Krogh et al. (1976), Langford and Morin (1976), Breaks et al. (1978), Bartlett (1978), is reviewed and summarized by Chipera (1985) and Roob (1987). Recent work, of note, conducted in the ERSP and not summarized in these reviews, includes: Ayres and Thurston (1985), Beakhouse (1985), Blackburn et al. (1985), Percival and Card (1985), Schwerdtner et al. (1985), Card and Ciesielski (1986), Card (1990), Percival (1990), Weber and Mezger (1990), Beakhouse

and McNutt (1991).

Workers at the University of North Dakota (UND), involved in a long term petrologic study to define the pressure and temperature conditions in the Lac Seul area are: Henke (1984), Baumann (1985), Chipera (1985), and Roob (1987). The major cities and highways in the Lac Seul area are identified in Figure 4. In addition to collecting samples for geothermobarometric analysis, UND workers in ERSP worked on the following projects. Specific study areas are outlined in Figure 5. Henke (1984) collected basic information throughout the western Superior Province, in and around the ERSP, Uchi Subprovince and Wabigoon Subprovince as well as the Bird River Greenstone Belt. Baumann (1985) studied an area wholly within the ERSP in attempt to determine if the intruded portions of the migmatites were derived in situ or were injected from elsewhere. Chipera (Chipera, 1985; Chipera and Perkins, 1988) evaluated a variety of geothermometers and geobarometers that were applicable to the ERSP and performed rudimentary gravity modelling for a profile based on previously existing Bouguer gravity data. Roob (1987) studied an area of low grade rocks south of Lac Seul in an attempt to determine if the area, located south of the plutonic domain of the ERSP, was part of the Wabigoon Subprovince (as it had been previously classified) or if it was a low grade extension of the ERSP.



Figure 4. Geographic location map of petrology study area, Lac Seul, Ontario. Displays location of major roads and lakes.

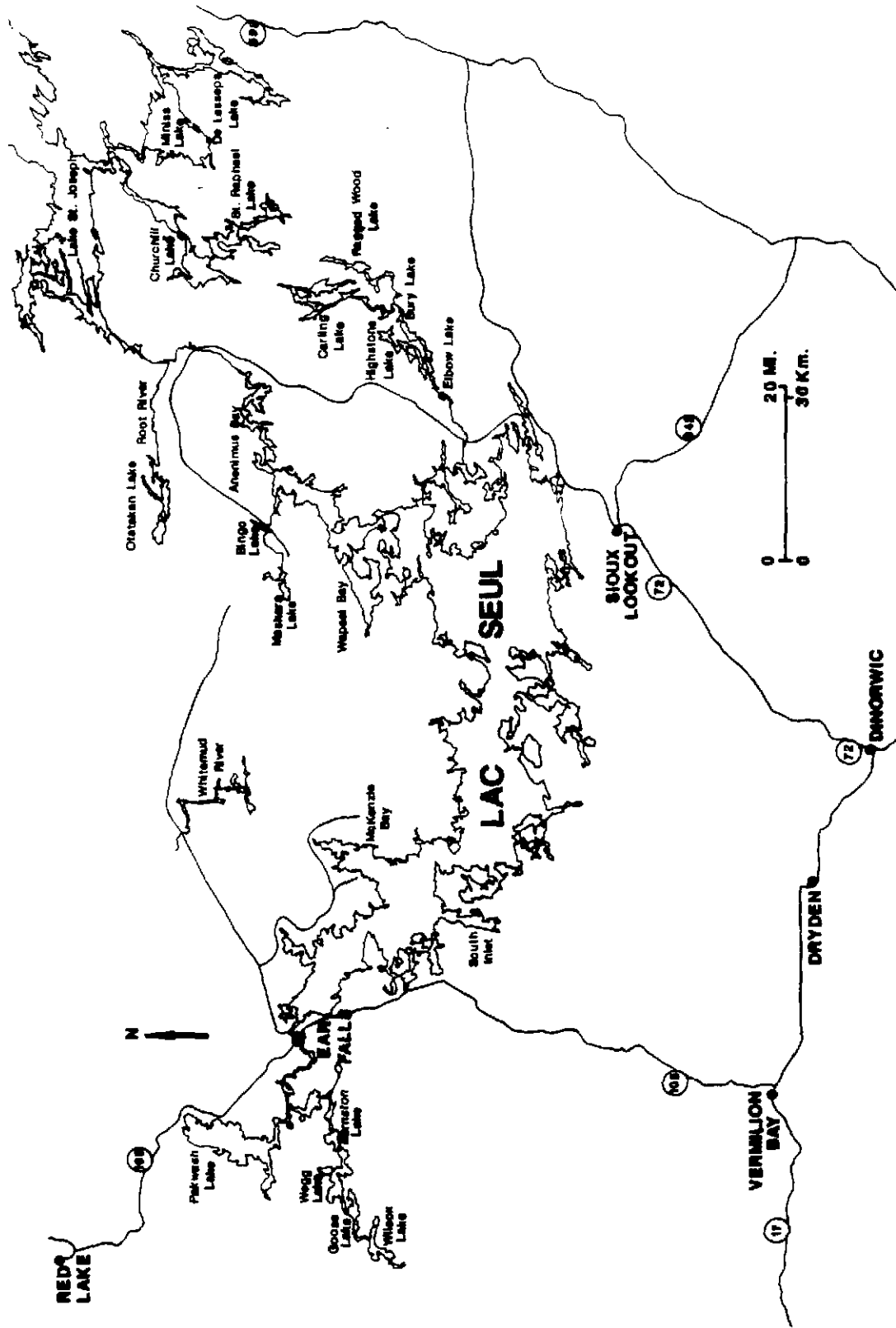
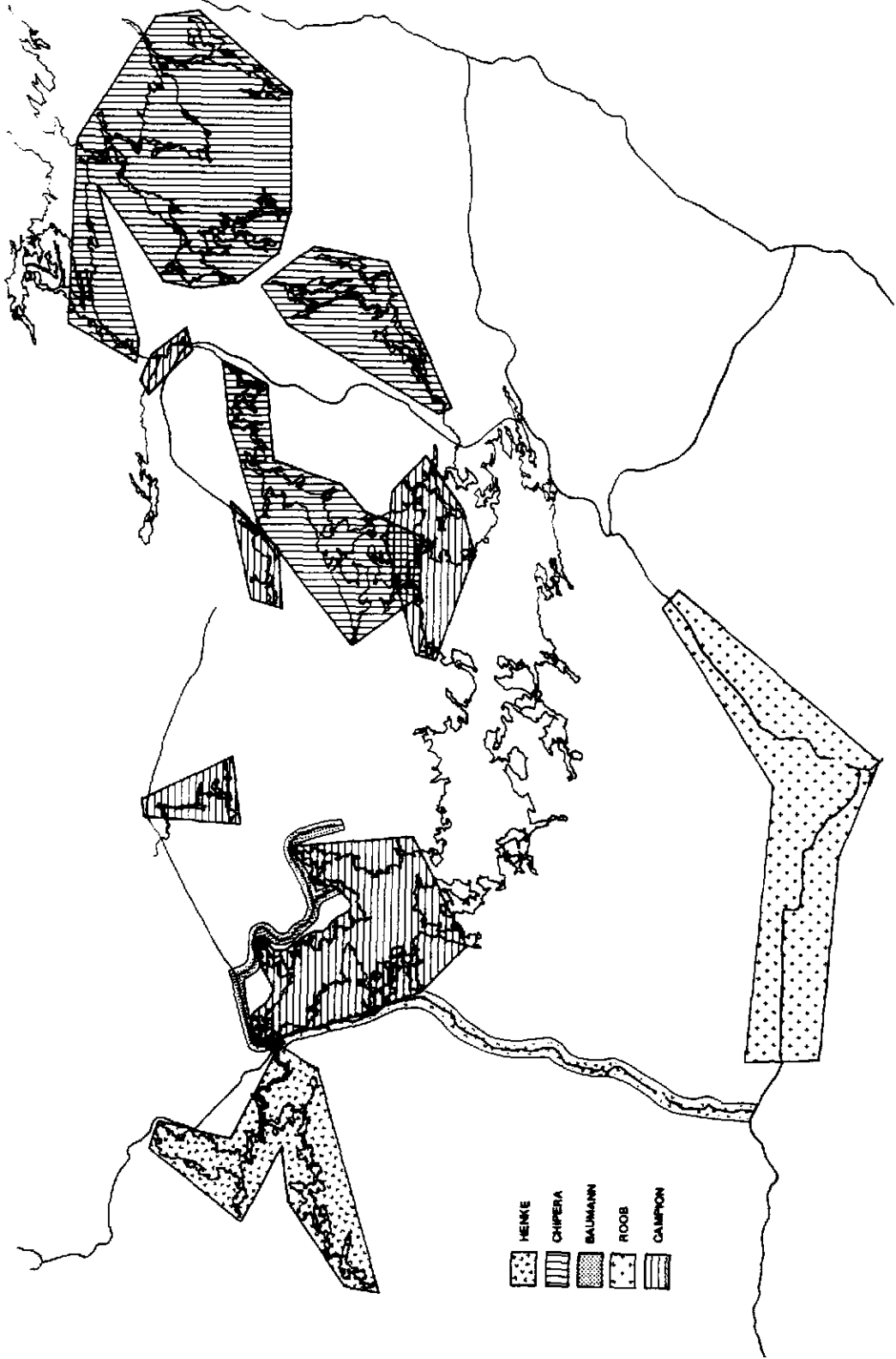


Figure 5. Location map of study areas for Henke (1984), Baumann (1985), Chipera (1985), Roob (1987) and Campion.



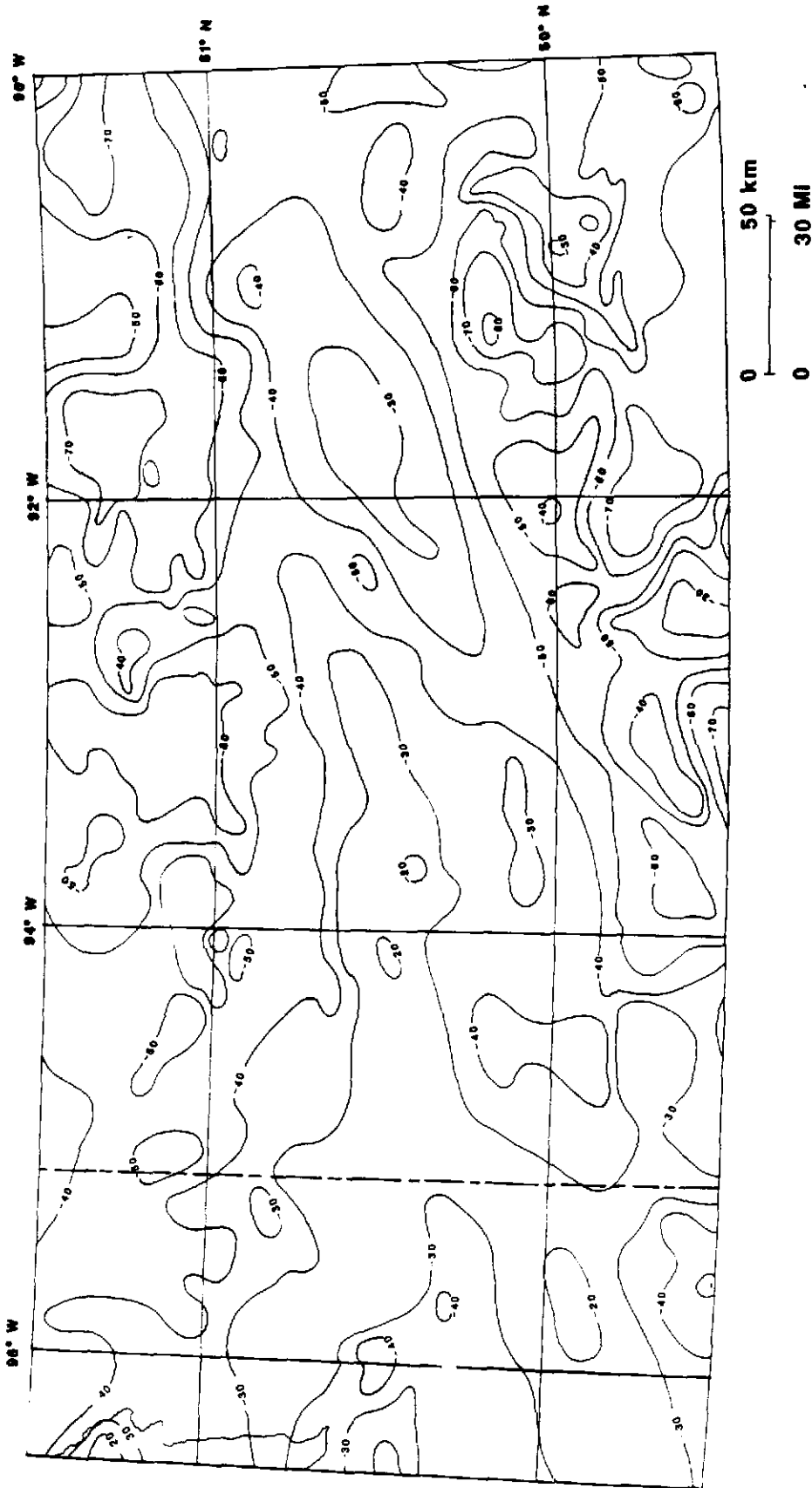
For this study, samples were collected from areas of the Lac Seul region not previously investigated by UND workers. Chemical analyses of these samples were obtained and used in geothermobarometric calculations to estimate temperatures and pressures of rock formation. The results were integrated with those of all previous University of North Dakota workers in the Lac Seul area (Henke, 1984; Baumann, 1985; Chipera, 1985; Roob, 1987), to summarize and interpret the temperature and pressure distribution across the entire Lac Seul region of the ERSP.

In order to provide another perspective on the tectonic regime that produced the present day ERSP, a gravity survey was conducted in Manitoba and the resulting Bouguer gravity anomaly modelled. Other existing gravity data (Gravity and Geodynamic Division; Energy, Mines and Resources Canada, 1981, Manuscript Map No. 48090) was examined as well; this data is displayed in Figure 6. Gravity modelling was performed to hypothesize the subsurface conditions underlying the ERSP and adjacent subprovinces.

Collection and synthesis of petrographic, geochemical and geophysical data permit a multidisciplinary approach to interpretation of the tectonic history of the ERSP. Using different techniques to characterize the terrane enables the investigator to impose limits on the resulting hypothesis of tectonic development. Integrating the

Figure 6. Bouguer gravity map of a portion of the Superior Province.

(Gravity and Geodynamics Division; Energy, Mines and Resources Canada, 1981, Manuscript Map No. 48090 and 48096)



different properties identified will serve to substantiate the resulting model. Examples of other multidisciplinary studies are: Smithson and Brown (1977), Fountain and Salisbury (1981), Percival and McGrath (1986), Fountain and Christensen (1989), Percival (1990), Weber and Mezger (1990).



## METAMORPHIC PETROLOGY AND GEOTHERMOBAROMETRY

### Methodology

During the summers of 1985 and 1986 rock samples were collected in the Lac Seul area. Most sampling was focused on the northeast and northwest portions of Lac Seul where the metasedimentary rocks are located (see Campion field areas Fig. 5, sample locations in Figures 7 and 8). Some sampling was done on the accessible lakes and rivers north of Lac Seul, as well as at some roadcuts. Preliminary geologic maps (Breaks and others, 1976a; 1976b; Breaks, Bond, Harris and Desnoyers, 1976; Breaks, Bond, Harris, Westerman and Desnoyers, 1976) were used to identify areas where minerals of interest had been reported and these areas were sampled.

Several samples were taken at each location. Samples were selected based on their freshness and geographic distribution and, if possible, the presence of garnet. This resulted in a sampling bias towards garnetiferous rocks and it is therefore possible that some orthopyroxene-bearing metasediments were overlooked.

Eighty-seven samples were cut and thin-sectioned. Thin sections were examined, using a petrographic microscope to identify minerals and textures present (see Appendix A). Mineral assemblages appropriate for geothermobarometry were determined, and the grains best suited for microprobe analysis were marked, carbon-coated and analyzed.

Figure 7. Eastern sample location map for the Campion field area. Displays the location of samples where geothermometry and/or geobarometry values were calculated.

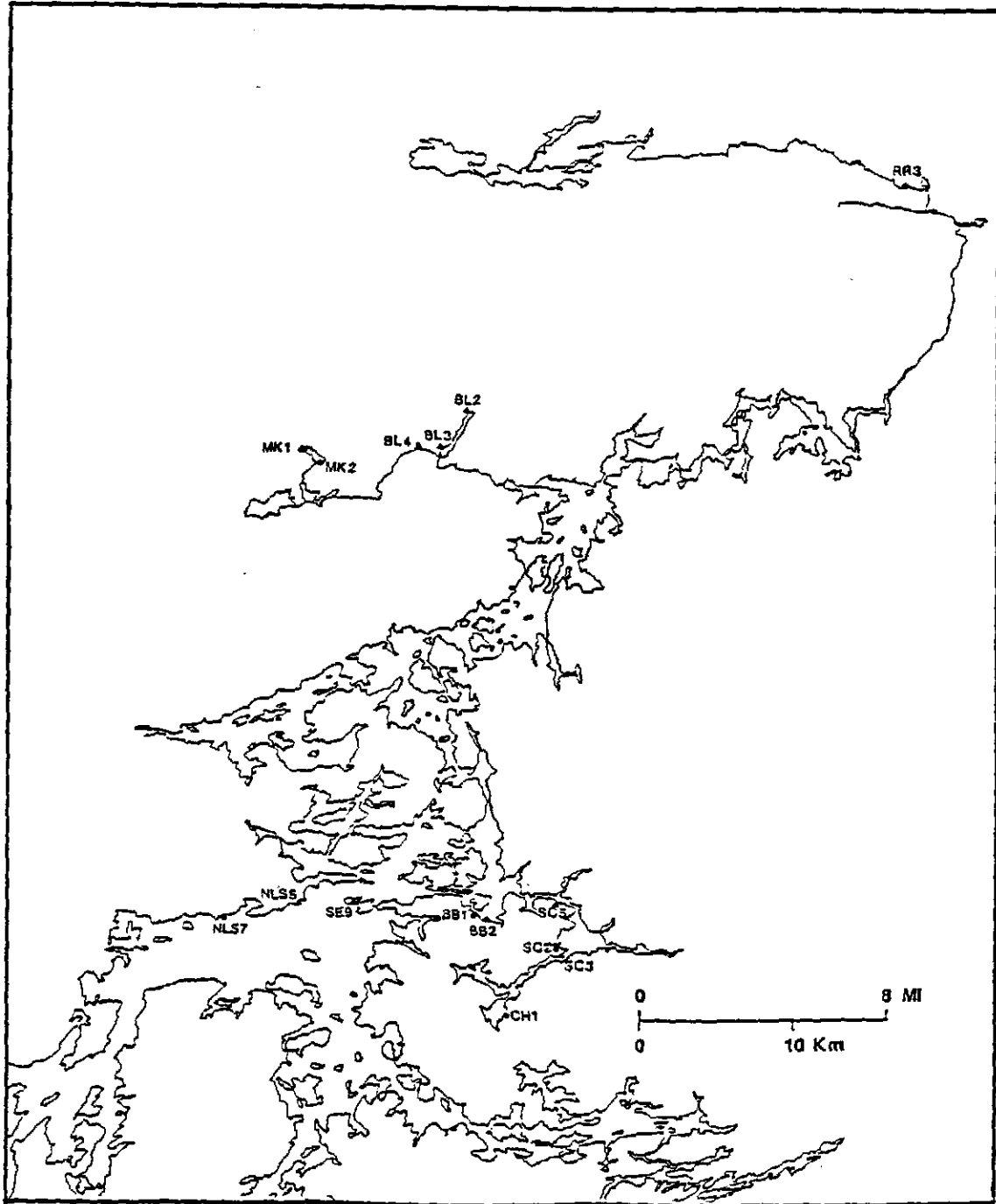
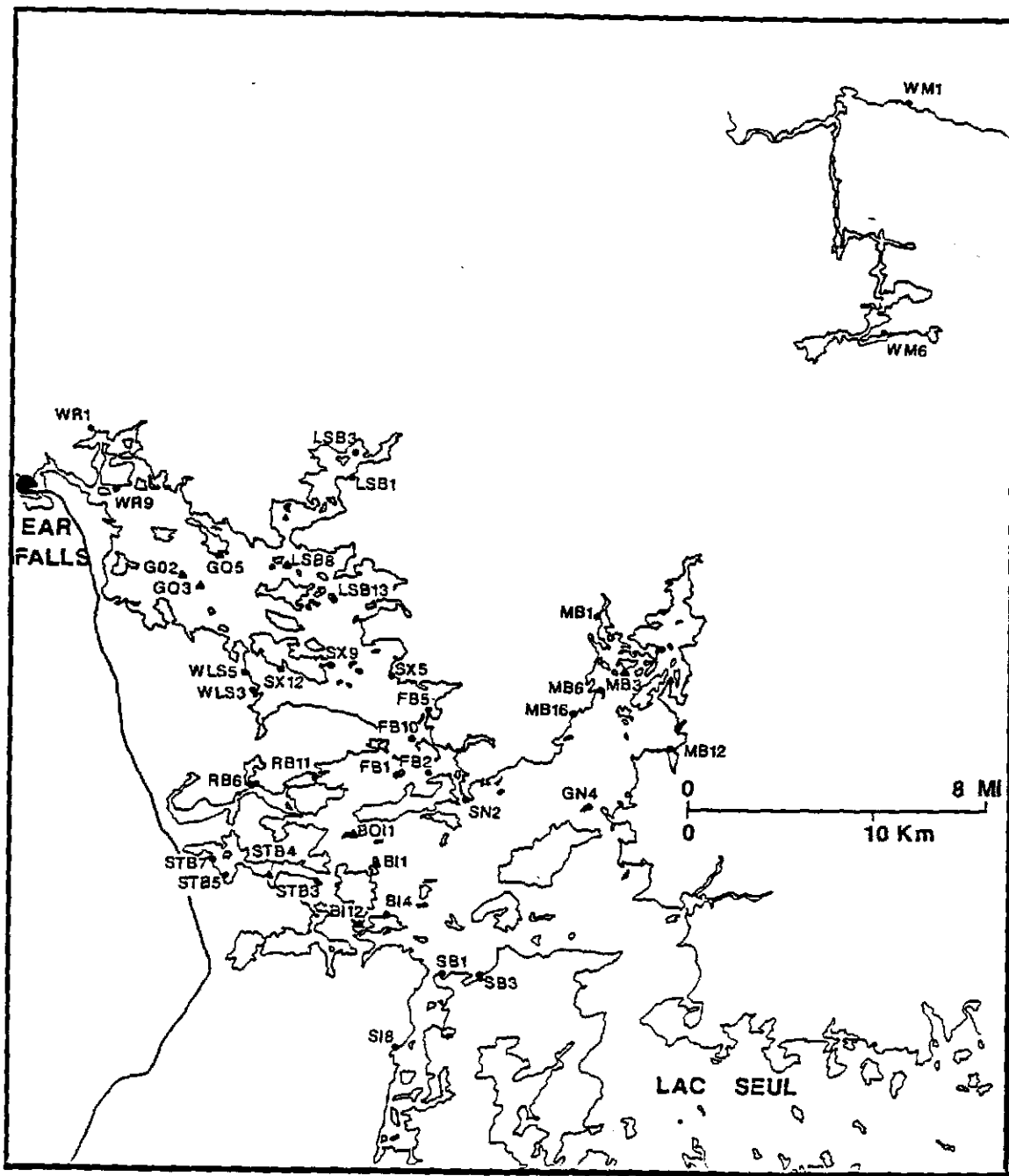


Figure 8. Western sample location map for the Campion field area. Displays the location of samples where geothermometry and/or geobarometry values were calculated.



### Microprobe Analysis

Chemical analyses were obtained using a JEOL 35C scanning electron microscope/electron probe microanalyzer operated at an accelerating voltage of 15 Kev and a beam current of 1000 picoamps. Energy dispersive spectra were collected and reduced to chemical analyses using a Bence Albee correction program on a Tracor Northern TN 2000 system. Minerals analyzed were garnet, biotite, cordierite, plagioclase, and orthopyroxene. These analyses are reported in Appendix B.

Standards of natural minerals were used. Six analyses of each standard were collected and averaged before any of the field specimens were analyzed. Correction factors were recalibrated using the averaged standard analyses as described by Roob (1987). Garnet R1134 was used to calibrate Si, Al, Fe, Mg and Ca. Plagioclase (Barton1) was used to calibrate Ca in plagioclase. Rhodonite R1826 was used to calibrate Mn concentrations. Early in the project Biotite 4166 was used to calibrate for Ti, Na and K. Later Orthoclase Orla was used for K, Albite Tib for Na, and Ilmenite R1959 for Ti.

Four to six analyses were taken for each mineral in a given geothermobarometric assemblage. Several mineral grains in different thin sections were checked for compositional zoning, all examples were found to be homogeneous. However, analyses were taken in the center of

the grain, if possible, to avoid obtaining chemical data from the rim of the mineral which may have been altered or undergone retrogression. Several grains of each phase (if there were several grains available) were analyzed, with a counting time of 45 or 60 seconds.

Five garnet-biotite geothermometers were employed (Thompson, 1976; Ferry and Spear, 1978; Perchuk and Lavrent'eva, 1983; Ganguly and Saxena, 1984; Indares and Martignole, 1985). Three different calibrations for garnet, plagioclase, sillimanite, quartz geobarometer were applied (Ghent, 1976; Newton and Haselton, 1981; Perchuk et al., 1981).

#### **Rock Descriptions**

Within the metasedimentary units, three compositionally distinct rock types were found. The vast majority of metasediments can be classified as a migmatitic biotite gneiss. In hand specimen the biotite gneiss can be further subdivided on the basis of texture into three subtypes: 1) massive biotite gneiss, 2) banded biotite gneiss, 3) biotite phyllite/schist. The biotite phyllite/schist is relatively minor in comparison to the other two textural types, and difficult to sample due to weathering.

The two other compositional varieties, amphibolite and metamorphosed iron formation, are less abundant than the migmatitic biotite gneiss. Amphibolite is minor in total

abundance but not uncommon as layers within the biotite gneiss. Metamorphosed iron formation was sampled at only one locality.

### **Migmatitic Biotite Gneiss**

All three varieties of the migmatitic biotite gneiss are dominantly composed of euhedral to subhedral quartz, feldspar, and biotite. Accessory minerals include apatite, zircon, epidote and opaques. Porphyroblasts of garnet and cordierite as well as minor occurrences of orthopyroxene and sillimanite may be present.

Garnet porphyroblasts are commonly poikiloblastic. Cordierite porphyroblasts are anhedral and poikiloblastic. Garnet is more common than cordierite. In some samples garnet and cordierite found together. Sillimanite is found in two specimens (BI12 and LSB8B). Sample LSB8B has fibrolite much like that reported throughout the Lac Seul area (Henke, 1984; Baumann, 1985; Chipera, 1985; Roob, 1987). Sample BI12 has well-developed needles of sillimanite which are not mantled by another mineral. Fibrolite is more commonly reported in the Lac Seul region, and coarse needles of sillimanite are rare.

Orthopyroxene is present in one sample (G03) of the migmatized biotite gneiss rock type. The orthopyroxene porphyroblasts are subhedral and not poikiloblastic.

The three sub-types of the migmatitic biotite gneiss have well-developed foliation parallel to bedding.



Migmatization is ubiquitous in the Lac Seul region, and therefore all the the rock types described here contain some veins of melted material. However, the layered biotite gneiss rock type typically contains more anatectic material than the other rock types.

Massive Biotite Gneiss The massive biotite gneiss is medium to coarse-grained and possesses well-developed foliation. In hand specimen biotite has well-developed preferred orientation. This foliation may not be readily apparent because biotite comprises no more than 15 percent of the rock. The massive biotite gneiss corresponds to the wacke rock type described by Henke (1984), Baumann (1985), Chipera (1985), and Roob (19867).

Layered Biotite Gneiss The layered biotite gneiss sub-type is a medium to coarse-grained, compositionally layered gneiss. Typically this rock type is more coarse-grained than the massive biotite gneiss sub-type described above. Compositional layers are well defined, exhibit well-developed lit-par-lit fabric, and range in thickness from millimeters to meters. These layers consist of leucocratic bands of quartz and feldspar alternating with strongly foliated layers of biotite, quartz, and feldspar, +/- porphyroblasts of garnet and/or cordierite.

Biotite Phyllite/Schist The third sub-type is a fine to medium-grained, well-foliated, biotite schist. The foliation is defined by biotite and varies texturally from

phyllitic to schistose. The biotite phyllite/schist is the least common of the migmatitic biotite gneiss sub-types.

#### **Mafic Amphibolite/Granulite Schist**

The medium-grained, moderately foliated amphibolite rock type is composed of plagioclase, quartz, clinopyroxene, amphibole and less common orthopyroxene. If orthopyroxene is present the rock type is classified as a mafic granulite schist--but this is not readily ascertained in the field. Common accessory minerals are epidote, apatite, zircon, and opaques. Foliation is defined by lineated amphibole grains. The mafic amphibolite/granulite schist rock type occurs as conformable layers within the migmatitic biotite gneiss. The conformable nature and the moderate grain size of the amphibolites in this field area indicate that they were derived from a basalt flow or possibly an ash deposit protolith.

#### **Metamorphosed Iron Formation**

A small unit of metamorphosed banded iron formation was found on the extreme northern border of the study area. This rock type is composed of magnetite, garnet, and quartz. Banding occurs as 0.5 to 1.5 centimeter layers of magnetite and quartz, alternating with layers of quartz and garnet. This rock type has not been reported by the previous UND workers, but it is reported to occur within the northern metasedimentary domain of the ERSP in both

Figure 9A. Isograd location map of Lac Seul study area. The map is based on data obtained by Henke (1984), Baumann (1985), Chipera (1985), Roob (1987) and Campion.

LEGEND

|                         |                       |
|-------------------------|-----------------------|
| ———                     | faults                |
| ▣▣▣▣▣▣▣▣                | andalusite-in         |
| ○○○○○○○○○○              | second sillimanite-in |
| — · — · — · — · — ·     | garnet-in             |
| -----                   | garnet-cordierite-in  |
| ●●●●●●●●                | fibrolite-in          |
| ▼ · ▼ · ▼ · ▼ · ▼ · ▼ · | clinopyroxene-in      |
| ▬▬▬▬▬▬▬▬                | orthopyroxene-in      |
| .....                   | spinel-in             |

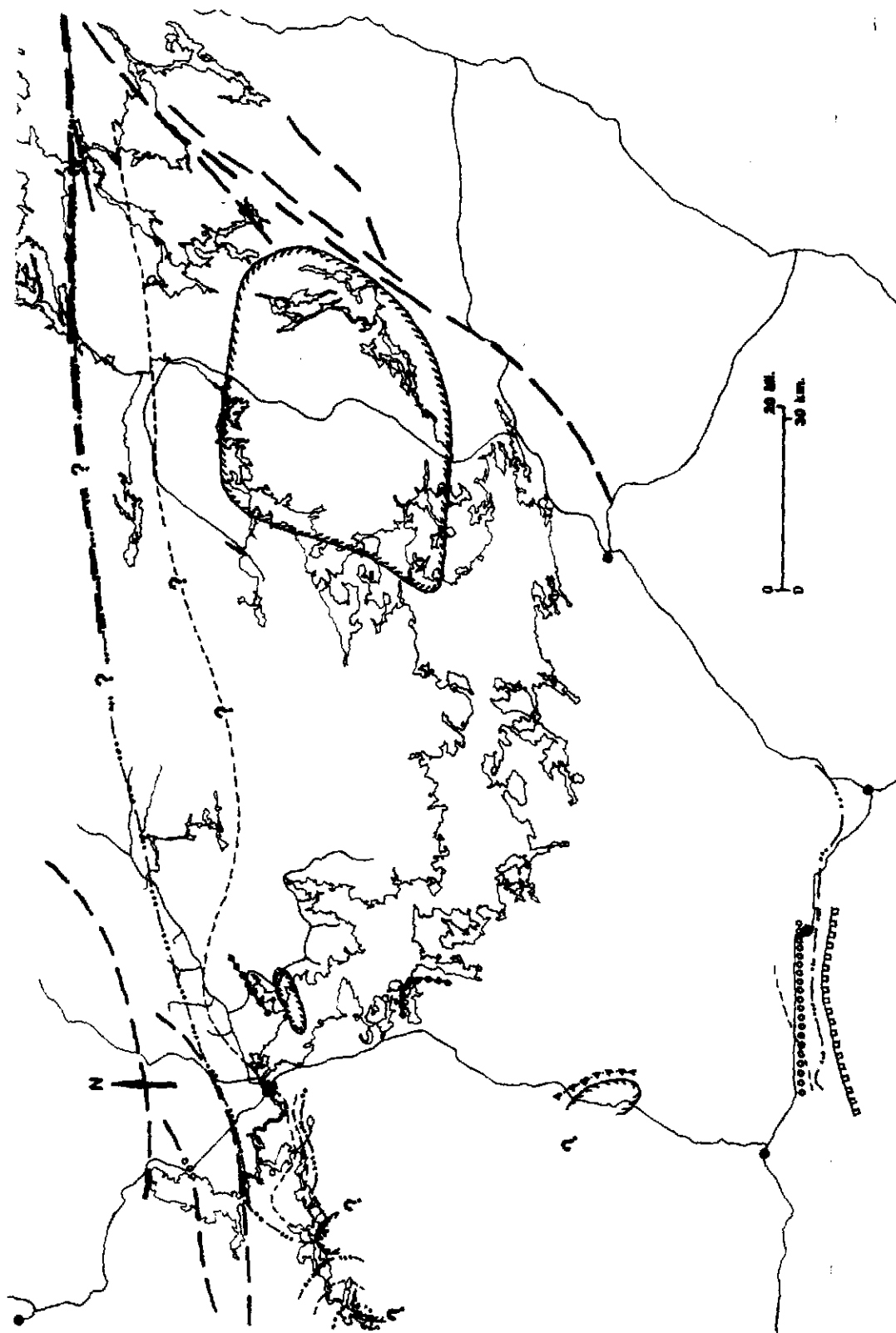
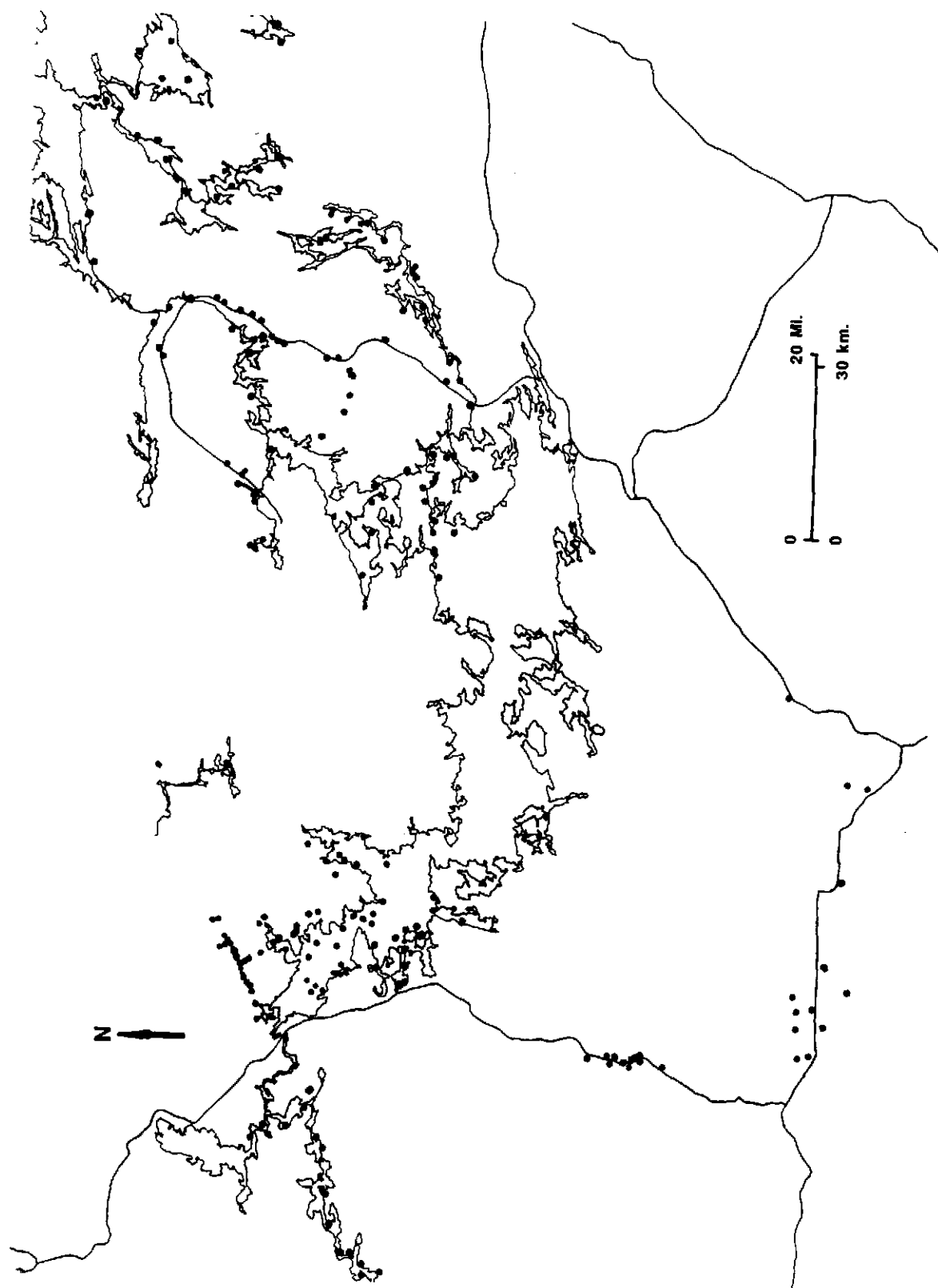


Figure 9B. Distribution of sample locations used to plot isograds. Based on data obtained by Henke (1984), Baumann (1985), Chipera (1985), Roob (1987) and Campion.



were taken directly from the theses of the other UND workers. The location of orthopyroxene occurrences is shown in Figure 10.

Figure 11 is a phase diagram showing some reactions which are relevant to this region plotted in pressure/temperature space. It may be used to constrain the pressure/temperature conditions of metamorphism. The index minerals identified by this study serve to bracket the temperature conditions of formation between reactions 4 and 11 in Figure 11, and pressure conditions to the sillimanite field shown by reaction 12. This corresponds to temperatures ranging from approximately 525 to 800 °C. The pressure range is confined between 3 and 5 kbars at 525 °C and is essentially unlimited at temperatures greater than 700 °C.

The range of conditions indicated by the mineral assemblages throughout the Lac Seul area are somewhat broader. Roob (1987) references reaction 1 in Figure 11 as a possible mechanism to produce andalusite, which occurs at approximately 425 °C and 3 kbar. Reaction 11 in Figure 11 is not indicated anywhere in the work of UND students, as orthopyroxene has not been found to coexist with cordierite.

Many reactions discussed in the literature are relevant to the metasedimentary rocks of the ERSP. In general, the reactions discussed below have been studied

Figure 10. Orthopyroxene occurrences in the Lac Seul area. The map is based on data obtained by Henke (1984), Baumann (1985), Chipera (1985), Roob (1987) and Champion. Open circles represent occurrences of orthopyroxene and garnet. Solid circles represent occurrences of orthopyroxene without garnet.



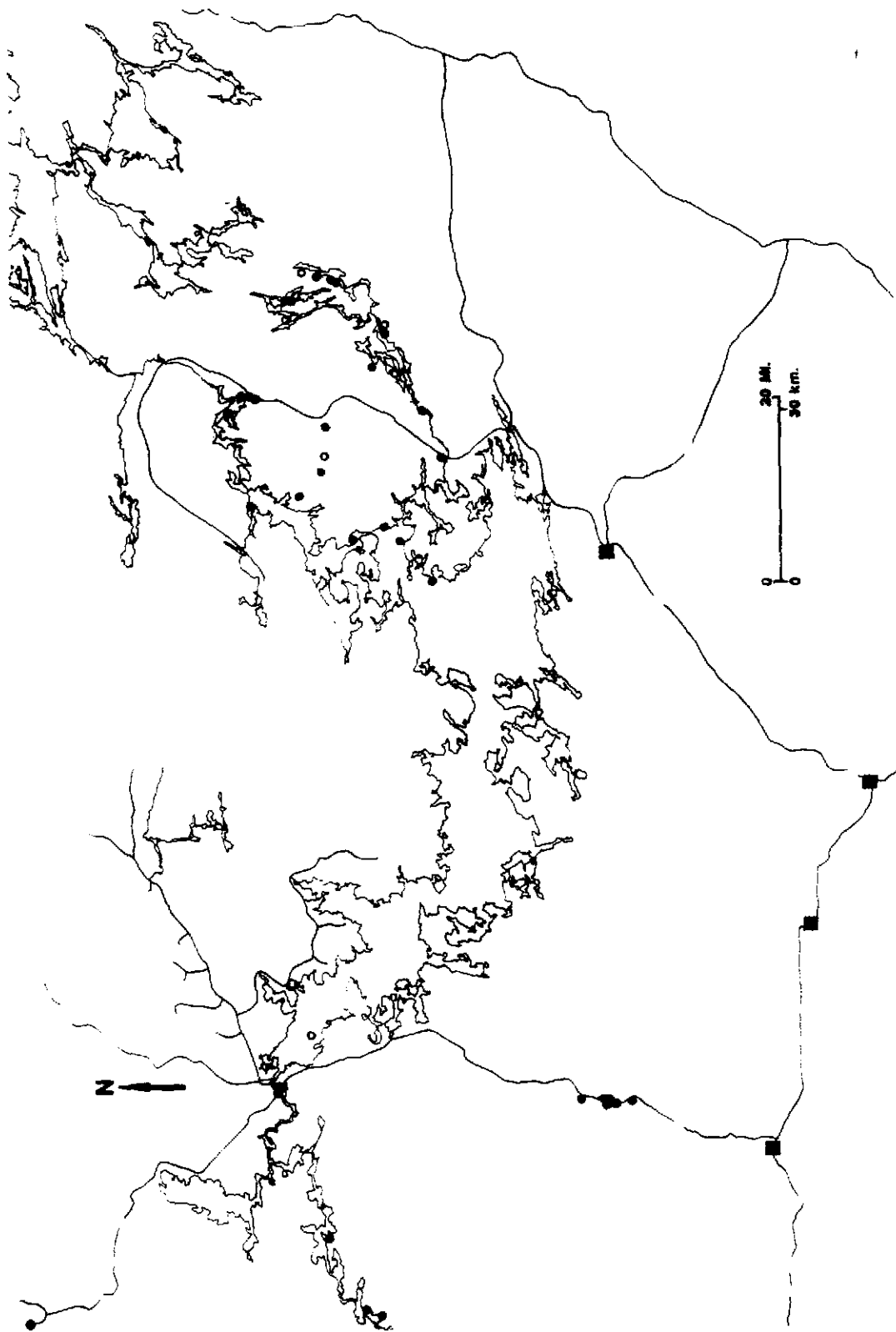


Figure 11. Mineralogical phase equilibria.

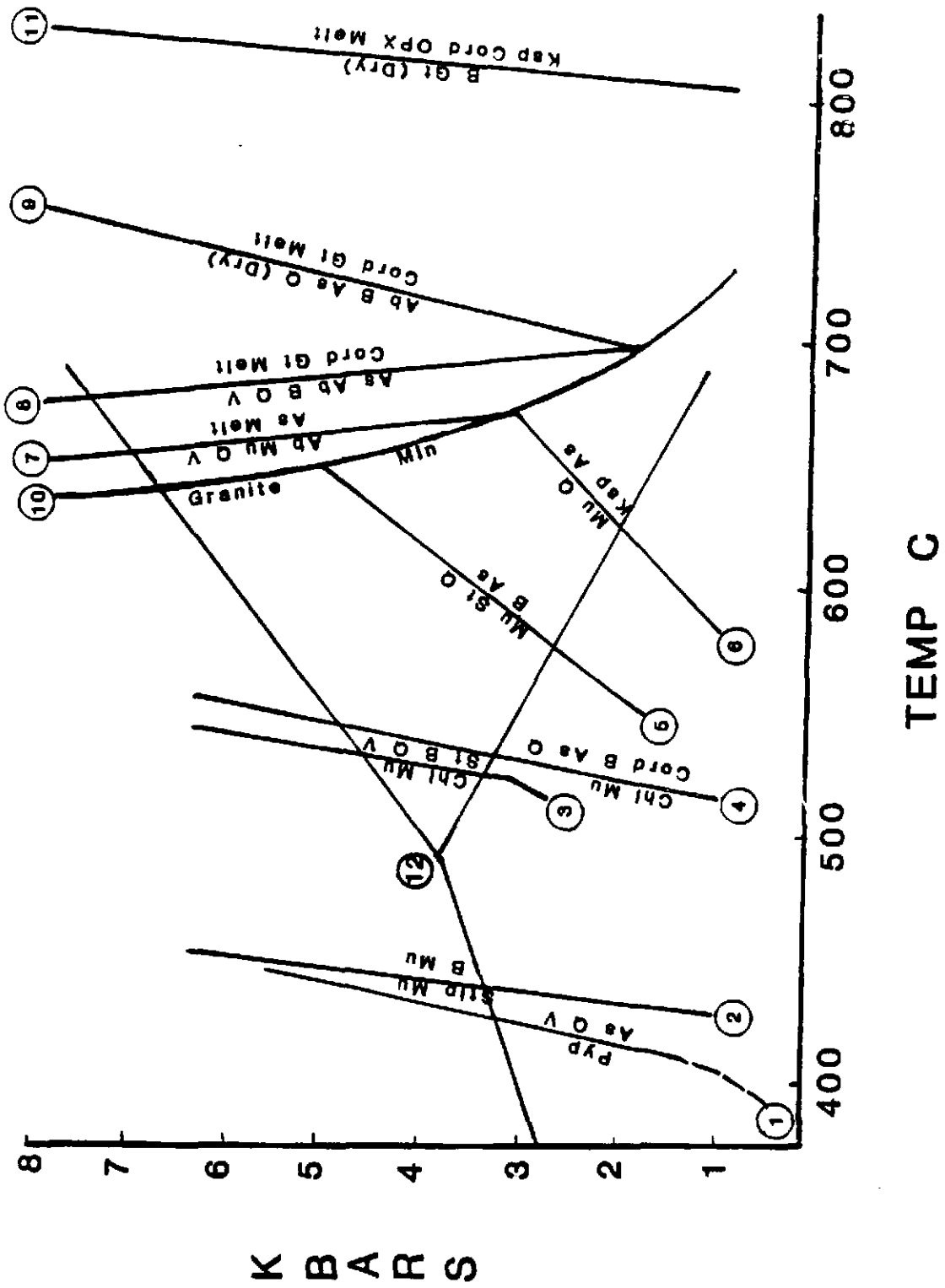
(Obtained from Roob, 1987)

Key

|                     |                      |
|---------------------|----------------------|
| Ab = Albite         | AS = $Al_2SiO_5$     |
| B = Biotite         | Chl = Chlorite       |
| Cord = Cordierite   | Gt = Garnet          |
| Ksp = K-Feldspar    | Ms = Muscovite       |
| OPX = Orthopyroxene | Q = Quartz           |
| St = Staurolite     | Stlp = Stilpnomelane |
| V = $H_2O$ Vapor    | Pyp = Pyrophyllite   |

MINERALOGICAL REACTIONS:

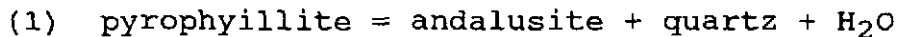
- 1  $Pyp = As + Q + V$   
(Holdaway, 1971)
- 2  $Stlp + Mu = B + Mu$   
(Winkler, 1979)
- 3  $Chl + Mu = St + B + Q + V$   
(Hoschek, 1969)
- 4  $Chl + Mu = Cord + B + AS + Q$   
(Winkler, 1979)
- 5  $Mu + St + Q = B + AS$   
(Hoschek, 1969)
- 6  $Mu + Q = Ksp + AS$   
(Winkler, 1979)
- 7  $Ab + Mu + Q + V = AS + Melt$   
(Winkler, 1979)
- 8  $Ab + B + AS + Q + V = Cord + Gt + Melt(Wet)$   
(Grant, 1973)
- 9  $Ab + B + AS + Q = Cord + Gt + Melt(Dry)$   
(Grant, 1973)
- 10 Granite Minimum Melt  
(Winkler, 1979)
- 11  $B + Gt = Ksp + Cord + OPX + Melt(Dry)$   
(Grant, 1973)
- 12 Holdaway's aluminosilicate triple point  
(Holdaway, 1971)



experimentally or evaluated thermodynamically. Relevant reactions are listed in order of relative metamorphic grade and grouped according to index minerals involved in the reaction. Because of the exhaustive efforts of Henke (1984), Baumann (1985), Chipera (1985), and Roob (1987), discussion of these reactions will be kept to a minimum--for a more complete listing and discussion refer to those documents. The pressure and temperature conditions at which the reactions occur may be found in Table 1.

#### **Reactions Involving Andalusite**

The andalusite isograd represents the lowest metamorphic grade and is located in the extreme southern portion of the Lac Seul region (Fig. 9). The presence of andalusite may be a result of:



#### **Reactions Involving Chlorite**

Like andalusite, primary chlorite is reported only in the southern part of this area. The chlorite-out isograd is not defined by Roob (1987) and is not shown in Figure 9A. However, the breakdown of chlorite may be important to the formation of several significant index minerals.

Reactions (2) and (3) both produce garnet and biotite--a widely distributed assemblage in the Lac Seul region:

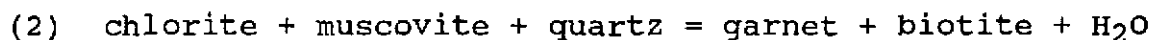


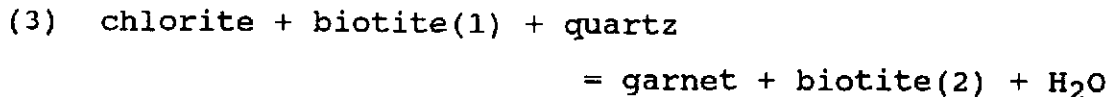
TABLE 1

## RELEVANT REACTIONS--TEMPERATURE/PRESSURE CONDITIONS OF FORMATION

| N    | REACTION   | TEMPERATURE<br>(CELSIUS) | PRESSURE<br>(KBARS)  | REFERENCE   |
|------|--|--------------------------|----------------------|---|
| (1)  | pyrophyllite = andalusite + qtz + H <sub>2</sub> O                                   | 400<br>430               | NR<br>4              | Holdaway (1971)<br>Winkler (1979)                                   |
| (2)  | chlorite + muscovite + qtz = garnet + biotite + H <sub>2</sub> O                     | 500-600                  | 4-5                  | Winkler (1979)  |
| (3)  | chlorite + biotite(1) + qtz = garnet + biotite(2) + H <sub>2</sub> O                 | 500-600                  | 4-5                  | Winkler (1979)  |
| (4)  | actinolite + epidote + chlorite + qtz = hornblende                                   | est. at 500              | NR                   | Winkler (1979)  |
| (5)  | chlorite + muscovite + qtz = biotite + cordierite + Al <sub>2</sub> SiO <sub>5</sub> | 505-555<br>580-600<br>NR | 0.5-4<br>3.5-7<br>NR | Winkler (1979)<br>Speer (1982)<br>Hess (1969)                       |
| (6)  | chlorite + muscovite = staurolite + biotite + qtz + H <sub>2</sub> O                 | 540-565                  | 4-7                  | Winkler (1979)  |
| (7)  | muscovite + chlorite + qtz = cordierite + biotite + H <sub>2</sub> O                 | 625<br>600-650           | 5<br>4.7-6.7         | Thompson (1976)<br>Schreyer and Seifert (1969)                      |
| (8)  | muscovite + qtz = sillimanite + k-feldspar + H <sub>2</sub> O                        | 740-790                  | 6-10                 | Winkler (1979)  |
| (9)  | muscovite + qtz + plag + H <sub>2</sub> O = sillimanite + melt                       | 640-655                  | 3-8                  | Winkler (1979)  |
| (10) | biotite + sillimanite + qtz = K-feldspar + cordierite + H <sub>2</sub> O             | 620-720<br>650-800<br>NR | 2-4.5<br>3-4.5<br>NR | Holdaway et al. (1977)<br>Holdaway et al. (1977)<br>Thompson (1976) |
| (11) | muscovite + biotite + qtz = garnet + K-feldspar + H <sub>2</sub> O                   | NR                       | NR                   | Thompson (1976)   |
| (12) | muscovite + biotite + qtz = cordierite + K-feldspar + H <sub>2</sub> O               | NR                       | NR                   | Thompson (1976)   |
| (13) | cordierite + biotite + qtz = garnet + K-feldspar + H <sub>2</sub> O                  | 640-665<br>665-695<br>NR | 2.5-3<br>4.3-5<br>NR | Hoffer (1976)<br>Schreyer and Seifert (1969)<br>Thompson (1976)     |

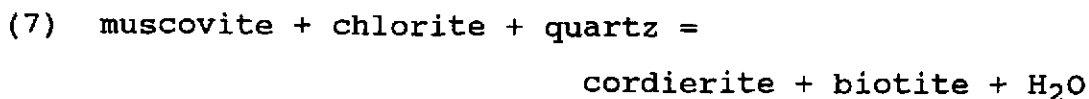
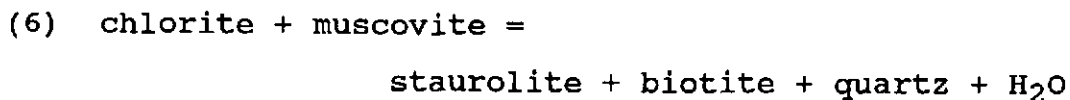
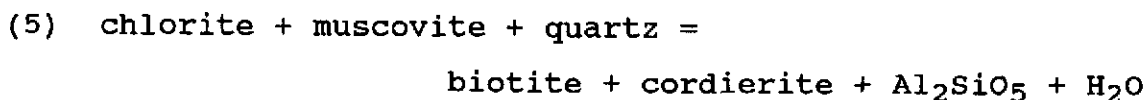
TABLE 1 CONTINUED

| N    | REACTION  | TEMPERATURE<br>(CELSIUS) | PRESSURE<br>(KBARS) | REFERENCE   |
|------|---|--------------------------|---------------------|---|
| (14) | biotite + Na-feldspar + $Al_2SiO_5$ + $H_2O$ = cordierite + garnet + melt | 650 - 700                | 1.5 - 7.5           | Grant (1973)  |
| (15) | biotite + qtz + $H_2O$ = orthopyroxene + melt                             | 750 - 800<br>NR          | NR<br>NR            | Breaks et al. (1978)<br>Winkler (1979)  |
| (16) | hornblende + qtz = orthopyroxene + clinopyroxene + plag + $H_2O$          | >710<br>NR               | 6-10<br>NR          | Bohlen et al. (1983)<br>Grant (1985)  |
| (17) | garnet + sillimanite = cordierite + spinel                                | 700                      | 5.5                 | Harris (1982)   |
| (18) | Fe-garnet + Mg-biotite = Mg-garnet + Fe-biotite                           | variable                 | variable            | Thompson (1976)<br>Ferry and Spear (1978)<br>Martignole and Sisi (1981)<br>Martignole and Sisi (1981)<br>Perchuk and Lavrent'eva (1983) |
| (19) | 3 anorthite = grossular + 2 sillimanite + qtz                             | variable                 | variable            | Ghent (1976)<br>Newton and Haselton (1981)<br>Perchuk et al. (1981)   |



Reaction (4) applies to the rocks of more mafic composition found in the area.

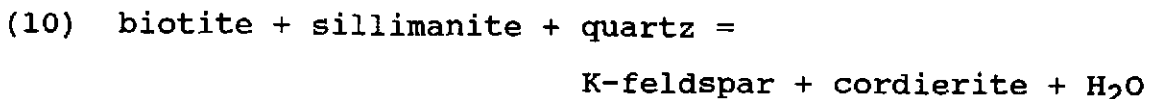
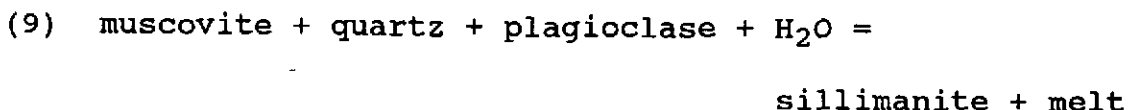
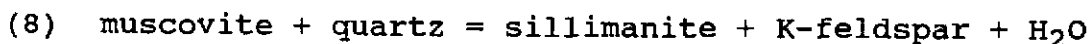
(4) actinolite + epidote + chlorite + quartz = hornblende  
Winkler (1979) describes the boundary between low and medium grade metamorphism by the first appearance of cordierite or staurolite. Reactions (5) and (7) may account for the common occurrence of cordierite in the area. Only one sample containing staurolite has been collected by UND workers. Reaction (6) not only describes a possible mechanism for the formation of staurolite, but Winkler (1979) also reports that this reaction coincides with the first appearance of cordierite--see reactions (5) and (7).



#### Reactions Involving Sillimanite

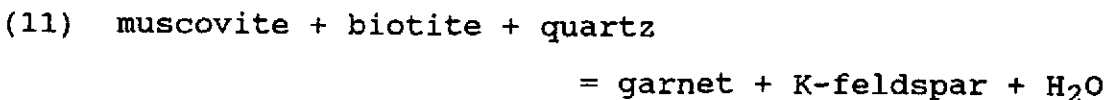
Reaction (8) represents the second sillimanite isograd which is defined by the coexistence of sillimanite and potassium feldspar without the presence of muscovite. Winkler (1979) defines the transition to high-grade metamorphism as the breakdown of muscovite in the presence

of quartz. Reaction (9) is the result of the intersection of reaction (8) and the granite minimum melting curve.



### Reactions Involving Garnet

Although reactions (2) and (3) have already been discussed above in terms of chlorite, for completeness they are also mentioned here. Thompson (1976) reports the position and orientation of reaction (11) in relative pressure/temperature space. Although this reaction has not been calibrated to specific pressure/temperature conditions, it bears noting.

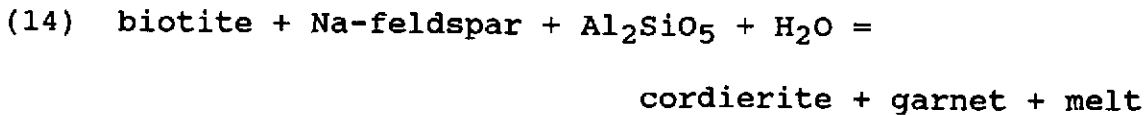
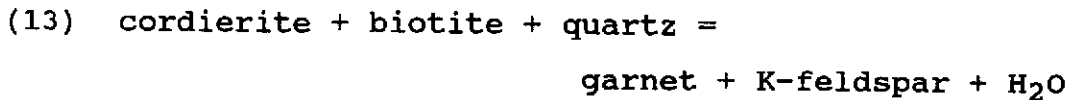
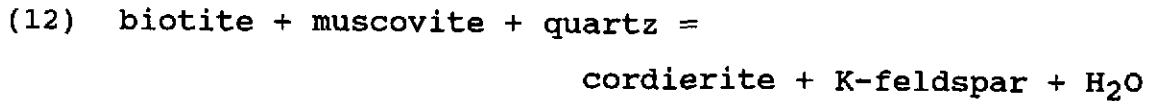


### Reactions Involving Cordierite and Cordierite/Garnet

Reactions (5), (7) and (10) involve cordierite. Reactions (12) and (13) are both reported by Thompson (1976) in relative pressure/temperature space, but reaction (13) is also reported by Hoffer (1976) and Schreyer et al. (1969) who have calibrated the pressure/temperature conditions of the reaction. Winkler (1979) states that the almandine-rich garnet and cordierite assemblage is found in a specific pressure/temperature range in the granulite



facies. Reaction (14) is significant, not only because it exhibits several of the phases so common in the Lac Seul area, but because it is the second melting reaction to be presented.



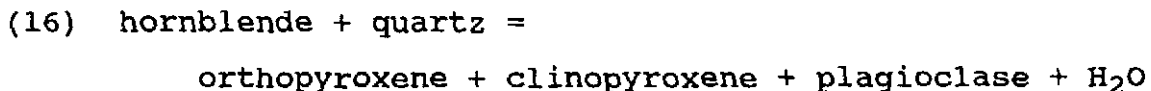
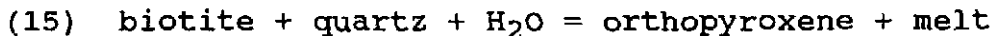
Baumann (1985) considers fibrolite found throughout the area to be a metastable remnant of reaction 14, isolated from further reaction by cordierite rims. The significance of fibrolite, in this area, versus coarse sillimanite is uncertain. Fibrolite is often considered to be a disequilibrium texture, however, its persistence over such a wide area in the ERSP may be attributed to the bulk composition of the rocks rather than metastability.

#### **Reactions Involving Orthopyroxene**

The orthopyroxene rocks represent the highest grade of metamorphism in the ERSP. Mafic granulites are not uncommon in the eastern Lac Seul region, but are rare in the west. Garnet-bearing granulites are rare in the area as a whole, it is speculated that the amount of aluminum in the more pelitic rocks has stabilized cordierite as a high

temperature phase and discouraged the formation of orthopyroxene.

Reaction (15) is noteworthy because it demonstrates how orthopyroxene can be produced from a pelitic assemblage without creating potassium feldspar as a discrete phase. Instead this reaction produces a melt which could be siphoned off and transported elsewhere. The temperature/pressure conditions of reaction (15) reported by Bohlen et al. (1983) are too high compared to the temperatures found by UND workers, determined through geothermometry. But the experiments executed by Bohlen et al. (1983) were done on the magnesium end-members and are therefore expected to take place at higher temperatures. Like reaction (4), reaction (16) applies to the amphibolites in the region.



#### Reactions Involving Spinel

Spinel was found in the extreme western portion of the Lac Seul area. It is unclear why spinel occurs in such a small area or what impact its presence has on metamorphic grade. The coexistence of quartz indicates that spinel is metastable. The temperatures calculated using geothermometry are somewhat low for this reaction, but are not unreasonable.

(17) garnet + sillimanite = cordierite + spinel

### Results of Geothermometry

The only geothermometer used was the garnet-biotite geothermometer. This was done to achieve consistent temperature results across the entire region. This geothermometer is based on the exchange reaction:

(18) Fe-garnet + Mg-biotite = Mg-garnet + Fe-biotite

As with many minerals, there is a complete solid-solution between the iron and magnesium end-members of both garnet and biotite. Because there is no need for a change in oxygen coordination or volume when Fe is exchanged for Mg in this reaction, it is essentially pressure-independent. Hence, this reaction serves well as a geothermometer. As temperature increases, the relative amount of magnesium in garnet increases and the amount of iron in biotite increases.

Five different garnet-biotite calibrations were used. The resulting temperatures are listed in Table 2. Within the field area of the current study, temperatures calculated using the Perchuk and Lavrent'eva (1983) calibration ranged from 577 to 751 °C. Temperatures from this calibration needed to be calculated for the Henke field area, these results are found in Table 3. The results of this study fit well with those of the four other studies in the Lac Seul region. In the western Lac Seul area the temperatures from the Baumann study area are in

TABLE 2  
 BIOTITE-GARNET EQUILIBRIA  
 Temperatures in Degrees C  
 at 5 Kbars

| Sample | Gt<br>Mg/Mg+Fe | Bio<br>ln Kd | THO    | F-S | P-L | G-S | I-M-1 | I-M-2 |     |
|--------|----------------|--------------|--------|-----|-----|-----|-------|-------|-----|
| BB1    | 0.226          | 0.486        | -1.172 | 737 | 820 | 699 | 713   | 693   | 712 |
| BB2B   | 0.213          | 0.496        | -1.295 | 694 | 756 | 670 | 686   | 653   | 705 |
| BI1B   | 0.173          | 0.444        | -1.340 | 679 | 734 | 660 | 680   | 629   | 653 |
| BI4B   | 0.166          | 0.438        | -1.543 | 618 | 646 | 617 | 637   | 568   | 617 |
| BI12   | 0.116          | 0.381        | -1.544 | 618 | 646 | 617 | 641   | 567   | 581 |
| BL2A   | 0.271          | 0.586        | -1.337 | 680 | 736 | 661 | 612   | 615   | 642 |
| BL2B   | 0.257          | 0.543        | -1.235 | 715 | 786 | 684 | 663   | 647   | 672 |
| BL3A   | 0.212          | 0.501        | -1.313 | 688 | 747 | 666 | 668   | 627   | 663 |
| BL4B   | 0.256          | 0.537        | -1.218 | 721 | 796 | 688 | 667   | 674   | 692 |
| BOI1A  | 0.197          | 0.510        | -1.441 | 648 | 688 | 638 | 618   | 565   | 587 |
| CH1A   | 0.209          | 0.516        | -1.392 | 663 | 710 | 649 | 638   | 609   | 647 |
| CH1C   | 0.226          | 0.489        | -1.192 | 730 | 809 | 694 | 718   | 704   | 748 |
| FB1    | 0.228          | 0.516        | -1.282 | 699 | 763 | 673 | 680   | 675   | 718 |
| FB2C   | 0.233          | 0.559        | -1.427 | 652 | 694 | 641 | 597   | 593   | 613 |
| FB5A   | 0.281          | 0.573        | -1.232 | 716 | 788 | 685 | 646   | 627   | 650 |
| FB10   | 0.276          | 0.425        | -1.320 | 686 | 744 | 665 | 636   | 612   | 652 |
| GN4B   | 0.230          | 0.630        | -1.749 | 563 | 571 | 577 | 531   | 544   | 619 |
| GO2C   | 0.197          | 0.476        | -1.308 | 690 | 750 | 667 | 679   | 629   | 658 |
| GO3    | 0.270          | 0.557        | -1.226 | 718 | 791 | 686 | 694   | 689   | 744 |
| G05A   | 0.229          | 0.551        | -1.419 | 654 | 698 | 643 | 603   | 570   | 591 |
| LPC2A  | 0.159          | 0.476        | -1.569 | 611 | 636 | 612 | 634   | 579   | 664 |
| LPC7A  | 0.237          | 0.549        | -1.365 | 671 | 722 | 655 | 620   | 620   | 645 |
| LPC9A  | 0.216          | 0.464        | -1.143 | 748 | 837 | 706 | 736   | 674   | 695 |
| LPC9B  | 0.252          | 0.544        | -1.263 | 705 | 772 | 678 | 662   | 634   | 667 |
| LSB1A  | 0.223          | 0.494        | -1.225 | 718 | 792 | 686 | 690   | 644   | 666 |
| LSB3A  | 0.238          | 0.564        | -1.421 | 654 | 697 | 643 | 596   | 588   | 609 |
| LSB8B  | 0.222          | 0.490        | -1.225 | 718 | 792 | 686 | 696   | 638   | 668 |
| LSB13A | 0.229          | 0.527        | -1.328 | 683 | 740 | 663 | 660   | 651   | 692 |
| MB1A   | 0.270          | 0.680        | -1.433 | 650 | 692 | 640 | 570   | 577   | 597 |
| MB3    | 0.268          | 0.560        | -1.243 | 712 | 782 | 682 | 643   | 635   | 650 |
| MB6C   | 0.213          | 0.546        | -1.492 | 633 | 667 | 628 | 592   | 554   | 584 |
| MB12   | 0.155          | 0.431        | -1.412 | 657 | 701 | 644 | 723   | 664   | 794 |
| MB16   | 0.253          | 0.597        | -1.473 | 638 | 675 | 632 | 567   | 575   | 596 |
| MK1A   | 0.182          | 0.511        | -1.545 | 617 | 646 | 617 | 599   | 550   | 582 |
| MK1B   | 0.168          | 0.468        | -1.473 | 638 | 675 | 632 | 649   | 608   | 669 |
| MK2A   | 0.186          | 0.490        | -1.435 | 649 | 691 | 639 | 643   | 612   | 659 |

TABLE 2 (CONT.)

## BIOTITE-GARNET EQUILIBRIA

Temperatures in Degrees C  
at 5 Kbars

| Sample | Gt<br>Mg/Mg+Fe | Bio<br>ln Kd | THO    | F-S | P-L | G-S | I-M-1 | I-M-2 |     |
|--------|----------------|--------------|--------|-----|-----|-----|-------|-------|-----|
| NLS5B  | 0.203          | 0.458        | -1.204 | 726 | 803 | 691 | 721   | 672   | 700 |
| NLS5C  | 0.258          | 0.477        | -0.967 | 818 | 949 | 751 | 805   | 777   | 805 |
| NLS7A  | 0.201          | 0.492        | -1.348 | 677 | 730 | 658 | 659   | 637   | 671 |
| RB6A   | 0.209          | 0.508        | -1.361 | 673 | 724 | 655 | 649   | 616   | 652 |
| RB11C  | 0.196          | 0.542        | -1.579 | 608 | 632 | 610 | 574   | 558   | 592 |
| RR3C   | 0.134          | 0.441        | -1.632 | 593 | 612 | 600 | 649   | 564   | 695 |
| RR5B   | 0.171          | 0.487        | -1.525 | 623 | 653 | 621 | 641   | 573   | 658 |
| SB1A   | 0.134          | 0.445        | -1.641 | 591 | 609 | 598 | 648   | 573   | 689 |
| SB3A   | 0.130          | 0.461        | -1.738 | 566 | 575 | 580 | 628   | 560   | 679 |
| SC2B   | 0.191          | 0.492        | -1.412 | 656 | 701 | 644 | 682   | 625   | 725 |
| SC3D   | 0.220          | 0.508        | -1.305 | 691 | 751 | 668 | 661   | 630   | 658 |
| SC5    | 0.167          | 0.461        | -1.448 | 646 | 685 | 637 | 644   | 570   | 604 |
| SE9A   | 0.262          | 0.577        | -1.345 | 678 | 732 | 659 | 612   | 617   | 641 |
| SI8    | 0.143          | 0.437        | -1.541 | 619 | 647 | 618 | 631   | 575   | 613 |
| SN2    | 0.199          | 0.518        | -1.460 | 642 | 680 | 634 | 619   | 601   | 638 |
| STB3B  | 0.203          | 0.528        | -1.479 | 636 | 672 | 630 | 619   | 587   | 637 |
| STB4B  | 0.190          | 0.543        | -1.618 | 597 | 618 | 602 | 557   | 536   | 552 |
| STB5A  | 0.196          | 0.490        | -1.334 | 681 | 737 | 661 | 670   | 639   | 678 |
| STB7A  | 0.194          | 0.511        | -1.468 | 640 | 677 | 633 | 638   | 583   | 641 |
| SX5D   | 0.218          | 0.551        | -1.482 | 636 | 671 | 630 | 589   | 558   | 582 |
| SX9    | 0.237          | 0.522        | -1.262 | 705 | 773 | 678 | 673   | 650   | 684 |
| SX12   | 0.272          | 0.600        | -1.390 | 664 | 711 | 649 | 587   | 580   | 601 |
| WLS3B  | 0.209          | 0.526        | -1.437 | 649 | 690 | 639 | 618   | 572   | 603 |
| WLS11A | 0.221          | 0.506        | -1.285 | 698 | 761 | 673 | 704   | 649   | 717 |
| WM1C   | 0.143          | 0.428        | -1.501 | 630 | 663 | 626 | 662   | 633   | 665 |
| WM6A   | 0.239          | 0.585        | -1.503 | 629 | 662 | 625 | 577   | 603   | 641 |
| WR1    | 0.178          | 0.512        | -1.575 | 609 | 633 | 611 | 603   | 541   | 588 |
| WR9A   | 0.188          | 0.517        | -1.532 | 621 | 651 | 619 | 628   | 578   | 663 |

$$\ln Kd = ((X_{Mg}/X_{Fe})_{Gt} / (X_{Mg}/X_{Fe})_{Bio})$$

F-S = Ferry and Spear (1978)

P-L = Perchuk and Lavrent'eva (1983)

T-H = Thompson (1976)

G-S = Ganguly and Saxena (1984)

I-M-1 = Indares and Martignole (1985) thermodynamic data

I-M-2 = Indares and Martignole (1985) thermodynamic and  
empirical data

TABLE 3

CALCULATED PERCHUK AND LAVRENT'EVA THERMOMETRY RESULTS  
HENKE (1984) FIELD AREA

Temperatures in Degrees C  
at 5 kbars

| Sample | Garnet<br>Xmg/Xfe | Biotite<br>Xmg/Xfe | ln Kd | Temperature |
|--------|-------------------|--------------------|-------|-------------|
| D4     | 0.268             | 0.978              | -1.3  | 680         |
| D5     | 0.218             | 0.582              | -1.0  | 757         |
| D7     | 0.268             | 1.141              | -1.4  | 646         |
| G2B    | 0.340             | 1.203              | -1.3  | 688         |
| G52C   | 0.187             | 1.045              | -1.7  | 592         |
| G53A   | 0.206             | 0.831              | -1.4  | 658         |
| G55A   | 0.222             | 1.132              | -1.6  | 609         |
| G63A   | 0.326             | 1.049              | -1.2  | 710         |
| G68B   | 0.202             | 1.075              | -1.7  | 601         |
| G69A   | 0.321             | 1.227              | -1.3  | 670         |
| G79A   | 0.364             | 1.336              | -1.3  | 673         |
| G89    | 0.240             | 1.096              | -1.5  | 628         |
| G98C   | 0.216             | 1.139              | -1.7  | 599         |
| G102   | 0.196             | 0.972              | -1.6  | 611         |
| G103A  | 0.147             | 0.724              | -1.6  | 611         |
| MF1A   | 0.236             | 0.880              | -1.3  | 670         |
| MF4A   | 0.179             | 1.049              | -1.8  | 578         |
| MF16   | 0.212             | 1.092              | -1.6  | 603         |
| MF19   | 0.184             | 0.996              | -1.7  | 593         |
| RL52   | 0.226             | 0.767              | -1.2  | 692         |
| RL120  | 0.186             | 0.815              | -1.5  | 635         |
| RL360  | 0.241             | 1.203              | -1.6  | 609         |

the upper 600's and lower 700's, whereas the temperatures reported in the adjoining portion of the Campion study are in mid to upper 600's.

Similarly, in the eastern Lac Seul area, the portions of the Chipera study that are adjacent to the Campion field area show temperatures in the lower 700's, and the Campion temperatures are in the upper 600's. The somewhat lower temperatures reported from the Campion field area correspond to the gradual decline in grade towards the southern Lac Seul region.

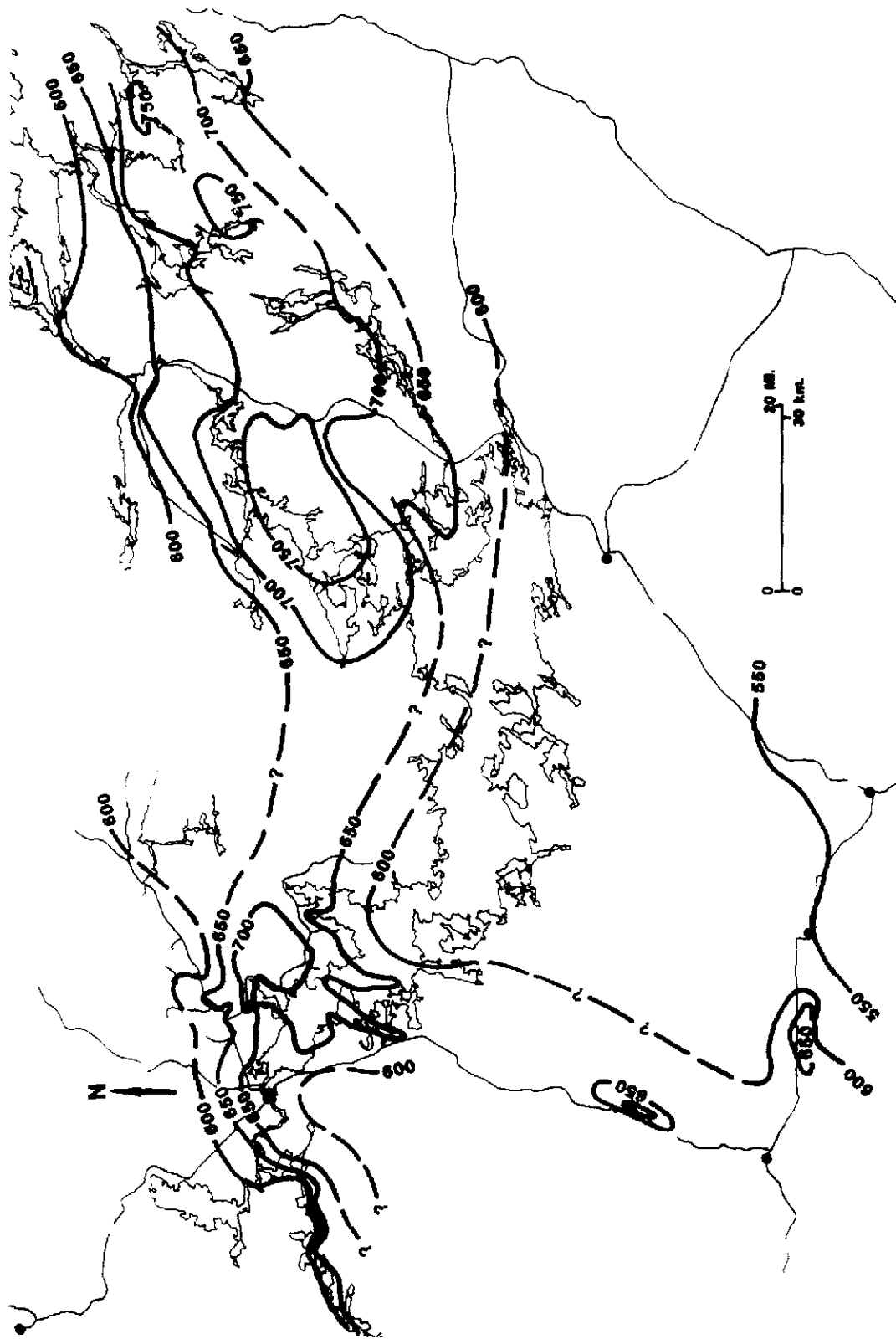
A map of hand-contoured temperature results based on the Perchuk and Lavrent'eva (1983) calibration for all five studies can be seen in Figure 12. This calibration was chosen for display because there is general agreement that it yields the most consistent results for the area (Chipera, 1985; Chipera and Perkins, 1988). There are still gaps in the distribution of samples throughout the Lac Seul region, however, the diagram does give a better estimate of the temperature conditions throughout the region as a whole, than has been previously presented. As was found by other workers, the resulting temperature gradient shows some correspondence with the successive appearance of index minerals of increasing grade. This relationship will be described in more detail below.

The additional detail supplied to the data by this study has changed the appearance of the isotherms in the

Figure 12. Hand contoured isotherms in Lac Seul study area. The map is based on data obtained by Henke (1984), Baumann (1985), Chipera (1985), Roob (1987) and Campion.

(Perchuk and Lavrent'eva, 1983)



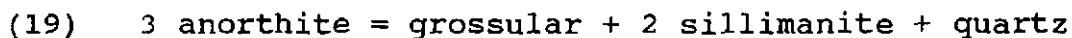


Lac Seul area. Unlike the results presented by other workers whose data distribution was limited, showing very linear contours sub-parallel to the subprovince boundaries, this additional information results in a pattern of thermal basins and domes. The contours are much more erratic than those shown by other UND workers in the area. Overall, the highest temperatures are recorded in the mid-northern portion of the subprovince, with temperatures falling off sharply to the north and more gradually to the south.

#### Results of Geobarometry

Three calibrations were used to obtain pressure estimates using the garnet-plagioclase-sillimanite-quartz geobarometer: Ghent (1976), Newton and Haselton (1981), Perchuk et al. (1981). Results are found in Table 4.

This geobarometer is based on the following reaction:



In this reaction the aluminum in anorthite is in tetrahedral coordination, whereas aluminum is octahedrally coordinated in both sillimanite and grossular. Because aluminum in grossular and sillimanite is more densely packed, there is a volume decrease associated with this reaction. The volume decrease, gives the reaction a strong pressure dependence, making it an excellent geobarometer.

There was only one sample in this study area which contains well-developed needles of sillimanite. Therefore, in the absence of coarse sillimanite, the pressures

TABLE 4

## GARNET-PLAGIOCLASE-SILLIMANITE-QUARTZ GEOBAROMETER RESULTS

Pressure in Kb

| Sample | Temp | Xan   | Xgr   | lnK  | Ghent<br>(1976) | Newton<br>Hasleton<br>(1981) | Perchuk<br>et al.<br>(1981) |
|--------|------|-------|-------|------|-----------------|------------------------------|-----------------------------|
| BI12   | 617  | 0.267 | 0.028 | -7.8 | 5.5             | 2.8                          | 2.7                         |
| BL2A   | 661  | 0.277 | 0.029 | -7.3 | 6.1             | 4.1                          | 4.7                         |
| BL2B   | 684  | 0.269 | 0.029 | -7.3 | 6.5             | 4.4                          | 4.9                         |
| BL3A   | 666  | 0.276 | 0.029 | -7.4 | 6.1             | 4.0                          | 4.3                         |
| BL4B   | 688  | 0.320 | 0.031 | -7.5 | 6.1             | 4.2                          | 4.9                         |
| BOI1A  | 638  | 0.274 | 0.030 | -7.4 | 5.9             | 3.7                          | 3.9                         |
| GO2C   | 667  | 0.272 | 0.028 | -7.5 | 6.3             | 3.9                          | 4.0                         |
| GO5A   | 643  | 0.275 | 0.026 | -7.7 | 5.4             | 3.3                          | 3.7                         |
| LPC9A  | 706  | 0.239 | 0.027 | -7.0 | 7.0             | 5.2                          | 4.8                         |
| LSB1A  | 686  | 0.218 | 0.022 | -6.6 | 6.3             | 5.4                          | 4.0                         |
| LSB8B  | 686  | 0.244 | 0.025 | -7.3 | 6.3             | 4.4                          | 4.2                         |
| MB3    | 682  | 0.246 | 0.024 | -7.3 | 6.1             | 4.4                          | 4.4                         |
| MK1B   | 632  | 0.253 | 0.027 | -7.6 | 5.8             | 3.4                          | 3.4                         |
| NLS5C  | 751  | 0.260 | 0.028 | -6.9 | 7.4             | 5.8                          | 5.7                         |
| SC3D   | 668  | 0.256 | 0.027 | -7.3 | 6.3             | 4.2                          | 4.2                         |
| SC5    | 637  | 0.214 | 0.023 | -7.4 | 5.9             | 3.7                          | 3.1                         |
| SN2    | 634  | 0.272 | 0.031 | -7.3 | 6.0             | 3.8                          | 4.0                         |
| STB4   | 602  | 0.320 | 0.036 | -7.5 | 5.5             | 3.1                          | 3.8                         |

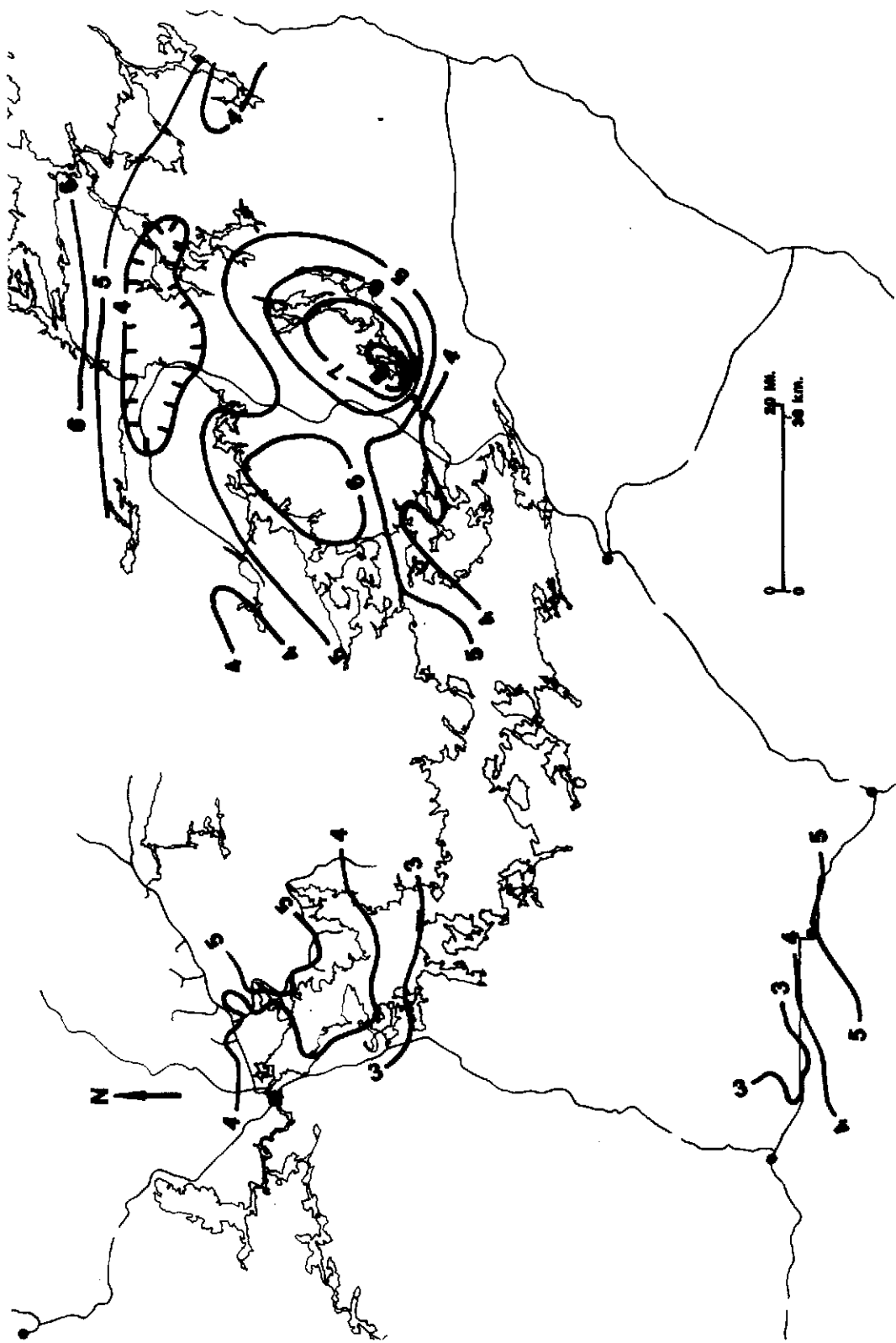
$$\ln K = \ln \left( \frac{(\text{agr})^3}{(\text{aan})^3} \right)$$

$$\text{Xan} = \frac{\text{Ca}}{\text{Ca} + \text{Na} + \text{K}} \text{ in Plagioclase}$$

$$\text{Xgr} = \frac{\text{Fe}}{\text{Ca} + \text{Fe} + \text{Mg} + \text{Mn}} \text{ in Garnet}$$

Figure 13. Hand contoured isobars in Lac Seul study area. The map is based on data obtained by Henke (1984), Baumann (1985), Chipera (1985), Roob (1987) and Campion.

(Perchuk, Podlesskii and Aranovich, 1981)



Lac Seul region, than it was with the temperature data. However, the areas of highest pressure roughly correspond to the areas of highest temperature.

One pressure data point was eliminated from this diagram. The data point corresponds to sample Z4B in the Roob field area; it was calculated to have a pressure estimate of 8.3 kb. This seems unreasonably high for the other pressure estimates in the area.

#### **Summary and Discussion of Metamorphism**

The information obtained during this study confirmed the isograd boundaries found by the other workers in this area and did not define additional isograds. The pressure and temperature data collected during this study corresponded to the surrounding areas well. Due to inaccessibility and limited outcrop, there are still gaps remaining in the data between the eastern and western portions of the Lac Seul region.

The lowest metamorphic grade in the Lac Seul region is found in the Roob study area, and the northwestern portion of the Baumann area. In the south, the andalusite, second sillmanite, garnet-in, and garnet-corderite-in isograds are present. Andalusite-out corresponds with approximately 4-5 kb and 550-600 °C. Garnet-corderite-in and the garnet-in isograds correspond to approximately 4 kb and 600-650 °C. The second sillmanite isograd occurs at 3-4 kb and 650 °C.

The sparse amount of data in the Roob area makes these comparisons difficult.

It must be emphasized that there are several reactions that produce H<sub>2</sub>O vapor and melts. The presence of water greatly influences the temperature conditions of melting. These reactions are likely to be responsible for the vapor-present migmatization so prevalent in the region.

Baumann (1985) reported an isograd of stable sillimanite in the extreme northern Lac Seul study area occurring between 4-5 kb and 650-700 °C. This is displayed as the isograd between coarse sillimanite and fibrolite in Figure 9A. All other sillimanite reported in the area is considered metastable by Baumann and Chipera, due either to its fibrolitic habit or to its presence within the center of cordierite grains where it had been prevented from further reacting to form more stable phases. However, during this study coarse sillimanite was found in the southwestern part of Lac Seul near South Bay (sample BI12). This indicates a decrease in metamorphic grade in the southern portion of the Campion field area. The decrease in metamorphic grade is indicated by pressures of less than 3 kb and temperatures of less than 650 °C, in the South Bay area.

Coexisting garnet and cordierite were found throughout the field area of this study, which supports the placement of the garnet-in isograds of Chipera (1985) and Roob

(1987), as well as the garnet-cordierite-in isograd of Baumann (1985) and Chipera (1985). The garnet-in isograd corresponds approximately 6 kb and 600 °C and is parallel to the Lake St. Joseph Fault in the Chipera field area. The garnet-corderite-in isograd corresponds to the 650 °C isotherm in the eastern Lac Seul area as well as in western Lac Seul area. The isotherms in the west are more erratic than in the east. In the Henke area the garnet-corderite isograd in the north extends well below the 600 °C isotherm. The garnet-corderite-in isograd corresponds to the 4 kb isobar at the northern and southern edges of the Lac Seul region.

South of the garnet/cordierite-in isograds and north of the occurrence of coarse sillimanite in South Bay there are a few occurrences of orthopyroxene. Twelve samples from the western Lac Seul area contain orthopyroxene, one is from this study, two are from the Baumann study, and nine are from the Henke study, six from Highway 105 and three Wegg and Wilcox Lakes. There are a number of samples containing orthopyroxene in the eastern Lac Seul region, three from this study and several from the Chipera study. All orthopyroxene samples reported by UND workers in the Lac Seul area are shown on Figure 10. Most of the orthopyroxene-bearing samples have a more mafic composition than the biotite gneisses common to the region, and are not garnetiferous. In the Campion area, these samples



correspond to the mafic amphibolite/granulite schist rock type. There are a few samples containing both garnet and orthopyroxene and they are indicated by open circles in Figure 10. As expected, these samples correspond to the highest temperatures and pressures in the area. The orthopyroxene shows the best agreement with temperatures greater than 650 °C and in the eastern Lac Seul area the best correspondence with pressure is greater than 6 kb but occurs in areas where pressure is as low as 4 kb. In the western Lac Seul region orthopyroxene occurs at pressures between 4 and 5 kb.

Henke reported three samples containing spinel in the far western portion of the Lac Seul area. These are the only samples reported by the UND workers that contained spinel. This area recorded higher than average temperatures, but not the highest in the Lac Seul region.

## GRAVITY GEOPHYSICS AND MODELLING

### Methods

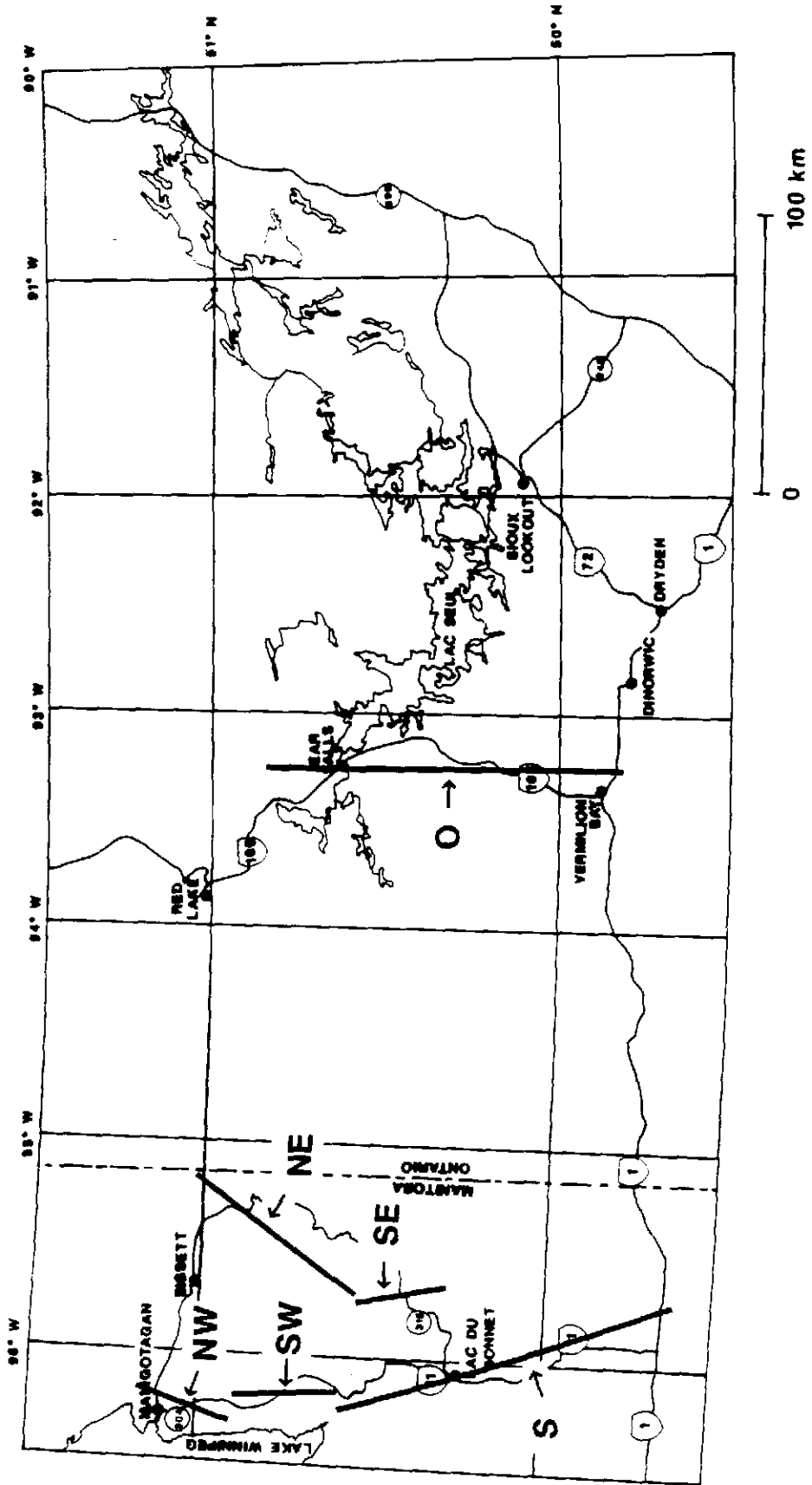
Gravity surveys are useful to understand the density of rocks underlying the survey area, and how these densities correspond to the rocks seen at the surface. If there is little correspondence between rock densities at the surface and the gravity signal, then it can be assumed that there are bodies at depth that differ from those on the surface. The ample bedrock exposure and relatively good geographic control in the ERSP, Uchi, and Wabigoon subprovinces east of Lake Winnipeg provided an excellent area to conduct a gravity survey. This information could be used to estimate the subsurface structure of the ERSP and adjacent subprovinces. Combined with the metamorphic conditions of the ERSP, the resulting gravity models could be used to decipher the tectonic development of the area. A gravity survey was conducted in southwestern Manitoba during the summer of 1986. Data were collected along Highways 11, 315, 304 and 314 in Manitoba (Fig. 14).

Along the northern limbs of the survey, gravity stations were spaced at approximately one-half mile intervals. Along the southern limb of the survey a one-mile station spacing was used because the geology is less complex. Stations were chosen and flagged prior to data collection and the distance between stations was determined using an automobile odometer. To attain an accuracy of 1

Figure 14. Location map of modelled gravity profiles in Manitoba and Ontario.

LEGEND

NW - Northwest Profile  
SW - Southwest Profile  
NE - Northeast Profile  
SE - Southeast Profile  
S - South Profile  
O - Ontario Profile



milligal for this survey, the station locations were determined to +/- 400 feet in a north-south direction, and the elevation was determined to +/- 10 feet (Telford and others, 1976). Some stations were located at reference points such as streams or road intersections to further assure accuracy.

Elevation was determined with an altimeter because the contour interval on the available topographic maps was too large. The altimeter was calibrated at established benchmarks whose location and elevation were provided by the Surveys and Mapping Branch of the Manitoba Department of Energy, Mines and Resources. The altimeter reading and the time were recorded at each station. The altimeter was recalibrated at the appropriate benchmark approximately once per hour to avoid inaccuracy due to changes in the ambient air pressure. Altimeter measurements for each station were corrected by linear interpolation, using the differences in consecutive benchmark elevation readings.

Gravity measurements were collected using a Lacoste and Romberg Model G gravity meter. Several gravity base stations were established within the survey. All gravity stations were located within two hours driving time to north or south of a base station; this distance varied due to terrain. It was necessary to return to the base station at approximately two hour intervals in order to limit the amount of change between successive base station readings

due to machine drift and earth tides. Three gravity readings and the time were recorded at each station. The intermediate value of the three measurements was used in the reduction calculations.

As with the elevation measurements, the gravity readings were corrected for machine drift and earth tides by linear interpolation of measurements between successive base station readings. Corrections were calculated by hand. All other corrections used to reduce the raw data to a Bouguer gravity anomaly were performed with a computer program, described below. All observed gravity readings were multiplied by the appropriate meter constant (supplied by Lacoste and Romberg). Latitude, free-air and Bouguer corrections were applied according to the procedure outlined in Telford et al. (1976).

The Bouguer anomaly was tied to a Bouguer gravity map of the region (Manuscript Map #48096, Gravity and Geodynamics Division, Earth, Mines and Resources, 1981). This was done by using the gravity measurement from the gravity station at the Air Government Center in Lac du Bonnet, Manitoba. After data reduction, the difference between the observed gravity measured at Lac du Bonnet station and the value shown for the same location on the Bouguer gravity map was added as a constant to all the reduced data. The reduced data and location information for each profile are tabulated in Appendix C. A portion of

the reduced data points used for the Bouguer anomaly gravity map (#48090) was obtained from the Gravity and Geodynamics Division, Earth Physics Branch of the Department of Energy, Mines and Resources, Canada and used to create a gravity profile. This profile is located in southwestern Ontario along Highway 105 between Vermilion Bay and Red Lake.

The modeling program used, Gravity, is published by the Environmental Simulations Laboratory of Southern Illinois University (Malinconico and Larson, 1985). Two of the assumptions on which this program bases its calculations are that the strike of the bodies being modeled is oriented perpendicular to the profile and that their strike-length is infinite. Neither of these assumptions is entirely valid. Strictly speaking, no geological body has an infinite strike length. However, most of the non-plutonic bodies in the region are several times longer in strike-length than in width. Thus, for those cases, these two assumptions are essentially valid. The roads where the gravity data were collected are not oriented perpendicular to the strike of the geological bodies in the region. Furthermore, there are many plutonic rock bodies in the region and the orientation of their boundaries is highly variable. To achieve a generalized model, gravity profiles and geologic contacts were projected onto straight lines oriented perpendicular to the

larger supracrustal rock bodies in the area. However, because neither underlying assumption is completely met for this study, the resulting gravity models cannot produce the most accurate picture possible. There is enough conformity to validate use of modelling to take an initial look at the area. Three-dimensional modeling would address the problems due to both of these assumptions, but adequate computer facilities were not available.

A Bouguer anomaly is based on an assumed average crustal density of 2.67 g/cc, which is true for the upper crust. However, the average density of the lower and middle crust is closer to 2.8-2.9 g/cc, and this should be taken into account to properly model regions of the lower crust. The models in this thesis focussed on surface bedrock shallow features and therefore did not account for the greater average density of the lower crust.

The Geological Map of Manitoba (Manitoba Mineral Resources Division, 1979) and the Geological Highway Map of Northern Ontario (Ontario Geological Survey, 1979) were used to determine rock types as well as the location of contacts between rock units along the surveyed roadways. The relevant rock descriptions and unit names used on these maps are provided in Tables 5A and 5B. The rock descriptions from these maps were used with tables of rock densities from Turcotte and Schubert (1982), Telford



TABLE 5A

## ROCK UNITS USED IN MANITOBA GRAVITY MODELS

Rock units present on gravity profiles in Manitoba. Taken from Geological Map of Manitoba, Map 79-2.

---

[1] Basalt, minor andesite, minor sedimentary and mafic intrusive rocks; ultramafic rocks

[2] Felsic to intermediate, mainly pyroclastic volcanic rocks; some flows, minor intrusive and sedimentary rocks.

[3] Graywacke, mudstone, conglomerate, arkose, banded iron formation.

[4] Gabbro, gabbronorite; (4a) diorite; (4b) anorthosite.

[5] Amphibolite; (5a) mafic and minor ultramafic granulite, banded iron formation, quartzite, and calc-silicate rocks.

[6] Metasedimentary gneiss.

[8] Tonalite, minor granodiorite, granite, related gneiss: tonalitic and granodioritic gneiss, migmatitic gneiss, augen-gneiss; inclusions of units (5) and (6); (8b) undifferentiated granitic rocks.

[11] Graywacke, conglomerate, arkose, arenite.

[12] Granodiorite, minor tonalite and migmatite.

[13] Granite, minor granodiorite.

ultramafic rocks - serpentized peridotite, serpentinite, pyroxenite, differentiated ultramafic/mafic intrusions.

---

TABLE 5B

## ROCK UNITS USED IN ONTARIO GRAVITY MODEL

Rock units present on gravity profile in Ontario. Taken from Geologic Highway Map, Northern Ontario, Map 2440.

---

[1] Basaltic and andesitic flows, tuffs, and breccias. (Corresponds to rock types [1] and [5] from Manitoba)

[2] Rhyolitic, dacitic, and andesitic flows, tuffs, and breccias. (Corresponds to rock type [2] from Manitoba)

[3] Conglomerate, sandstone, mudstone, marble, chert, iron formation and related migmatites. (Corresponds to rock types [3], [6] and [11] from Manitoba)

[4] Diorite, gabbro, norite, pyroxenite, peridotite, dunite, serpentite. (Corresponds to rock type [4] from Manitoba)

[5m] Granitic, metasedimentary, and minor metavolcanic migmatite. (Corresponds to rock type [8] from Manitoba)

[5] Granitic rocks, syenite, pegmatite, unsubdivided migmatite. (Corresponds to rock types [12] and [13] from Manitoba)

---

(1976), and Gibb (1967). The bodies and density contrasts are included in the figure captions.

### **Results**

The location of the gravity surveys in Manitoba and Ontario are presented in Figure 14. This diagram displays the projected profiles, as oriented generally perpendicular to the strike of the contacts between rock units along the profile. The Bouguer gravity values for each profile in Manitoba are graphically displayed on Figure 15, using the same scale for each profile. The Bouguer gravity values for the Ontario profile are shown in Figure 16.

#### **Northwest Profile--Manitoba**

The northwest profile extends from Wanipigow southward to the the east-west trending fault in the northern metasedimentary terrane of the ERSP (Fig. 14). The Bouguer gravity values vary along the profile from a maximum of -12.5 mgals to a minimum of -29.06 mgals (Fig. 15). The profile has been projected at  $19^{\circ}$ , it is 29.68 kilometers long, and includes 44 stations. This is the shortest of the five profiles from the Manitoba gravity survey.

This profile is positioned over the bulk of the of the northern metasedimentary domain of the ERSP with its northern end just crossing into the Uchi Greenstone Belt. The northwest profile, as well as the southwest profile, is located just east of Lake Winnipeg, which is the western

Figure 15. Bouguer gravity profiles of data collected during this study from Highways 11, 304, 314 and 315, Manitoba. The Bouguer gravity data for each profile is plotted using the same vertical and horizontal scales.

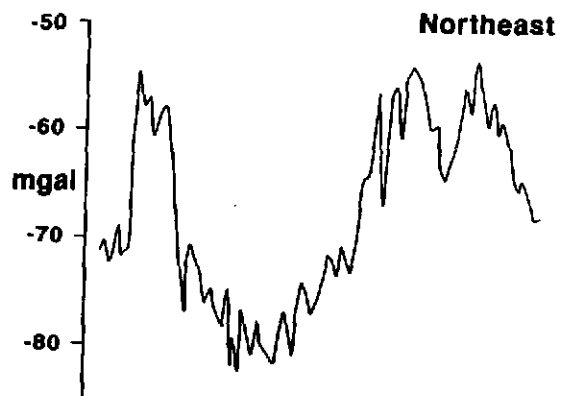
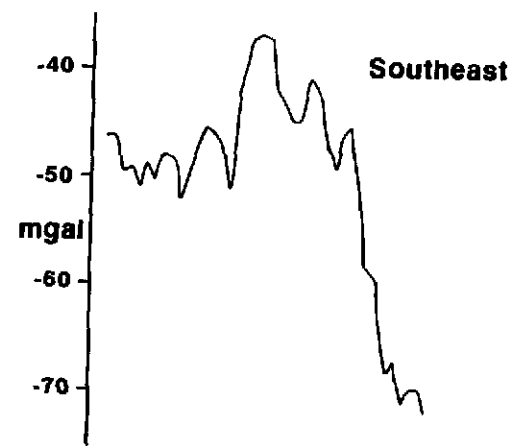
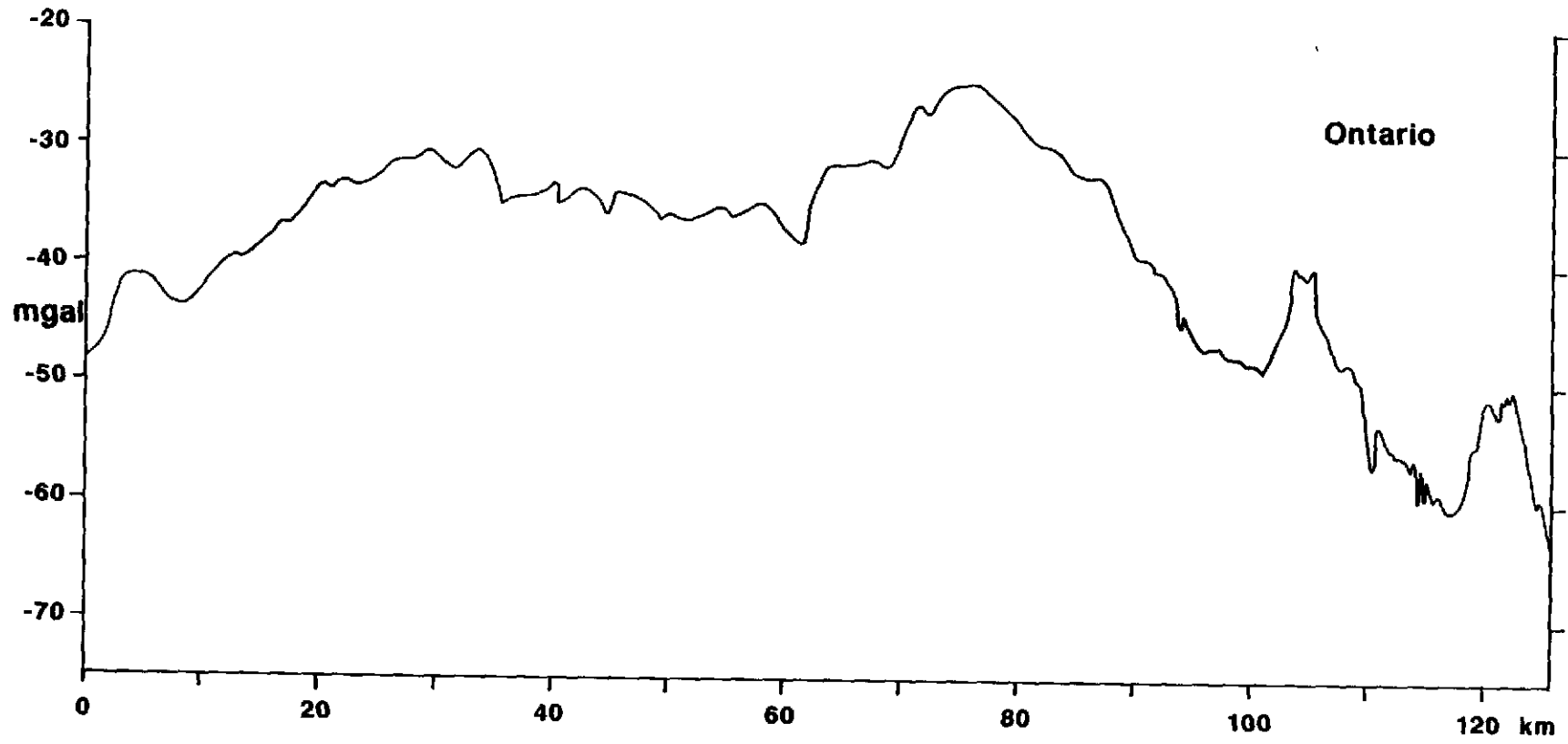


Figure 16. Bouguer gravity profile of data collected on Highway 105, Ontario (Gravity and Geodynamic Division; Energy Mines and Resources Canada, Manuscript Map No. 48090).



limit of the Superior Province of the Canadian Shield. The geology of the northern domain of the ERSP, at this location, consists primarily of metasedimentary gneisses interlayered with tonalites, tonalitic gneisses, and migmatites. Basalts and conformable graywackes intruded by gabbros, together with serpentized ultramafics and migmatites comprise this portion of the southern Uchi Greenstone Belt.

There are ten different bodies in this model (Fig. 17). Nine bodies correspond to the surficial geology: three of these bodies represent interlayered metasedimentary gneisses and tonalites with a density contrast of +0.09 g/cc, three smaller bodies represent tonalitic and granodioritic gneisses with a density contrast of +0.02 g/cc, one small body of tonalite with a density contrast of +0.03 g/cc, one body representing a rather large package of metasedimentary gneisses with a density contrast of +0.09 g/cc, and one body of gabbro with a density contrast of +0.33 g/cc. Although there are serpentized ultramafics near this area, these bodies are small and localized enough that it was not considered necessary to include them in the model; these rocks have been included in the polygon representing the denser mafic rocks. One large subsurface body with a density contrast of -0.09 g/cc is shown in this model; this is thought to



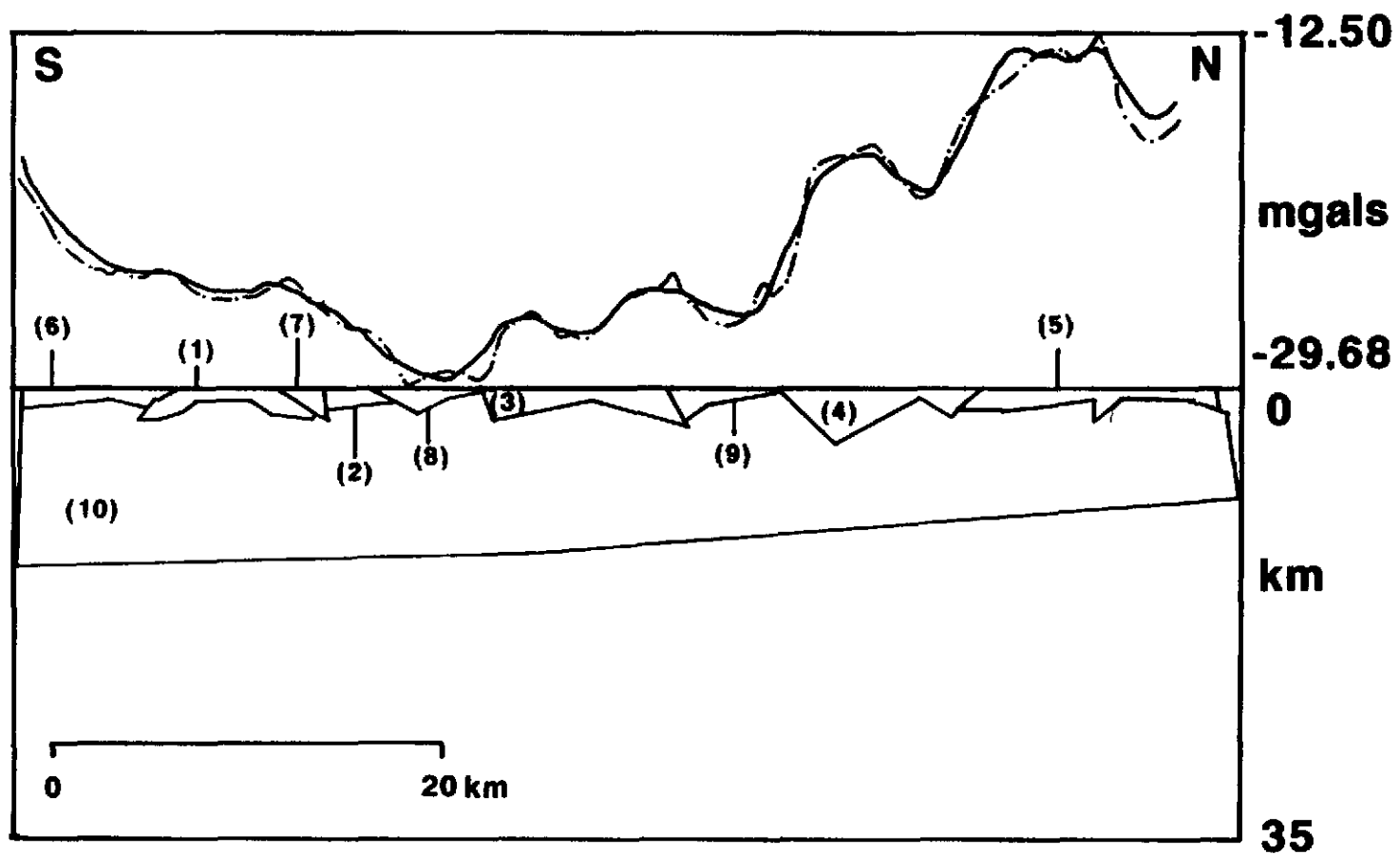
Figure 17. Observed and calculated profiles with modelled polygons--Northwest profile, Manitoba.

LEGEND

(see Table 5A for rock type)

| Polygon # | Rock Type  | Density Contrast |
|-----------|------------|------------------|
| (1)       | [6,8]      | +0.09            |
| (2)       | [6,8]      | +0.09            |
| (3)       | [6,8]      | +0.09            |
| (4)       | [6]        | +0.09            |
| (5)       | [4]        | +0.33            |
| (6)       | [8a]       | +0.02            |
| (7)       | [8a]       | +0.02            |
| (8)       | [8a]       | +0.02            |
| (9)       | [8]        | +0.03            |
| (10)      | subsurface | -0.09            |

# Northwest Profile



correspond to the abundant granitoids (rock type 13) throughout this part of the Superior Province.

#### **Southwest Profile--Manitoba**

The northernmost portion of the southwest profile is located just south of the fault which defines the southernmost end of the northwest profile (Fig. 14) and extends southward to Powerview, Manitoba. The southwest profile is 35.99 kilometers long. It has been projected with an orientation of  $355^{\circ}$ , includes 49 stations, and has gravity measurements range from a maximum of -9.81 mgals (the highest maximum of all five profiles in the Manitoba survey) to a minimum of -24.19 mgals (Fig. 15).

The northern portion of the southwest profile is underlain by the metasedimentary domain of the ERSP and is characterized by an assemblage of metasedimentary gneisses, tonalitic and granodioritic gneisses, and felsic igneous rocks. A variety of granitoid bodies underly the southern portion of this profile. A large granitic body is modelled under the entire profile. This body would correspond to the granites (rock type 13) found elsewhere in the area.

The signal produced in this profile has the lowest amplitude of all five profiles. On a large scale, this profile begins and ends in the intermediate values of its range. There is a gravity high in the north which corresponds to the metasedimentary rocks of the ERSP. South of this area is an irregular gravity low produced by the

presence of felsic to intermediate plutonic rocks and gneisses.

Ten bodies were used to model this profile (Fig. 18). These consist of: one large metasedimentary body with a density contrast of +0.14 g/cc, two bodies consisting of a mixture of metasedimentary rocks and tonalites and other felsic plutonics with a density contrast of +0.09 g/cc, three bodies which represent tonalitic and granodioritic gneisses with density contrasts of +0.04 g/cc, two small bodies with a density contrast of +0.03 g/cc corresponding to a granodioritic composition, one body of tonalite with a density contrast of +0.07 g/cc, and finally a large body with a density contrast of -0.09 g/cc underlying all of the bodies in the model (rock type 13). These density contrasts are slightly greater than the density contrasts chosen for the same rock types in the other models. In the other models the density contrasts are as follows; metasediments = +0.09 g/cc, granodiorites = +0.01 g/cc, tonalites = +0.03 g/cc, tonalitic gneisses = +0.02 g/cc.

#### **South Profile--Manitoba**

The south profile extends from Powerview in the north to just south of the Trans-Canada Highway in the south (Fig. 14). It is 98.2 kilometers long, has been projected with an orientation of  $339^{\circ}$ , and consists of 75 stations. This profile is the longest profile and has the smoothest signal (Fig. 15). The smoothness of the signal may be due

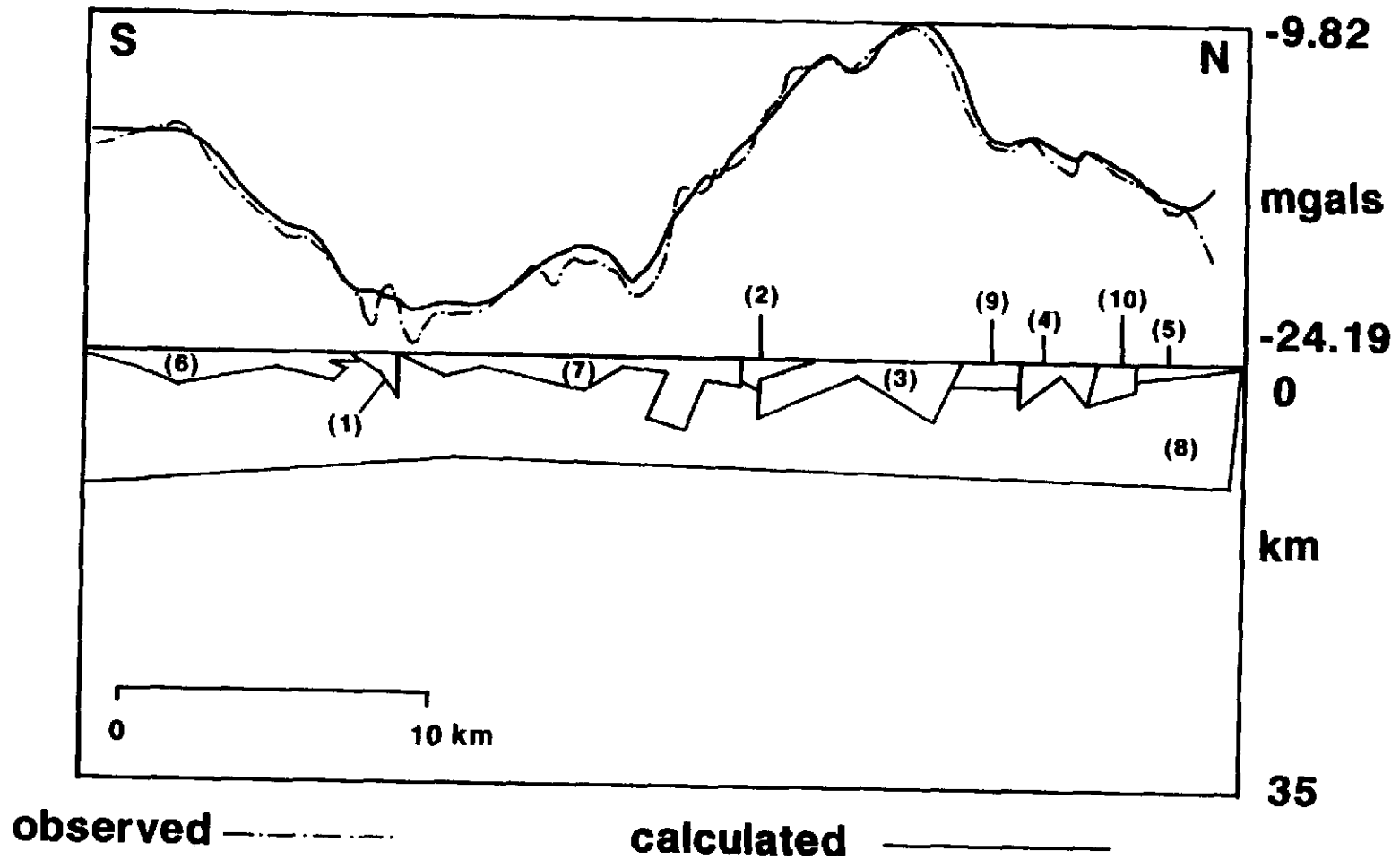
Figure 18. Observed and calculated profiles with modelled polygons--Southwest profile, Manitoba.

LEGEND

(see Table 5A for rock type)

| Polygon # | Rock Type  | Density Contrast |
|-----------|------------|------------------|
| (1)       | [12]       | +0.03            |
| (2)       | [12]       | +0.03            |
| (3)       | [6]        | +0.14            |
| (4)       | [6,8]      | +0.09            |
| (5)       | [6,8]      | +0.09            |
| (6)       | [8]        | +0.07            |
| (7)       | [8a]       | +0.04            |
| (8)       | subsurface | -0.09            |
| (9)       | [8a]       | +0.04            |
| (10)      | [8a]       | -0.04            |

# Southwest Profile



to the uninterrupted granitoid intrusions in the area. However, the smoothness of the signal may be due to the thin layer of glacial overburden dampening the affect of small bodies at the bedrock surface, or the largest station spacing of all the profiles. This profile exhibits the greatest relief in observed gravity, with a maximum reading is -14.19 mgals and the minimum of -65.44 mgals. Felsic to intermediate plutonic rocks comprise the majority of the local geological bodies. This profile traverses the southern plutonic domain of the ERSP and the northern limit of the Wabigoon Subprovince; in this area the Wabigoon consists primarily of felsic to intermediate plutonic rocks. With the exception of a single small mafic body, these subprovinces are geophysically indistinct in this area.

Fourteen bodies were used to model this profile; all except two represent felsic to intermediate intrusive bodies (Fig. 19). The first exception is the small mafic body mentioned above with a density contrast of +0.1 g/cc. This density is lower than should be expected for mafic rocks and was chosen because the body is small and is oriented close to parallel to the traverse. The second exception is a thin body covering the southern half of the entire model which represents the veneer of glacial drift in this area and has been given a density contrast of -0.8 g/cc. The remaining twelve bodies are as follows: one

Figure 19. Observed and calculated profiles with modelled polygons--South profile, Manitoba.

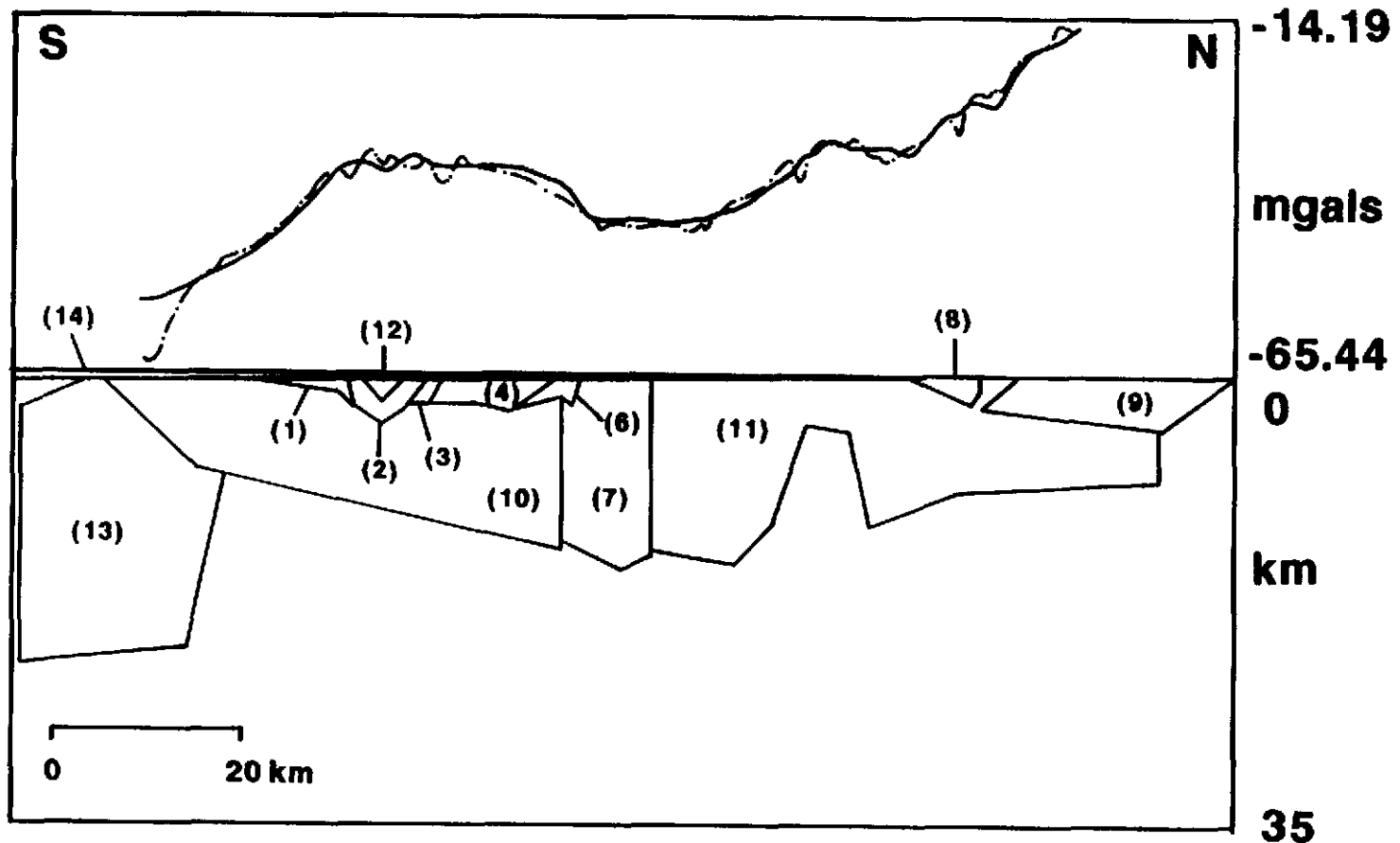
LEGEND

(see Table 5A for rock type)

| Polygon # | Rock Type    | Density Contrast |
|-----------|--------------|------------------|
| (1)       | [5]          | +0.10            |
| (2)       | [8]          | +0.03            |
| (3)       | [12]         | +0.01            |
| (4)       | [8]          | +0.03            |
| (6)       | [12]         | +0.01            |
| (7)       | [8b]         | -0.08            |
| (8)       | [8]          | +0.03            |
| (9)       | [8]          | +0.03            |
| (10)      | [13]         | -0.09            |
| (11)      | [13]         | -0.09            |
| (12)      | [13]         | -0.09            |
| (13)      | subsurface   | -0.11            |
| (14)      | glacial seds | -0.80            |



# South Profile



observed - - - - -

calculated ———

body of undifferentiated granitic rocks with a density contrast of  $-0.08$  g/cc, four bodies of tonalite with minor granodiorite having density contrasts of  $+0.03$  g/cc, two bodies of granodiorite with minor tonalite having density contrasts of  $+0.01$  g/cc, and three bodies of granite with minor granodiorite and density contrasts of  $-0.09$  g/cc.

#### **Northeast Profile--Manitoba**

The northeast profile exhibits the most irregular observed gravity anomaly of all of the Manitoba profiles (Fig. 14). It has a length of 40.63 km, is oriented at  $36^{\circ}$  and contains 83 stations. Overall, this profile has the lowest observed gravity measurements, ranging in magnitude from  $-82.56$  mgals to  $-54$  mgals.

The northeast profile traverses some of the most complicated geology in the area. At its northern end is the Uchi Greenstone Belt, which in this area consists of a typical greenstone package of interbedded basalt flows, felsic to intermediate extrusives (primarily pyroclastics), and weakly metamorphosed immature sediments which have been intruded by gabbro/gabbronorites. The rocks of the Uchi Greenstone Belt are separated from the northern domain of the ERSP by a fault which trends northwest in this area. The southern half of the profile traverses over an assemblage of metasedimentary gneisses and tonalites which represent the northern metasedimentary domain of the ERSP, and then passes into an area of granites and minor

granodiorites. The southern end terminates in the middle of a large body of tonalite.

Two distinct gravity highs of approximately equal magnitude and wavelength occur in the north, and a large, wide gravity low extends through the middle and southern portion of the profile. At the far southern end of the profile there is a sharp gravity high of the same magnitude as the two highs at the northern end of the profile.

The large amount of high frequency signal in this profile, due to the complicated near surface geology, poses significant problems to the modeller. The complex near surface geology, which must be accounted for, imposes such a large number of variables that the modelled features at depth may be questionable. However, for the sake of consistency with other models in this study, both near-surface and deeper bodies have been included in this model.

There are twenty-one bodies used to model this profile (Fig. 20). Nineteen of the bodies are exposed at the surface. In the northern portion of the model there are three basaltic bodies with density contrasts of +0.3 g/cc, as well as three gabbroic bodies with density contrasts of +0.33 g/cc. Also in the north, there are two bodies which represent felsic to intermediate intrusives with differing density contrasts of +0.03 g/cc and -0.03 g/cc. The middle portion of this model (ERSP) contains three bodies of metasediments with density contrasts of +0.12 g/cc, four

# Northeast Profile

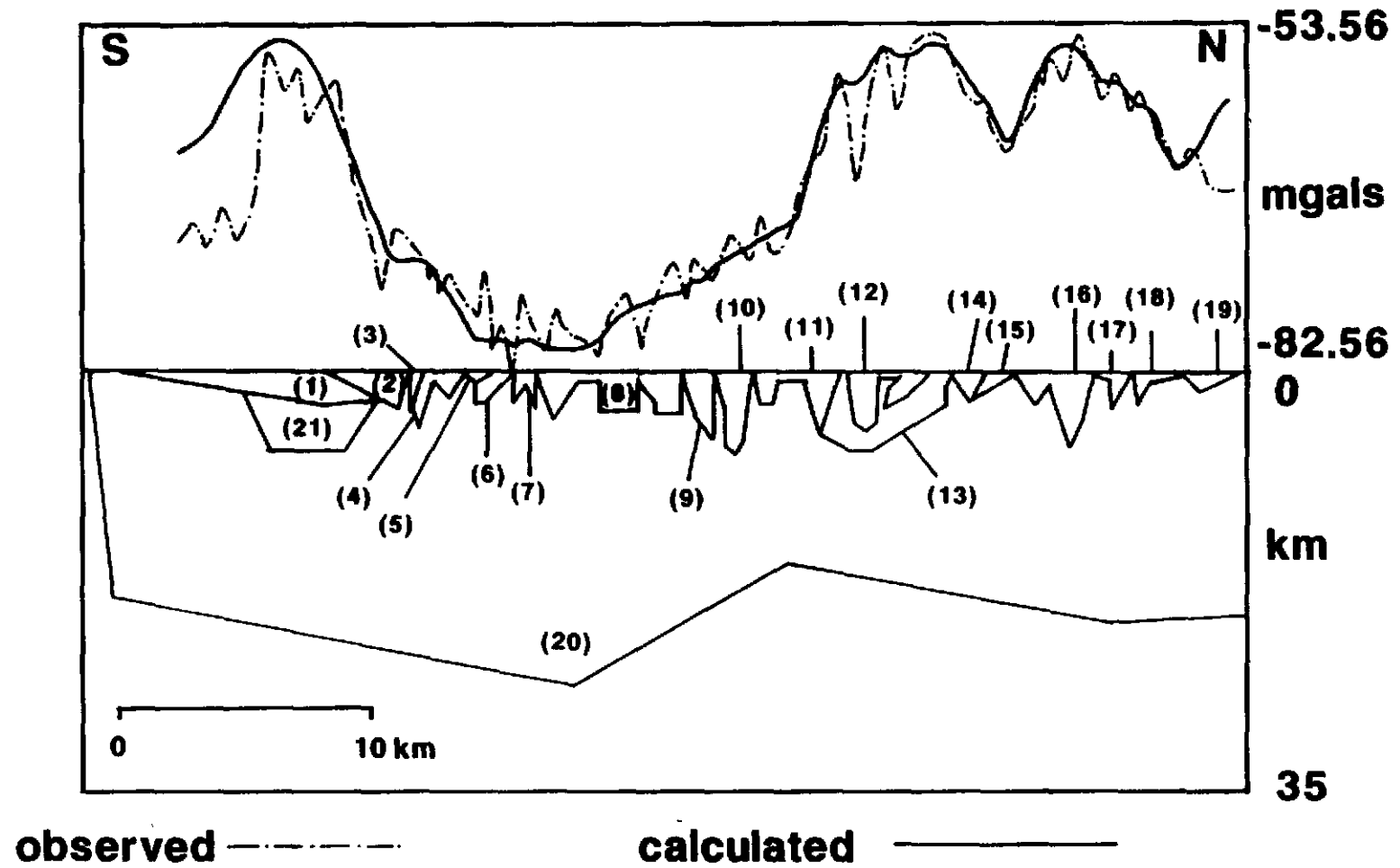


Figure 20. Observed and calculated profiles with modelled polygons--Northeast profile, Manitoba.

LEGEND

(see Table 5A for rock type)

| Polygon # | Rock Type  | Density Contrast |
|-----------|------------|------------------|
| (1)       | [8]        | +0.03            |
| (2)       | [13]       | -0.09            |
| (3)       | [8a]       | +0.02            |
| (4)       | [6,8]      | +0.09            |
| (5)       | [8a]       | +0.02            |
| (6)       | [6,8]      | +0.09            |
| (7)       | [3]        | +0.12            |
| (8)       | [6,8]      | +0.09            |
| (9)       | [3]        | +0.12            |
| (10)      | [6,8]      | +0.09            |
| (11)      | [3]        | +0.12            |
| (12)      | [2]        | +0.03            |
| (13)      | [4]        | +0.33            |
| (14)      | [1]        | +0.30            |
| (15)      | [4]        | +0.33            |
| (16)      | [1]        | +0.30            |
| (17)      | [4]        | +0.33            |
| (18)      | [1]        | +0.30            |
| (19)      | [2]        | -0.03            |
| (20)      | subsurface | -0.17            |
| (21)      | subsurface | +0.33            |

bodies which represent a mixture of metasediments and tonalite and granodiorites with a density contrast of +0.09 g/cc, and two bodies with a density contrast of +0.02 g/cc representing tonalitic and granodioritic gneisses and migmatites. There are two bodies at the surface at the extreme southern end of this profile the northernmost of these two bodies has a density contrast of -0.09 g/cc and consists of granite, whereas the southernmost surface body represents tonalite and has a density contrast of +0.03 g/cc. Because there is no surface feature which would account for the steep gravity high at the southern end of this profile, a subsurface body was added to this model with a density contrast of +0.33 g/cc and represents a gabbroic body. Finally, as with most of the other models, there is a large subsurface body with a density contrast of -0.09 g/cc (corresponding to rock type 13) considered to be a thick layer of granite.

A small body of basalt outcrops near the southern end of this profile. This unit was not included in the model because of its limited lateral extent and its position on only one side of the gravity survey.

#### **Southeast Profile--Manitoba**

The southeast profile has a length of 29.98 km with an orientation of  $347^{\circ}$  and forty-two stations (Fig. 14 and 15). The range in values of observed gravity is from a maximum of -37 to a minimum of -71.75 mgals. At its

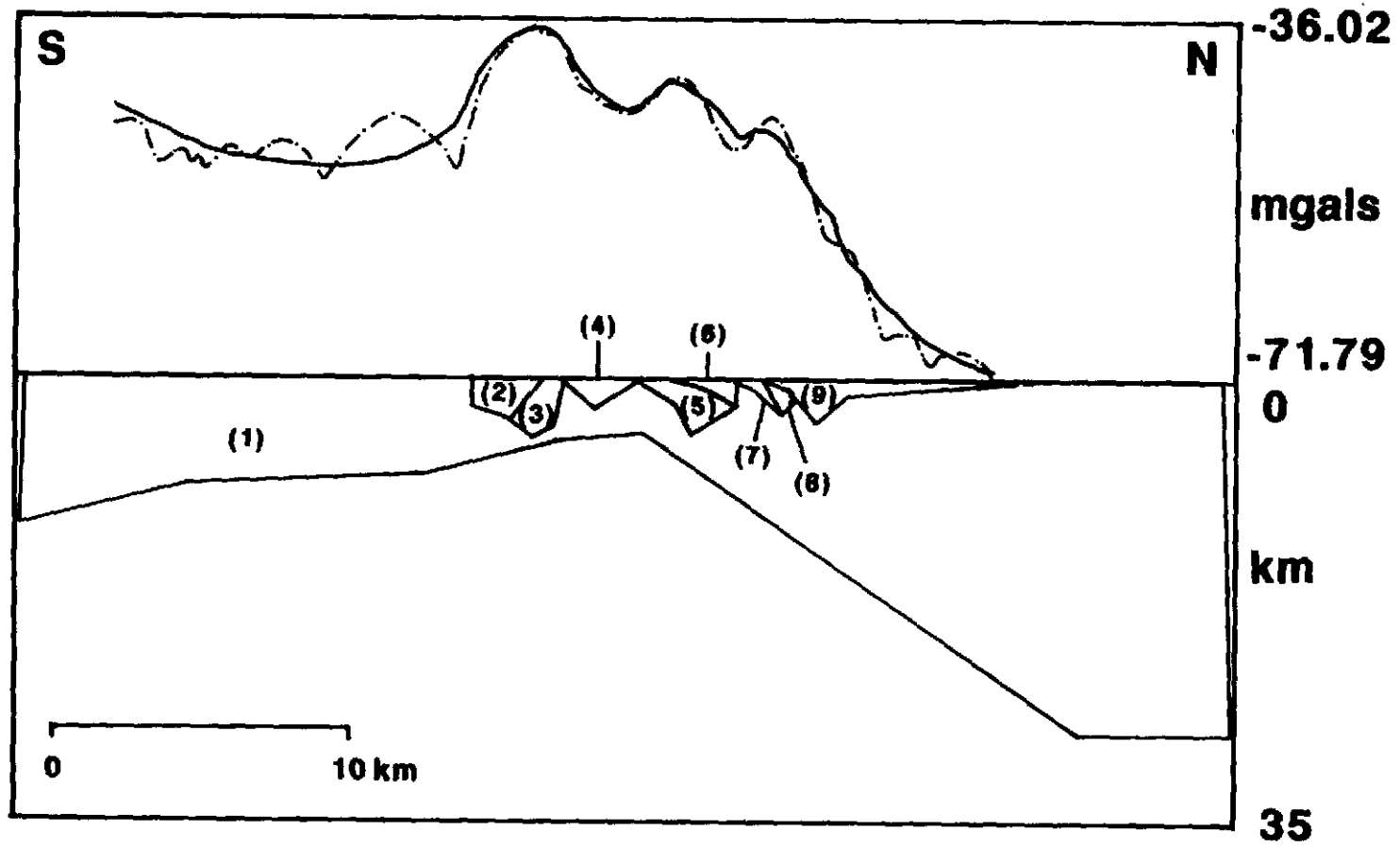
Figure 21. Observed and calculated profiles with modelled polygons--Southeast profile, Manitoba.

LEGEND

(see Table 5A for rock type)

| Polygon # | Rock Type   | Density Contrast |
|-----------|-------------|------------------|
| (1)       | [13]        | -0.16            |
| (2)       | [2]         | +0.02            |
| (3)       | [11]        | +0.15            |
| (4)       | [2]         | -0.02            |
| (5)       | [11]        | +0.15            |
| (6)       | [2]         | +0.03            |
| (7)       | [3]         | +0.12            |
| (8)       | ultramafics | +0.43            |
| (9)       | [8]         | +0.03            |

# Southeast Profile



observed - - - - -

calculated - - - - -



ultramafics rock representing an ultramafic sill with a density contrast of +0.43 g/cc. Just north of the Bird River Greenstone Belt there is a body of tonalite included that has a density contrast of +0.03 g/cc.

### **Ontario Profile**

The rock units on the Northern Ontario Geologic Highway Map (Ontario Geological Survey, 1979) have been grouped differently than those described in Manitoba. There are fewer rock types in Ontario and both the intrusive and extrusive igneous rocks are grouped on the Geologic Highway Map such that the density contrasts are different than those used in the Manitoba models. Tables 5A and 5B show how the rock types in the Manitoba and the Ontario profiles correspond to one another.

The Ontario profile is located approximately three degrees longitude to the east of the Manitoba profiles (Fig. 15). As mentioned previously, the Ontario data were collected along Highway 105, by other workers prior to this study. The profile is 126.35 km long, is oriented parallel to longitude, and contains 161 stations (Fig. 16). The observed gravity measurements vary from -24.43 to -63.82 mgals and are intermediate to the range exhibited by the Manitoba profiles.

The distinction between the southern domain of the ERSP and the Wabigoon Subprovince is more obvious in this part of Ontario than in the area containing the Manitoba

profiles. The southern limit of the Ontario profile just enters the Wabigoon Subprovince at the town of Vermilion Bay, whereas the northern end of this profile crosses into more of the Uchi Greenstone Belt than do the Manitoba profiles. The middle portion of this profile crosses both the northern and southern domains of the ERSP, which are uninterrupted by the Bird River or Separation Lake Greenstone Belts. There are only three geologic units defined in the middle portion of this profile: 1) granitic rocks, syenites, and pegmatites; 2) granites and metasediments with minor metavolcanic migmatites; 3) sandstones, mudstones, conglomerates, and related migmatites.

Eighteen bodies were used to model this profile (Fig. 22). There are several large bodies which represent the granitic rocks that outcrop at the surface in small patches, these are modelled as larger bodies at depth, similar to most of the Manitoba profiles. These granitic bodies have a density contrast of  $-0.08$  g/cc. Five bodies with a density contrast of  $+0.03$  g/cc represent granites with metasedimentary and minor metavolcanic migmatites. Two bodies of metasediments are modelled with a density contrast of  $+0.12$  g/cc. Three bodies of basaltic and andesitic flows with a density contrast of  $+0.13$  g/cc are modelled; one body lies within the Wabigoon Subprovince and two are located in the Uchi Subprovince. There is one body

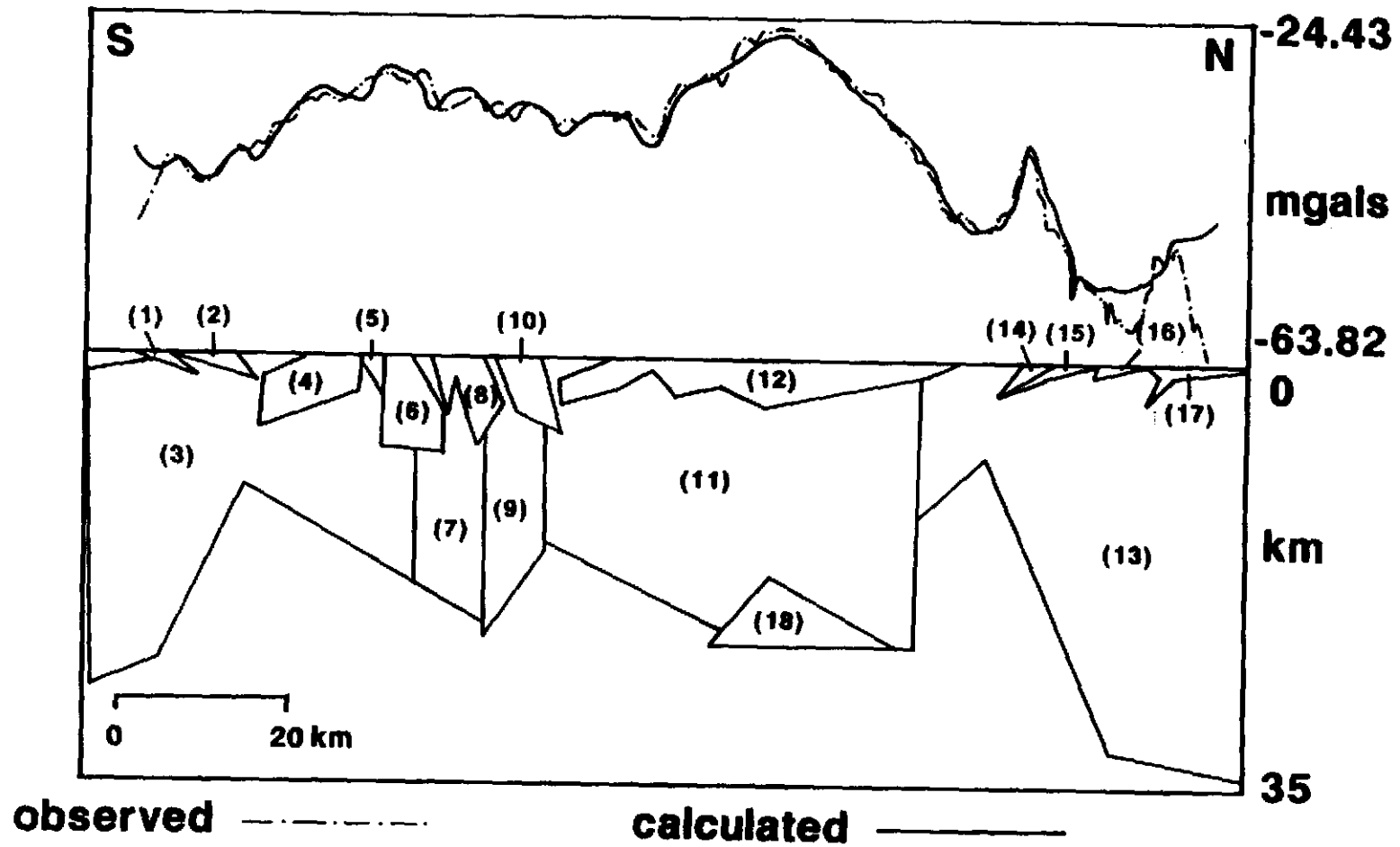
Figure 22. Observed and calculated profiles with modelled polygons--Ontario.

LEGEND

(see Table 5B for rock type)

| Polygon # | Rock Type  | Density Contrast |
|-----------|------------|------------------|
| (1)       | [1]        | +0.13            |
| (2)       | [5m]       | +0.03            |
| (3)       | [5]        | -0.08            |
| (4)       | [5m]       | +0.03            |
| (5)       | [3]        | +0.12            |
| (6)       | [5m]       | +0.03            |
| (7)       | [5]        | -0.08            |
| (8)       | [5m]       | +0.03            |
| (9)       | [5]        | -0.08            |
| (10)      | [5m]       | +0.03            |
| (11)      | [5]        | -0.08            |
| (12)      | [3]        | +0.12            |
| (13)      | [5]        | -0.08            |
| (14)      | [4]        | +0.25            |
| (15)      | [1]        | +0.13            |
| (16)      | [2]        | -0.03            |
| (17)      | [1]        | +0.13            |
| (18)      | subsurface | +0.33            |

# Ontario Profile



of rhyolitic, dacitic, and andesitic flows modelled in the Uchi Subprovince with a density contrast of  $-0.03$  g/cc. Finally there is one body with no surface expression. This polygon has a density contrast of  $+0.33$  g/cc, and may represent a portion of crust that could be raised mantle.

#### **Summary and Discussion of Gravity Models**

All of the profiles modelled for this study show evidence of significant granitoid bodies underlying their entire length. The density contrasts of these granitoid bodies ranges from  $-0.16$  g/cc to  $+0.07$  g/cc. Typically these density contrasts are  $-0.09$  g/cc for the granite lithology and  $+0.03$  g/cc for the tonalite lithology. The lower surface of these bodies is typically irregular and ranges from 35 km depth at the deepest point to less than 6 km for the shallowest granitoid body. The supracrustal rocks are subdivided differently in Ontario versus Manitoba, but the density contrasts are relatively consistent within each profile. The supracrustals are modelled as relatively shallow features.

The northeast profile covers the area with the most complicated geology. At the southern end of this profile are two granitoid bodies. The northern metasedimentary domain of the ERSP is in the middle of the profile and is succeeded northward by the mafic and felsic volcanics and the mafic plutonics of the Uchi Subprovince. The high variability and the low gravity values near the

metasedimentary rocks of the ERSP may be due to crustal thinning in this area.

The south profile crosses the least complicated geology of all the profiles modelled. The entire area is characterized by a number of granitoid intrusions, with the exception of one small amphibolite body. However, this profile traverses the only area covered by glacial overburden, modelled as a very thin veneer with a density contrast of  $-0.8$  g/cc. It could be debated whether the gravity low in this area is due to the thin, relatively low density cover or whether it is due to thicker or lighter granitoids in the area. This provides an example of the non-uniqueness of gravity models.

Only two models employ the use of dense subsurface bodies, the northeast and Ontario profiles. In the northeast profile a body is modelled at a depth of approximately 3-7 km with a density contrast of  $+0.33$  g/cc, which represents a mafic intrusion. This may have some relationship to the granulite occurrences reported nearby (Percival, 1989), however it is not as direct a relationship as is found between the gravity highs and granulite occurrences found in the Lac Seul area. In the Ontario profile a relatively small body is modelled at a depth of approximately 23-25 km with a density contrast of  $+0.33$ .

The above mentioned dense subsurface bodies modelled in the northeast and Ontario profiles may be an indication of crustal thinning and under and/or intra-plating. Hall and Hajnal (1969) and Hall and Brisbin (1982) interpreted the seismological data collected in the ERSP to indicate that the crust is thin and that rocks of mafic composition exist in the middle or lower crust. The gravity models in this study are consistent with this seismological interpretation. The thinner crust proposed by Hall and Hajnal (1969) and Hall and Brisbin (1982) on the basis of seismological evidence, and the presence of gravity highs indicative of dense bodies at depth, support the possibility of crustal underplating in this area. Crustal underplating is a proposed process in which mafic magmas are intruded into the lower (and sometimes middle) crust directly from the mantle. This process is considered to take place under extensional conditions (Fountain, 1989).

It was not necessary to model dense bodies at depth in all profiles. Most of the profiles did not require the addition of a dense body at depth to attain a good fit, but the potential existence of dense bodies underneath these profiles is not precluded by this fact. Therefore, determining whether crustal underplating has occurred in this area will require further investigation. Uniformitarian tectonic models proposed for this region have been collisional/compressional in nature and have not

addressed the possibility of extensional episodes. If underplating is the explanation for the thinner crust and the presence of mafic bodies at depth in this area, these crustal features may be the only geologic evidence that remains to indicate past extensional events.

In addition to the problems mentioned above, those of two-dimensional modelling and non-unique solutions, some other problems exist due to the nature of this project. First, since the profiles are not infinite in length there are, of course, edge effects. Also, because of the need to project these profiles perpendicular to the major structure in the area, the gravity data was broken into five profiles and, therefore, there are more edge effects. This, however, was weighed against the benefits of perpendicularity so the edge effects are regarded as unavoidable. The modelling did not make clear the vertical orientation of known faults in the region. In addition, the abundant small supracrustal bodies of variable densities did not make any tectonic organization readily apparent. The tectonic structure was further obscured by the enormous quantity of late granitoid intrusions throughout the ERSP and adjacent subprovinces. In spite of these problems, the ample exposure of bedrock geology in this area used to constrain the models, the correspondence of data collected for this study with previously published gravity data, the good fits achieved between observed and



modelled profiles, and agreement of the depths of all modelled bodies with the crustal thicknesses estimated by Braile et al. (1989), demonstrate the validity of gravity modelling to gain an understanding of the subsurface in the ERSP and adjacent subprovinces.

To gain a better understanding of the precise nature of the contacts between surface lithologies and the boundaries of these subprovinces, it would be useful to include some further geophysical work. The aeromagnetic data available in the area could be incorporated into the gravity modelling process. This would more precisely define the contacts between bodies of different magnetic susceptibilities (Telford and others, 1976). Furthermore, the nature of the boundaries between these Archean subprovinces remains unresolved. Gibbs et al. (1984), Percival et al. (1989), and Green et al. (1990) have produced detailed seismic reflection studies across Precambrian terranes of the Canadian Shield in order to gain a better understanding of the Great Lakes tectonic zone, Kapuskasing structural zone, and Grenville orogen, respectively. Collection of more data or reevaluation of existing seismic data may provide more information on the orientation of the boundaries of these subprovinces.

## DISCUSSION

In this discussion the results of this thesis and those of the other UND theses in the Lac Seul region will be related to current tectonic models for the ERSP and other Archean terranes. Other topics to be addressed below include continental crustal cross-sections, the common association of granulites and silicic igneous processes in high-grade gneiss terranes, and pressure-temperature-time (PTt) paths. Because this study employed both geochemical and geophysical techniques and because it examines crustal processes, a discussion of the more recent work involving continental crustal cross-sections is appropriate. A second topic of current interest relevant to the tectonic processes influencing the development of the ERSP, is the significance of the close association of granulite and granites. Lastly, previous estimations of PTt paths will be discussed and the validity of their application to the ERSP examined. Examination of these subjects will yield techniques and information to help constrain and improve the tectonic model developed for the ERSP.

### **Crustal Cross-sections, Geochemical/Geophysical Studies**

Most past studies of the earth's crust have been carried out by geophysicists or geochemists/petrologists. Few interdisciplinary investigations occurred in the literature until recently. The principal tools used in

geophysical investigations of the crust are seismic refraction and reflection, magnetics, and gravity methods. Xenoliths have provided the primary source of information to be used by geochemists and petrologists for deep crustal studies. These widely differing approaches have yielded much information on the nature of the the crust. Hamilton (1989), Fountain and Christensen (1989), Simpson and Jachens (1989), and Smithson (1989) summarize a number of the methods typically applied to crustal studies. However, many gaps in the theory of crustal processes remain.

Recently, a number of large-scale surface features have been inferred to be crustal cross-sections. Many of these studies have made use of both geophysical and geochemical/petrological techniques (see Fountain and Salisbury, 1981; Percival and McGrath, 1986; Weber and Mezger, 1990). These approaches have provided new understanding about crustal structure and development. The two regions within the Superior Province that provide excellent examples of crustal cross-sections; they are the Pikwitonei granulite domain and the Kapuskasing uplift (Percival and McGrath, 1986; Weber and Mezger, 1990). These areas display a large range of metamorphic temperatures and pressures, close association with faulting, and directly observable geologic relationships. This indicates that these cross-section are relatively complete. However, according to Fountain et al. (1990),

geophysical evidence indicates that the lowermost levels of the crust have not been found exposed on the surface.

The moderate pressures determined in this study, as well as other studies of the ERSP, preclude the possibility of the ERSP including lower crustal elements. The asymmetric distribution of pressure and temperature data and extensive faulting indicate that the middle and upper crustal levels of the ERSP have been thrust onto the boundary of the Uchi Subprovince.

#### **Granulites, Granites and Migmatization**

Several authors have written about the close association between granulites and granites (Newton, 1988; Clemens, 1990; Thompson, 1990; Vielzeuf and others, 1990). The large volumes of syntectonic intrusions in and around the ERSP as well as the pervasive migmatization warrant some discussion of this association.

Wells (1979, 1980) describes Archean rocks in West Greenland and concludes that the granulite and amphibolite facies assemblages were formed during prolonged emplacement of large volumes of acid- intermediate plutons under anhydrous conditions. Conversely, Harrison et al., (1990), and Arculus and Ruff (1990), report that granulite terranes may instead be the residuals left behind following metamorphism and dehydration melting, rather than the product of igneous intrusion. Vielzeuf et al. (1990) experimentally quantify the amount of granitoid melt which

can be derived from various rock types and suggest that the differences observed in the amount of melt production in different orogens may be due to the number of thermal events that occurred within those orogens. Newton (1988) attributes this theory of differentiation of granite and granulites from an initial host rock due to metamorphism to Fyfe (1973), but points out that lack of mobility makes transport of small amounts of siliceous melts away from the host rock problematic.

The amount of water present during these melting reactions should also be taken into account when developing a tectonic model. Thompson (1983) cautions that the production of a fluid phase during dehydration reactions, together with the presence of fluid inclusions in the rocks, is not conclusive evidence that the system is water-saturated. Although he acknowledges that fluid-present metamorphism does occur, he states that this would not be the case throughout the entire process of metamorphism. Clemens (1990) and Hyndman (1981) also point out that water-rich magmas are not very mobile and are driven upward by water pressure alone. According to these authors, only fluid-absent partial melting can create shallow large-scale granitoid bodies.

Large-scale granitoids are found throughout the ERSP and the adjacent greenstone belts. This is further demonstrated in the gravity models presented in this study.

The ERSP is highly migmatized and contains sporadic occurrences of granulites. As described above, several dehydration and melting reactions have been proposed for this area. The pressure and temperature results of this study and mineral reactions that occurred confirm that vapor-present partial melting took place at mid-crustal levels in the ERSP. However, Baumann (1985) concluded that the anatectic veins in migmatites could not have been derived wholly from in situ partial melting. Because of the relative immobility of hydrous partial melts, an additional explanation is needed for the presence of large-scale granitoid bodies in the region. It is suggested that both partial melting of ERSP supracrustals and emplacement of large-scale mantle-derived granitoids occurred.

#### **Pressure-Temperature-Time Paths**

Pressure and temperature conditions of metamorphism can be estimated using mineral assemblages with known stability fields or by geothermobarometric methods. Theoretically, under equilibrium conditions, the same mineral assemblage can be created independent of the path taken through various pressure and temperature conditions. However, information about the P-T-t path would be helpful in understanding the sequence of tectonic, thermal, and barometric processes that took place in a particular region.

England and Thompson (1984) published a detailed theoretical model of the pressure and temperature response to rapid crustal thickening, thermal relaxation, and erosional thinning (a clockwise PTt path). The accompanying article by Thompson and England (1984) discusses problems encountered when hypothesizing PTt paths from petrologic data. They illustrate different possible PTt paths using data sets from a number of areas. Bohlen (1987) states that the distinction between amphibolite and granulite facies rocks is more commonly one of temperature rather than pressure, and magmatic intrusion is responsible for the higher temperatures before and during crustal thickening--thus inferring an anti-clockwise PTt path for granulite occurrences. Thompson (1990) describes different PTt paths resulting in the formation of granulites; he also considers the conditions required to expose these granulites and suggests that multiple collisions are necessary to bring them to the surface. Ellis (1987) also concludes that a second orogeny is needed to exhume granulite facies rocks. Schumacher et al. (1990) describe granulites from Sri Lanka, primarily on the basis of textural evidence, they report two possible PTt paths for the same rocks. This demonstrates the complexity involved in deriving PTt paths. Typically, authors have employed the use of prograde (and less frequently retrograde) mineral assemblages and metamorphic textures, in some cases

along with detailed age relationships, to infer PTT paths. Such evidence is not abundant in the ERSP. Chipera (1985) proposed a clockwise PTT path for the ERSP, based primarily on his proposed tectonic model. There is little evidence to support this hypothesis but less to refute it.

### **Tectonic Model for the ERSP**

Modern models for the tectonic evolution of Archean terranes began to be developed in the 1960's. Various models have been applied to the Superior Province and are summarized in Chipera (1985). A recent article by Card (1990) provides a uniformitarian generalized accretionary model of the Superior Province as well as an excellent overview of geology and age relationships of all subprovinces within the Superior Province. Card considers the areas referred to in this document as the northern and southern domains of the ERSP to be separate terranes. He treats the southern domain of the ERSP as a distinct subprovince, called the Winnipeg River Subprovince. Considering the difference in age and lithology of the southern plutonic domain of the ERSP from the northern metasedimentary domain, it is appropriate to distinguish this as a subprovince. The northern plutonic domain of the ERSP will be referred to as the Winnipeg River Subprovince (WRSP) throughout the rest of this discussion.

The metasediments in the Lac Seul region of the northern domain of the ERSP display upper amphibolite to



lower granulite facies conditions. The moderate to low pressures recorded by these rocks are indicative of mid-crustal conditions, as is the presence of pervasive migmatization. The patchy distribution of medium to high temperatures (Fig. 11) is probably due to the abundant magmatic intrusions emplaced into the ERSP, Winnipeg River Batholith, and the Uchi, Wabigoon, and Bird River greenstone belts during the Kenoran orogeny. This temperature distribution resembles what might be expected from multiple convection cells. The steeper increase in temperature near the faulted northern contact with the Uchi Subprovince, as compared to the gradual decline in temperature towards the southern boundary with the WRSP, suggests the possibility of a cross-sectional exposure of the middle and upper portions of the continental crust. The eastern part of the Lac Seul region exhibits lower crustal conditions than the western Lac Seul region (Figures 10, 11, and 12). This might be due to the presence of the Minniss River fault intersecting the Lake St. Joseph fault at the eastern edge of the Lac Seul region. The two highest pressure measurements in the area occur on either side of the Minniss River fault. Furthermore, Chipera points out that the thermal axis is deflected to a parallel orientation near the Minniss River Fault.

Percival (1989) points out that although similar processes occur in all exposures of crustal cross-sections, comparisons to the present-day lower crust should be made only to those terranes with lower crustal exposures and whose exhumation was late in their tectonic history. The only examples of terranes with lower crustal exposures in the Superior Province are the Pikwitonei and Kapuskasing terranes.

Magmatic underplating has been proposed by Clemens (1990) to be the most common cause of silicic magmatism. Mafic granulites found in the eastern Lac Seul region may be a manifestation of underplating. Clemens (1990) contends that mafic granulites are the result of basaltic magmas injected during underplating and provide a heat source for the metamorphism and partial melting of shallower rocks. Underplating is controlled by extensional conditions and the temperature of the asthenosphere (Fountain, 1989). Fountain et al. (1990) consider the function of underplating in the process of continental crustal growth to be unresolved. The overall lack of large dense bodies at the base of the crust demonstrated in the gravity models presented by this study, suggest that Turcotte's (1989) delamination model may apply to this region.

As discussed above, it is appropriate to regard the southern plutonic domain of the ERSP (Winnipeg River

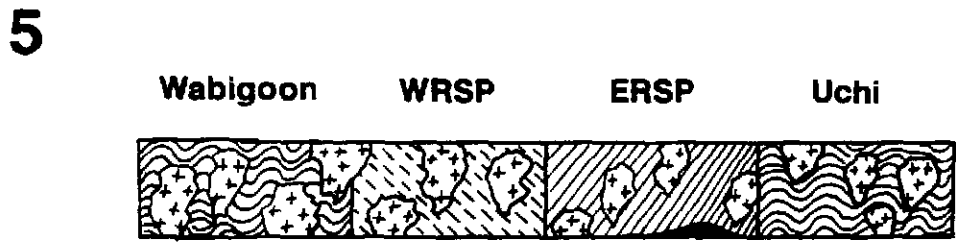
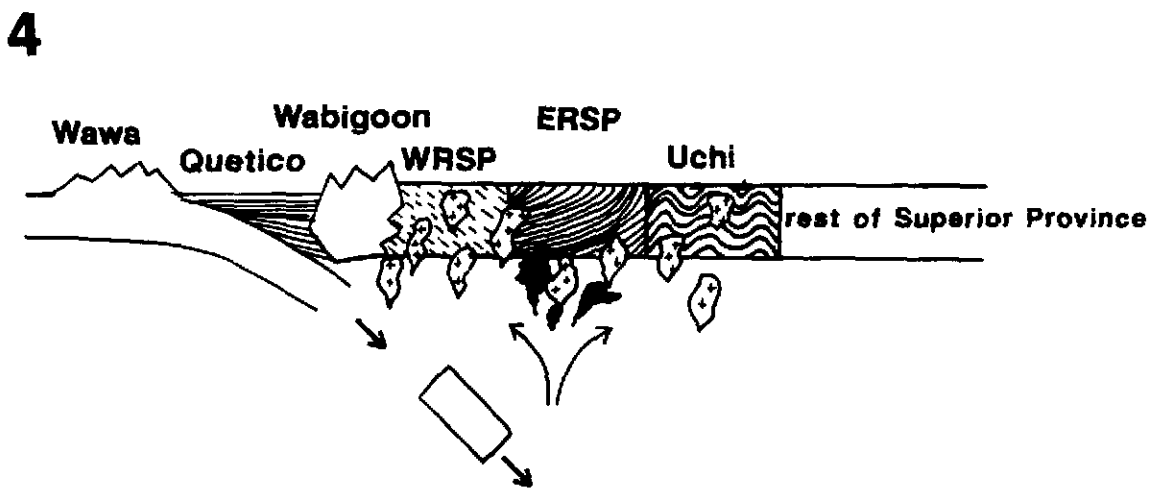
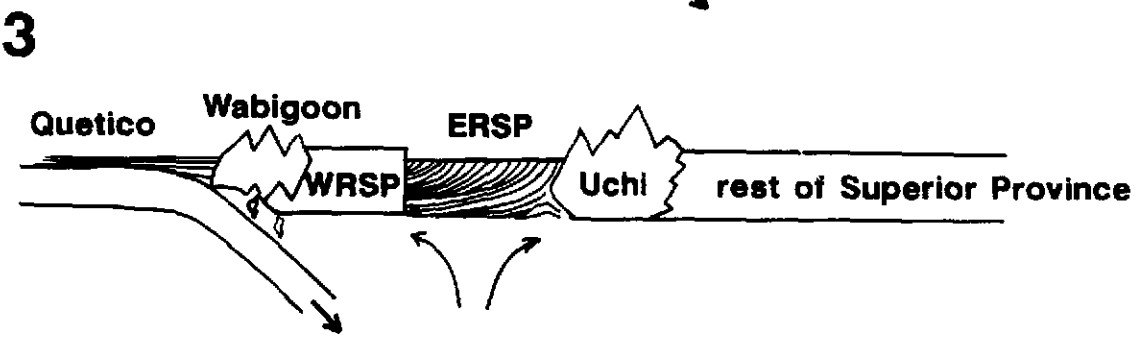
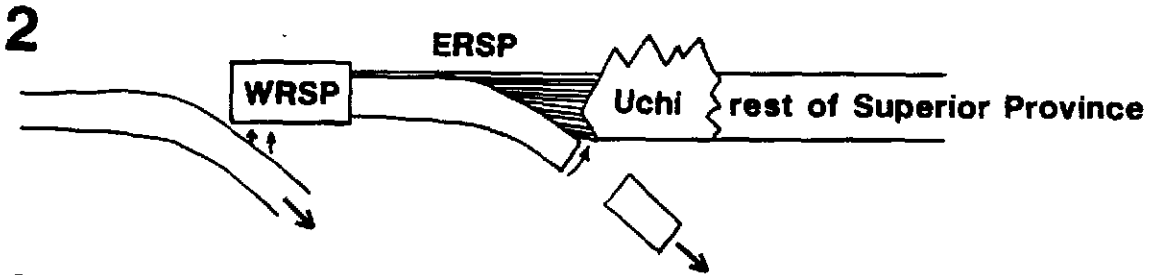
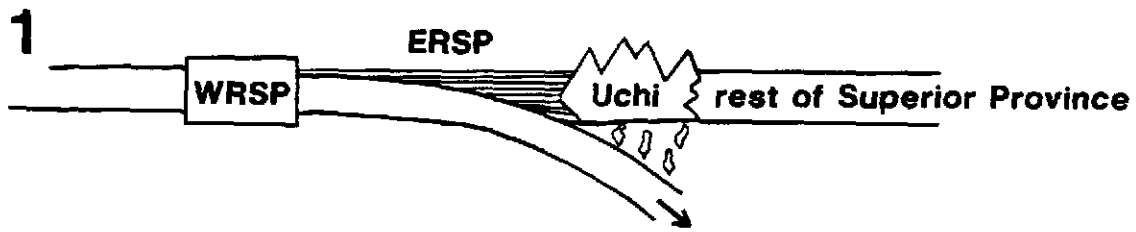
Subprovince--WRSP) as tectonically independent of the northern metasedimentary domain, because it is considerably older and compositionally distinct. The boundaries of the WRSP with the northern metasedimentary domain of the ERSP and with the Wabigoon Subprovince are obscured by later granitoid plutonism, and the characteristics of the boundary are controversial (Blackburn, 1980). It is therefore difficult to delineate the mode of accretion. Card (1990) reports sediments of crustal provenance dated at 3.0 Ga in the Wabigoon Subprovince. There are also gneisses in the Wabigoon that are this old and may be the most reasonable source of these sediments. However, the possibility exists that these sediments were derived from the WRSP. These age relationships imply that these subprovinces developed in close proximity. However, two late Archean batholiths in the Winnipeg River and Wabigoon subprovinces have been studied in detail by Beakhouse and McNutt (1991). These authors conclude that the batholiths were derived from different sources and therefore the WRSP and Wabigoon Subprovince developed independently. These late plutons could be derived by in situ partially melting of host rocks and therefore these subprovinces need not have developed separately.

A model showing the potential tectonic development of the ERSP based on the results of this study and others at UND, as well as incorporating elements from models

discussed in the literature, is presented in Figure 23. The abundance of granitoid intrusions in the Uchi, ERSP, WRSP and the Wabigoon subprovinces shown in the model is based on both the surface geology in the region and the results of gravity modelling. These intrusions have obscured the initial boundaries between these terranes and the gravity modelling was unable to decipher the orientation of these contacts. The model is similar to Card (1990) in that it is uniformitarian and accretionary. Elements of extension have been added to allow for underplating which could account for the abundance of granitoid in the region, as well as granulites.

Figure 23. Proposed tectonic evolution of ERSP and adjacent subprovinces.

1. Subduction beneath Superior Province, creation of Uchi subprovince as volcanic arc. Sedimentation into ERSP. WRSP carried into area by oceanic plate.
2. Deformation of ERSP begins. Descending plate under Uchi subprovince is broken off and subduction begins beneath WRSP.
3. Wabigoon volcanics are emplaced into WRSP and off-shore. Extensional forces begin under ERSP--similar to a back-arc basin. Underplating begins under (and possibly into) ERSP due to the plastic response of the wet sediments in the ERSP.
4. Migmatization within ERSP. Gneissoid emplacement due to anhydrous partial melting at the base of the crust. Heat source for this partial melting from underplating.
5. Quiescence, gradual delamination of most of underplated material in the lower crust.



## CONCLUSIONS AND RECOMMENDATIONS

This study contributes temperature and pressure estimations to areas not previously studied by UND workers in the ERSP. No previously unreported index minerals were found during this project and therefore no new isograds were delineated. The temperature of formation was calculated using garnet-biotite geothermometry. The temperature values obtained in this study range from 577 to 751 °C. The metamorphic pressures were estimated using the plagioclase-garnet-sillimanite-quartz geobarometers. The resulting pressure values ranged from 2.7 to 5.7 kb. Garnet is abundant throughout the field area of this study and coexisting garnet and cordierite are widespread in most of the area. This added data to the garnet-in and garnet/cordierite-in isograds reported by Baumann (1985), Chipera (1985). Sillimanite was found in two samples collected during this study--one coarsely crystalline, one fibrolitic. Orthopyroxene was found in three samples. One garnetiferous granulite was found near the granulites in the Baumann area. Two other non-garnetiferous granulites were found in the eastern Lac Seul area where the Chipera and Campion areas overlap.

The results of Henke (1984), Baumann (1985), Chipera (1985) and Roob (1987) were combined with those of this project to produce maps displaying the distribution of isograds, orthopyroxene occurrences, temperature, and

pressure throughout the Lac Seul region of the ERSP.

Several isograds were defined in the Lac Seul region by UND workers. The lowest metamorphic grade is indicated in the Roob study area by the presence of the andalusite-out isograd, corresponding to 4-5 kb and 550-600 °C. An isograd delineating coarse sillimanite versus fibrolite was defined in the Baumann study area, occurring between 4-5 kb and 650-700 °C. Well developed crystals of sillimanite were also encountered during this study in the southwestern part of Lac Seul. This sillimanite occurrence corresponds to conditions of less than 600 °C and less than 3 kb. The garnet/cordierite-in isograd corresponds to the 650 °C isotherm in the eastern and western Lac Seul samples. Orthopyroxene was identified in a number of samples. The majority of orthopyroxene-bearing samples are the mafic amphibolite/granulite schist rock type and are more mafic relative to the biotite gneisses that dominate the area. These rocks typically do not contain garnet. The orthopyroxene-bearing samples obtained the highest temperature and pressures in the area, with >650 °C and 6 kb in the eastern area, and pressure of 4-5 kb in the western area.

The isotherms occur in the shape of basins and domes, and are not linear contours parallel to the subprovince boundaries, as was previously suggested. The temperature values for the western Lac Seul area are in the upper 600's



°C to lower 700's °C. The temperature values in the east are in lower 700's °C in the Chipera study and upper 600's °C in this study. The temperature falls off abruptly to the north and more gradually to the south.

Pressures in the western and eastern Lac Seul areas ranged from 2.7 to 5.6 kb and 3.1 to 8.3 kb, respectively. The pressure contours are less linear and less parallel to the subprovince contacts than the temperature contours. Additionally, the orientation of isobars does not readily allow interpolation between the western and eastern areas. The areas of highest pressure roughly correspond to the areas of highest temperature.

The profiles modelled for this study strongly indicate the presence of significant granitoid bodies underlying the entire length of each profile. The lower surface of the granitoid bodies is irregular, ranging from 35 to <6 km.

The most complex geology was encountered in the northeast profile, traversing the Uchi and northern ERSP, and has the most variable gravity signal. The south profile is located in an area comprised largely of granitoids and had the lowest frequency signal. It was necessary in two models, the northeast profile and Ontario profile, to incorporate a dense subsurface body.

Seismological data for the ERSP indicates the crust is thin, with mafic rocks of the lower or middle crust at shallow depths. This suggests underplating may have

occurred in the area. The gravity highs found in the northeast and Ontario profiles, which are too large to be explained by surface features, support this hypothesis.

The gravity models must be interpreted with caution due to the problems associated with edge effects and the fact the model is a non-unique solution. Insights into the tectonic development of the region, based on gravity modelling, was hampered by the presence of abundant, small supracrustal bodies and immense subsurface granitoid intrusives. The gravity study did obtain subsurface information which is consistent with the estimated regional crustal thickness.

The tectonic development of the ERSP subprovince was evaluated in reference to continental crustal cross-sections, the association of granulites and felsic intrusives, and P-T paths. The moderate pressures determined for the ERSP indicate mid-crustal conditions. Evidence for thrusting of the middle and upper crust of the ERSP onto the Uchi is provided in the asymmetric temperature and pressure data distribution and extensive faulting. Huge granitoid bodies are exposed at the surface in the ERSP and adjacent subprovinces, with granulites and migmatization occurring in the ERSP. The gravity modelling also suggests abundant subsurface granitic bodies. Vapor-present melting is indicated by the pressure and temperature results for the Lac Seul area. Given the large

amount of granitoids in the area, it appears both partial melting and intrusion of massive felsic plutons took place. Evidence to decipher the PTT path for the ERSP is insufficient.

A uniformitarian accretionary tectonic model of the ERSP was developed to include formation of the Uchi and Wabigoon subprovinces, sedimentation into the ERSP, accretion of the WRSP, extension and underplating, and emplacement of granitoid intrusions.

Additional geophysical work, consisting of aeromagnetic and detailed seismic evaluation of the area, may provide more conclusive evidence of the subsurface structure and contacts between the subprovinces. More geochemical work could be done to obtain more age dates within the ERSP, as well as isotopic work of the igneous rocks to gain an understanding of the origin of the plutons and perhaps the conditions of metamorphism. Lastly, it may be worthwhile to do some more sampling, should accessibility improve, in the areas south of the Henke study, and in the smaller lakes north of Lac Seul to obtain a more complete data base.

APPENDICES

APPENDIX A  
THIN SECTION MINERALOGY

## APPENDIX A

## THIN SECTION MINERALOGY

## MINERAL ABBREVIATIONS

|                        |                     |
|------------------------|---------------------|
| Qtz = quartz           | Plag = plagioclase  |
| Orth = alkali feldspar | Perth = perthite    |
| Biot = biotite         | Garn = garnet       |
| Cord = cordierite      | Opx = orthopyroxene |
| Cpx = clinopyroxene    | Sill = sillimanite  |
| Amph = amphibole       | Musc = muscovite    |
| Zirc = zircon          | Apat = apatite      |
| Opaq = opaques         | Chlor = chlorite    |
| Epid = epidote         |                     |

## KEY

|                     |
|---------------------|
| X = mineral present |
| 2 = secondary       |
| F = fibrolite       |

## THIN SECTION MINERALOGY

| SAMPLE | Q<br>t<br>z | P<br>l<br>a<br>g | O<br>r<br>t<br>h | B<br>i<br>o<br>t | G<br>a<br>r<br>n | C<br>o<br>r<br>d | O<br>p<br>x | C<br>p<br>x | A<br>m<br>p<br>h | Z<br>i<br>r<br>c | A<br>p<br>a<br>t | O<br>p<br>a<br>q | C<br>h<br>l<br>o<br>r | M<br>u<br>s<br>c | E<br>p<br>i<br>d | S<br>i<br>l |
|--------|-------------|------------------|------------------|------------------|------------------|------------------|-------------|-------------|------------------|------------------|------------------|------------------|-----------------------|------------------|------------------|-------------|
| BB1    | X           | X                | X                | X                | X                |                  |             |             |                  | X                |                  | X                |                       |                  |                  |             |
| BB2B   | X           | X                | X                | X                | X                |                  |             |             |                  | X                |                  | X                |                       |                  |                  |             |
| BB3    | X           | X                |                  |                  |                  |                  | X           | X           | X                |                  |                  | X                |                       |                  |                  |             |
| BB4B   | X           | X                |                  | X                |                  |                  |             |             |                  | X                |                  | X                |                       |                  |                  |             |
| BB5A   | X           | X                | X                | X                |                  |                  | X           | X           | X                |                  | X                | X                | 2                     |                  | X                |             |
| BI1B   | X           |                  | X                | X                | X                |                  |             |             |                  |                  |                  | X                |                       | 2                |                  |             |
| BI4B   | X           | X                |                  | X                | X                |                  |             |             |                  | X                |                  |                  |                       |                  | X                |             |
| BI12   | X           | X                |                  | X                | X                | X                |             |             |                  | X                | X                |                  |                       |                  |                  | X           |
| BL2A   | X           | X                | X                | X                | X                | X                |             |             |                  |                  |                  |                  |                       |                  | X                |             |
| BL2B   | X           | X                | X                | X                | X                | X                |             |             |                  |                  |                  |                  |                       |                  |                  |             |
| BL3A   | X           | X                |                  | X                | X                | X                |             |             |                  | X                |                  | X                |                       |                  |                  |             |
| BL4B   | X           | X                |                  | X                | X                | X                |             |             |                  | X                |                  |                  |                       |                  | X                |             |
| BOI1A  | X           | X                |                  | X                | X                | X                |             |             |                  |                  |                  | X                |                       |                  |                  |             |
| CH1A   | X           | X                |                  | X                | X                |                  |             |             |                  | X                | X                |                  |                       |                  |                  |             |
| CH1C   | X           | X                | X                | X                | X                |                  |             |             |                  | X                |                  |                  |                       |                  |                  |             |
| CH2A   | X           | X                | X                | X                |                  |                  |             |             |                  | X                |                  | X                |                       |                  |                  |             |
| FB1    | X           | X                |                  | X                | X                |                  |             |             |                  | X                |                  |                  |                       |                  |                  |             |
| FB2C   | X           | X                |                  | X                | X                |                  |             |             |                  | X                |                  |                  |                       |                  |                  |             |
| FB5A   | X           | X                | X                | X                | X                |                  |             |             |                  |                  |                  |                  |                       |                  |                  |             |
| FB10   | X           | X                |                  | X                | X                |                  |             |             |                  | X                |                  |                  |                       |                  |                  |             |
| GN4B   | X           | X                |                  | X                | X                |                  |             |             |                  | X                | X                | X                |                       |                  |                  |             |
| GO2C   | X           | X                |                  | X                | X                | X                |             |             |                  |                  |                  |                  |                       |                  |                  |             |
| GO3    | X           | X                |                  | X                | X                |                  | X           |             |                  |                  |                  |                  |                       |                  |                  |             |
| GO5A   | X           | X                |                  | X                | X                | X                |             |             |                  | X                |                  | X                |                       |                  |                  |             |
| LPC2A  | X           | X                |                  | X                | X                |                  |             |             |                  |                  |                  | X                |                       | 2                |                  |             |
| LPC2B  | X           | X                |                  | X                |                  |                  |             |             |                  | X                |                  | X                | 2                     | 2                | X                |             |
| LPC5B  | X           | X                |                  | X                |                  |                  |             | X           |                  | X                | X                | X                |                       |                  |                  |             |
| LPC7A  | X           | X                |                  | X                | X                |                  |             |             |                  | X                |                  | X                |                       |                  |                  |             |
| LPC9A  | X           | X                | X                | X                | X                | X                |             |             |                  |                  | X                |                  |                       |                  | X                |             |
| LPC9B  | X           | X                |                  | X                | X                |                  |             |             |                  | X                |                  | X                |                       |                  |                  |             |
| LSB1A  | X           | X                | X                | X                | X                | X                |             |             |                  |                  |                  |                  |                       |                  |                  |             |
| LSB3A  | X           | X                |                  | X                | X                |                  |             |             |                  | X                |                  |                  |                       | 2                |                  |             |
| LSB8B  | X           | X                |                  | X                | X                | X                |             |             |                  |                  |                  |                  |                       |                  |                  | F           |
| LSB13A | X           | X                |                  | X                | X                |                  |             |             |                  | X                |                  |                  |                       |                  |                  |             |
| MB1A   | X           | X                |                  | X                | X                |                  |             |             |                  | X                |                  |                  |                       |                  |                  |             |
| MB3    | X           | X                | X                | X                | X                | X                |             |             |                  | X                |                  |                  |                       |                  |                  |             |
| MB6C   | X           |                  | X                | X                | X                |                  |             |             |                  |                  |                  |                  | 2                     |                  |                  |             |
| MB12   | X           | X                |                  | X                | X                |                  |             |             |                  | X                |                  |                  |                       |                  |                  |             |
| MB16   | X           | X                |                  | X                | X                |                  |             |             |                  | X                |                  |                  |                       |                  |                  |             |
| MK1A   | X           | X                |                  | X                | X                |                  |             |             |                  | X                |                  |                  |                       | 2                |                  |             |
| MK1B   | X           | X                |                  | X                | X                | X                |             |             |                  | X                |                  |                  |                       |                  |                  |             |

## THIN SECTION MINERALOGY (CONT.)

| SAMPLE | Q<br>t<br>z | P<br>l<br>a<br>g | O<br>r<br>t<br>h | B<br>i<br>o<br>t | G<br>a<br>r<br>n | C<br>o<br>r<br>d | O<br>p<br>x | C<br>p<br>x | A<br>m<br>p<br>h | Z<br>i<br>r<br>c | A<br>p<br>a<br>t | O<br>p<br>a<br>q | C<br>h<br>l<br>o<br>r | M<br>u<br>s<br>c | E<br>p<br>i<br>d | S<br>i<br>l |
|--------|-------------|------------------|------------------|------------------|------------------|------------------|-------------|-------------|------------------|------------------|------------------|------------------|-----------------------|------------------|------------------|-------------|
| MK2A   | X           | X                |                  | X                | X                |                  |             |             |                  | X                |                  |                  |                       |                  |                  |             |
| MK4B   | X           | X                | X                | X                |                  |                  |             |             |                  | X                |                  |                  | 2                     |                  |                  |             |
| MK5A   | X           | X                |                  | X                |                  |                  |             |             | X                |                  |                  |                  |                       |                  |                  |             |
| MR1B   | X           | X                |                  | X                |                  | X                |             | X           |                  |                  |                  | X                | 2                     |                  | X                |             |
| NLS1A  | X           | X                |                  | X                |                  |                  |             |             |                  |                  | X                | X                |                       |                  |                  |             |
| NLS3A  | X           | X                | X                | X                |                  |                  |             |             | X                |                  |                  | X                |                       |                  |                  |             |
| NLS3B  | X           | X                | X                | X                |                  |                  |             |             | X                |                  |                  | X                |                       |                  | X                |             |
| NLS5B  | X           | X                |                  | X                | X                |                  |             |             |                  | X                |                  | X                |                       |                  |                  |             |
| NLS5C  | X           | X                | X                | X                | X                | X                |             |             | X                |                  |                  | X                |                       |                  |                  |             |
| NLS7A  | X           | X                |                  | X                | X                |                  |             |             | X                |                  |                  |                  |                       |                  |                  |             |
| NLS9A  | X           | X                | X                | X                |                  |                  |             |             |                  |                  |                  |                  |                       |                  |                  |             |
| NLS10B | X           | X                |                  | X                |                  |                  |             |             |                  |                  |                  | X                |                       |                  |                  |             |
| RB6A   | X           | X                |                  | X                | X                |                  |             |             |                  |                  |                  | X                |                       |                  |                  | X           |
| RB11C  | X           | X                |                  | X                | X                |                  |             |             | X                |                  |                  |                  |                       |                  |                  |             |
| RR1    | X           | X                | X                | X                | X                |                  |             |             | X                |                  |                  | X                | 2                     | 2                |                  |             |
| RR3C   | X           |                  | X                | X                | X                |                  |             |             | X                |                  |                  | X                |                       | 2                |                  |             |
| RR5B   | X           | X                | X                | X                | X                |                  |             |             |                  | X                |                  | X                |                       |                  |                  |             |
| RR6    | X           |                  | X                | X                |                  | X                |             |             |                  |                  |                  | X                | 2                     |                  | X                |             |
| SB1A   | X           | X                |                  | X                | X                |                  |             |             | X                |                  |                  | X                |                       | 2                |                  |             |
| SB3A   | X           | X                |                  | X                | X                |                  |             |             |                  |                  |                  | X                | 2                     |                  |                  |             |
| SC2B   | X           | X                |                  | X                | X                |                  |             |             | X                | X                |                  |                  |                       |                  |                  |             |
| SC3D   | X           | X                |                  | X                | X                | X                |             |             | X                |                  |                  |                  |                       |                  |                  |             |
| SC5    | X           | X                | X                | X                | X                | X                |             |             | X                |                  |                  |                  |                       |                  |                  |             |
| SE1    | X           | X                |                  | X                |                  |                  |             |             | X                |                  |                  | X                |                       |                  |                  |             |
| SE3A   | X           | X                | X                | X                |                  |                  |             |             | X                | X                |                  | X                |                       |                  |                  |             |
| SE4B   | X           | X                |                  | X                |                  |                  |             | X           |                  |                  |                  | X                |                       |                  |                  |             |
| SE7A   |             | X                |                  | X                |                  |                  | X           |             | X                |                  |                  | X                |                       |                  |                  |             |
| SE9A   | X           | X                |                  | X                | X                |                  |             |             |                  |                  |                  |                  |                       |                  |                  |             |
| SI8    | X           | X                |                  | X                | X                |                  |             |             |                  |                  |                  |                  |                       |                  |                  | X           |
| SN2    | X           | X                |                  | X                | X                | X                |             |             | X                |                  |                  |                  |                       |                  |                  |             |
| STB3B  | X           | X                |                  | X                | X                |                  |             |             | X                |                  |                  | X                |                       |                  |                  |             |
| STB4B  | X           | X                |                  | X                | X                | X                |             |             | X                |                  |                  | X                |                       | 2                | X                |             |
| STB5A  | X           | X                |                  | X                | X                |                  |             |             |                  |                  |                  | X                | 2                     |                  |                  |             |
| STB7B  | X           | X                |                  | X                | X                |                  |             |             |                  |                  |                  |                  |                       |                  |                  |             |
| STL5   |             |                  |                  | X                |                  | X                |             |             |                  |                  |                  |                  |                       |                  |                  |             |
| SX5D   | X           | X                |                  | X                | X                |                  |             |             | X                |                  |                  | X                |                       |                  |                  | X           |
| SX9    | X           | X                |                  | X                | X                |                  |             |             |                  |                  |                  |                  |                       |                  |                  |             |
| SX12   | X           | X                |                  | X                | X                |                  |             |             |                  |                  |                  | X                | 2                     |                  |                  |             |
| WLS3B  | X           | X                |                  | X                | X                |                  |             |             |                  |                  |                  |                  |                       |                  |                  |             |
| WLS5B  | X           | X                |                  | X                | X                |                  |             |             |                  |                  |                  | X                | 2                     | 2                |                  |             |





APPENDIX B  
MICROPROBE ANALYSES

APPENDIX B  
MICROPORBE ANALYSES

I Garnet  
II Biotite  
III Cordierite  
IV Plagioclase

$$X_{Mg} = Mg/Mg+Fe$$

$$X_{Fe} = Fe/Mg+Fe$$

$$* = Fe^{+2}$$

## APPENDIX B I

## GARNET

$$X_{py} = \text{Mg}/\text{Mg}+\text{Fe}+\text{Ca}+\text{Mn}$$

$$X_{al} = \text{Fe}/\text{Mg}+\text{Fe}+\text{Ca}+\text{Mn}$$

$$X_{gr} = \text{Ca}/\text{Mg}+\text{Fe}+\text{Ca}+\text{Mn}$$

$$X_{sp} = \text{Mn}/\text{Mg}+\text{Fe}+\text{Ca}+\text{Mn}$$

## MICROPROBE ANALYSES

## GARNETS

|                                | BB1    | BB2B   | BI1B   | BI4B   | BI12   | BL2A   | BL2B   | BL3A  |
|--------------------------------|--------|--------|--------|--------|--------|--------|--------|-------|
| SiO <sub>2</sub>               | 38.01  | 37.44  | 37.81  | 37.42  | 37.45  | 38.69  | 37.88  | 37.05 |
| Al <sub>2</sub> O <sub>3</sub> | 21.44  | 21.39  | 21.68  | 21.21  | 21.18  | 21.92  | 21.76  | 21.17 |
| FeO                            | 34.43  | 32.71  | 35.28  | 34.77  | 38.02  | 32.70  | 32.70  | 33.63 |
| MgO                            | 5.65   | 4.98   | 4.14   | 3.25   | 2.80   | 6.81   | 6.33   | 5.10  |
| MnO                            | 0.53   | 2.71   | 1.13   | 2.75   | 0.59   | 1.35   | 1.04   | 1.76  |
| CaO                            | 1.17   | 1.12   | 0.82   | 1.38   | 0.98   | 1.06   | 1.04   | 1.04  |
| Total                          | 101.23 | 100.35 | 100.86 | 100.78 | 101.02 | 102.53 | 100.75 | 99.75 |

## Normalized moles based on 8 total cations

|                  |        |        |        |        |        |        |        |        |
|------------------|--------|--------|--------|--------|--------|--------|--------|--------|
| Si               | 2.975  | 2.968  | 2.996  | 2.989  | 2.998  | 2.968  | 2.961  | 2.954  |
| Al <sup>IV</sup> | 0.025  | 0.032  | 0.004  | 0.011  | 0.002  | 0.032  | 0.039  | 0.046  |
| Al <sup>VI</sup> | 1.953  | 1.966  | 2.020  | 1.986  | 1.996  | 1.949  | 1.965  | 1.944  |
| Fe <sup>+3</sup> | 0.071  | 0.066  | 0.001  | 0.025  | 0.006  | 0.083  | 0.082  | 0.102  |
| Fe <sup>+2</sup> | 2.183  | 2.102  | 2.337  | 2.298  | 2.540  | 2.014  | 2.055  | 2.140  |
| Mg               | 0.659  | 0.588  | 0.489  | 0.387  | 0.334  | 0.779  | 0.738  | 0.606  |
| Mn               | 0.035  | 0.182  | 0.076  | 0.186  | 0.040  | 0.088  | 0.069  | 0.119  |
| Ca               | 0.098  | 0.095  | 0.070  | 0.118  | 0.084  | 0.087  | 0.087  | 0.089  |
| Total            | 7.999  | 7.999  | 7.993  | 8.000  | 8.000  | 8.000  | 7.996  | 8.000  |
| O                | 12.011 | 12.005 | 12.009 | 12.005 | 12.007 | 12.016 | 12.009 | 12.014 |
| <br>             |        |        |        |        |        |        |        |        |
| X <sub>py</sub>  | 0.216  | 0.194  | 0.165  | 0.128  | 0.111  | 0.255  | 0.243  | 0.198  |
| X <sub>al</sub>  | 0.740  | 0.715  | 0.787  | 0.771  | 0.847  | 0.687  | 0.705  | 0.734  |
| X <sub>gr</sub>  | 0.032  | 0.031  | 0.023  | 0.039  | 0.028  | 0.029  | 0.029  | 0.029  |
| X <sub>sp</sub>  | 0.012  | 0.060  | 0.026  | 0.062  | 0.013  | 0.029  | 0.023  | 0.039  |

## MICROPROBE ANALYSES

## GARNETS

|                                | BL4B   | BO11A | CH1A   | CH1C   | FB1    | FB2C   | FB5A   | FB10   |
|--------------------------------|--------|-------|--------|--------|--------|--------|--------|--------|
| SiO <sub>2</sub>               | 37.81  | 37.96 | 37.51  | 38.14  | 38.43  | 38.01  | 38.89  | 39.70  |
| Al <sub>2</sub> O <sub>3</sub> | 21.65  | 21.37 | 21.41  | 21.49  | 21.75  | 21.55  | 21.94  | 22.33  |
| FeO                            | 32.92  | 33.82 | 33.41  | 33.62  | 32.51  | 33.42  | 31.88  | 30.59  |
| MgO                            | 6.35   | 4.68  | 4.97   | 5.51   | 5.39   | 5.71   | 7.00   | 6.54   |
| MnO                            | 0.51   | 1.01  | 1.94   | 2.16   | 1.95   | 0.93   | 1.03   | 1.63   |
| CaO                            | 1.13   | 1.04  | 1.07   | 1.01   | 1.60   | 1.02   | 0.91   | 2.22   |
| Total                          | 100.37 | 99.88 | 100.31 | 101.93 | 101.63 | 100.64 | 101.65 | 103.01 |

## Normalized moles based on 8 total cations

|                  |        |        |        |        |        |        |        |        |
|------------------|--------|--------|--------|--------|--------|--------|--------|--------|
| Si               | 2.966  | 3.023  | 2.975  | 2.971  | 2.995  | 2.986  | 3.000  | 3.022  |
| Al <sup>IV</sup> | 0.034  | 0.000  | 0.025  | 0.029  | 0.005  | 0.014  | 0.000  | 0.000  |
| Al <sup>VI</sup> | 1.968  | 2.006  | 1.976  | 1.943  | 1.993  | 1.982  | 1.995  | 2.003  |
| Fe <sup>+3</sup> | 0.065  | 0.000  | 0.050  | 0.086  | 0.012  | 0.044  | 0.004  | 0.000  |
| Fe <sup>+2</sup> | 2.095  | 2.252  | 2.166  | 2.104  | 2.106  | 2.152  | 2.053  | 1.947  |
| Mg               | 0.743  | 0.556  | 0.588  | 0.640  | 0.626  | 0.669  | 0.805  | 0.742  |
| Mn               | 0.034  | 0.068  | 0.130  | 0.143  | 0.129  | 0.062  | 0.067  | 0.105  |
| Ca               | 0.095  | 0.089  | 0.091  | 0.084  | 0.134  | 0.086  | 0.075  | 0.181  |
| Total            | 8.000  | 7.994  | 8.001  | 8.000  | 8.000  | 7.995  | 7.999  | 8.000  |
| O                | 12.007 | 12.020 | 12.000 | 12.013 | 12.008 | 12.011 | 12.000 | 12.039 |
| <br>             |        |        |        |        |        |        |        |        |
| X <sub>py</sub>  | 0.245  | 0.187  | 0.194  | 0.209  | 0.208  | 0.222  | 0.268  | 0.249  |
| X <sub>al</sub>  | 0.712  | 0.760  | 0.733  | 0.716  | 0.705  | 0.729  | 0.685  | 0.654  |
| X <sub>gr</sub>  | 0.031  | 0.030  | 0.030  | 0.028  | 0.044  | 0.029  | 0.025  | 0.061  |
| X <sub>sp</sub>  | 0.011  | 0.023  | 0.043  | 0.047  | 0.043  | 0.021  | 0.022  | 0.035  |

## MICROPROBE ANALYSES

## GARNETS

|                                | GN4B   | GO2C   | GO3    | GO5A   | LPC2A  | LPC7A  | LPC9A  | LPC9B  |
|--------------------------------|--------|--------|--------|--------|--------|--------|--------|--------|
| SiO <sub>2</sub>               | 38.92  | 38.26  | 39.06  | 37.94  | 37.70  | 39.18  | 38.25  | 38.75  |
| Al <sub>2</sub> O <sub>3</sub> | 21.54  | 21.63  | 21.93  | 21.68  | 21.03  | 22.20  | 21.98  | 21.91  |
| FeO                            | 29.86  | 34.10  | 29.77  | 33.77  | 32.75  | 33.31  | 35.02  | 31.75  |
| MgO                            | 5.01   | 4.70   | 6.17   | 5.63   | 3.48   | 5.82   | 5.43   | 6.02   |
| MnO                            | 4.94   | 1.40   | 2.14   | 1.04   | 5.42   | 1.18   | 0.73   | 1.44   |
| CaO                            | 1.88   | 1.00   | 2.56   | 0.95   | 1.47   | 0.95   | 0.98   | 1.28   |
| Total                          | 102.15 | 101.09 | 101.63 | 101.01 | 101.85 | 102.64 | 102.39 | 101.15 |

## Normalized moles based on 8 total cations

|                  |        |        |        |        |        |        |        |        |
|------------------|--------|--------|--------|--------|--------|--------|--------|--------|
| Si               | 3.002  | 3.015  | 3.018  | 2.975  | 2.979  | 3.017  | 2.965  | 3.019  |
| Al <sup>IV</sup> | 0.000  | 0.000  | 0.000  | 0.025  | 0.021  | 0.000  | 0.035  | 0.000  |
| Al <sup>VI</sup> | 1.973  | 2.009  | 1.997  | 1.979  | 1.938  | 2.105  | 1.973  | 2.012  |
| Fe <sup>+3</sup> | 0.000  | 0.000  | 0.000  | 0.047  | 0.082  | 0.000  | 0.062  | 0.000  |
| Fe <sup>+2</sup> | 1.941  | 2.247  | 1.923  | 2.168  | 2.082  | 2.145  | 2.208  | 2.069  |
| Mg               | 0.580  | 0.552  | 0.711  | 0.658  | 0.410  | 0.668  | 0.627  | 0.699  |
| Mn               | 0.325  | 0.093  | 0.140  | 0.069  | 0.363  | 0.077  | 0.048  | 0.095  |
| Ca               | 0.157  | 0.084  | 0.212  | 0.080  | 0.124  | 0.078  | 0.081  | 0.107  |
| Total            | 7.978  | 8.000  | 8.001  | 8.001  | 7.999  | 8.090  | 7.999  | 8.001  |
| O                | 12.011 | 12.019 | 12.024 | 12.008 | 12.005 | 12.024 | 12.000 | 12.032 |

|                 |       |       |       |       |       |       |       |       |
|-----------------|-------|-------|-------|-------|-------|-------|-------|-------|
| X <sub>py</sub> | 0.193 | 0.185 | 0.238 | 0.218 | 0.134 | 0.225 | 0.207 | 0.235 |
| X <sub>al</sub> | 0.646 | 0.755 | 0.644 | 0.733 | 0.707 | 0.723 | 0.750 | 0.697 |
| X <sub>gr</sub> | 0.052 | 0.028 | 0.071 | 0.026 | 0.041 | 0.026 | 0.027 | 0.036 |
| X <sub>sp</sub> | 0.108 | 0.031 | 0.047 | 0.023 | 0.118 | 0.026 | 0.016 | 0.032 |

## MICROPROBE ANALYSES

## GARNETS

|                                | LSB1A  | LSB3A  | LSB8B  | LSB13A | MB1A   | MB3    | MB6C   | MB12   |
|--------------------------------|--------|--------|--------|--------|--------|--------|--------|--------|
| SiO <sub>2</sub>               | 38.14  | 38.83  | 38.86  | 38.49  | 38.24  | 38.55  | 39.14  | 37.61  |
| Al <sub>2</sub> O <sub>3</sub> | 21.91  | 21.86  | 21.87  | 21.73  | 21.64  | 22.04  | 22.17  | 21.22  |
| FeO                            | 33.98  | 33.34  | 34.07  | 32.07  | 31.98  | 33.02  | 34.70  | 30.01  |
| MgO                            | 5.47   | 5.85   | 5.45   | 5.32   | 6.63   | 6.79   | 5.26   | 3.10   |
| MnO                            | 0.97   | 1.00   | 1.39   | 1.69   | 0.99   | 0.55   | 1.66   | 7.67   |
| CaO                            | 0.79   | 1.00   | 0.89   | 1.88   | 0.97   | 0.86   | 1.02   | 1.79   |
| Total                          | 101.26 | 101.88 | 102.53 | 101.18 | 100.45 | 101.81 | 103.95 | 101.40 |

## Normalized moles based on 8 total cations

|                  |        |        |        |        |        |        |        |        |
|------------------|--------|--------|--------|--------|--------|--------|--------|--------|
| Si               | 2.985  | 3.013  | 3.007  | 3.008  | 2.992  | 2.975  | 2.993  | 2.986  |
| Al <sup>IV</sup> | 0.015  | 0.000  | 0.000  | 0.000  | 0.008  | 0.025  | 0.007  | 0.014  |
| Al <sup>VI</sup> | 2.007  | 1.999  | 1.995  | 2.002  | 1.987  | 1.980  | 1.991  | 1.972  |
| Fe <sup>+3</sup> | 0.008  | 0.000  | 0.000  | 0.000  | 0.021  | 0.044  | 0.017  | 0.042  |
| Fe <sup>+2</sup> | 2.217  | 2.163  | 2.205  | 2.096  | 2.072  | 2.087  | 2.202  | 1.951  |
| Mg               | 0.638  | 0.677  | 0.629  | 0.620  | 0.773  | 0.781  | 0.600  | 0.367  |
| Mn               | 0.064  | 0.066  | 0.091  | 0.112  | 0.066  | 0.036  | 0.108  | 0.516  |
| Ca               | 0.066  | 0.083  | 0.074  | 0.157  | 0.081  | 0.071  | 0.084  | 0.152  |
| Total            | 8.000  | 8.001  | 8.001  | 7.995  | 8.000  | 7.999  | 8.002  | 8.000  |
| O                | 12.000 | 12.028 | 12.014 | 12.011 | 12.000 | 12.008 | 12.014 | 12.000 |
| <br>             |        |        |        |        |        |        |        |        |
| X <sub>py</sub>  | 0.213  | 0.226  | 0.210  | 0.208  | 0.257  | 0.259  | 0.199  | 0.121  |
| X <sub>al</sub>  | 0.743  | 0.724  | 0.735  | 0.702  | 0.695  | 0.706  | 0.737  | 0.658  |
| X <sub>gr</sub>  | 0.022  | 0.028  | 0.025  | 0.053  | 0.027  | 0.024  | 0.028  | 0.050  |
| X <sub>sp</sub>  | 0.021  | 0.022  | 0.030  | 0.037  | 0.022  | 0.012  | 0.036  | 0.170  |



## MICROPROBE ANALYSES

## GARNETS

|                                | MB16   | MK1A   | MK1B   | MK2A   | NLS5B  | NLS5C  | NLS7A  | RB6A   |
|--------------------------------|--------|--------|--------|--------|--------|--------|--------|--------|
| SiO <sub>2</sub>               | 38.89  | 38.37  | 37.84  | 38.17  | 38.31  | 38.17  | 38.28  | 38.02  |
| Al <sub>2</sub> O <sub>3</sub> | 21.89  | 21.66  | 21.58  | 21.61  | 21.57  | 21.80  | 21.58  | 21.78  |
| FeO                            | 33.03  | 34.97  | 34.01  | 34.37  | 35.25  | 32.86  | 34.68  | 34.55  |
| MgO                            | 6.29   | 4.38   | 3.85   | 4.41   | 5.02   | 6.39   | 4.89   | 5.14   |
| MnO                            | 1.07   | 1.64   | 3.73   | 2.72   | 1.24   | 0.97   | 1.79   | 1.89   |
| CaO                            | 1.03   | 1.53   | 0.97   | 1.02   | 0.96   | 1.01   | 0.87   | 1.03   |
| Total                          | 102.20 | 102.55 | 101.98 | 102.30 | 102.35 | 101.20 | 102.09 | 102.41 |

## Normalized moles based on 8 total cations

|                  |        |        |        |        |        |        |        |        |
|------------------|--------|--------|--------|--------|--------|--------|--------|--------|
| Si               | 3.000  | 2.989  | 2.978  | 2.983  | 2.982  | 2.971  | 2.989  | 2.954  |
| Al <sup>IV</sup> | 0.000  | 0.011  | 0.022  | 0.017  | 0.018  | 0.029  | 0.011  | 0.046  |
| Al <sup>VI</sup> | 1.990  | 1.977  | 1.980  | 1.974  | 1.961  | 1.971  | 1.975  | 1.949  |
| Fe <sup>+3</sup> | 0.009  | 0.034  | 0.043  | 0.043  | 0.057  | 0.058  | 0.036  | 0.096  |
| Fe <sup>+2</sup> | 2.122  | 2.244  | 2.196  | 2.204  | 2.238  | 2.082  | 2.229  | 2.149  |
| Mg               | 0.723  | 0.509  | 0.452  | 0.514  | 0.583  | 0.742  | 0.569  | 0.595  |
| Mn               | 0.070  | 0.108  | 0.249  | 0.180  | 0.082  | 0.064  | 0.118  | 0.124  |
| Ca               | 0.085  | 0.128  | 0.082  | 0.085  | 0.080  | 0.084  | 0.073  | 0.086  |
| Total            | 7.999  | 8.000  | 8.002  | 8.000  | 8.001  | 8.001  | 8.000  | 7.999  |
| O                | 12.009 | 12.006 | 12.000 | 12.016 | 12.009 | 12.006 | 12.000 | 12.011 |
| <br>             |        |        |        |        |        |        |        |        |
| X <sub>py</sub>  | 0.240  | 0.168  | 0.150  | 0.170  | 0.192  | 0.245  | 0.188  | 0.195  |
| X <sub>al</sub>  | 0.708  | 0.754  | 0.741  | 0.742  | 0.755  | 0.706  | 0.749  | 0.736  |
| X <sub>gr</sub>  | 0.028  | 0.042  | 0.027  | 0.028  | 0.026  | 0.028  | 0.024  | 0.028  |
| X <sub>sp</sub>  | 0.023  | 0.036  | 0.082  | 0.060  | 0.027  | 0.021  | 0.039  | 0.041  |

## MICROPROBE ANALYSES

## GARNETS

|                                | RB11C  | RR3C   | RR5B   | SB1A   | SB3A   | SC2B   | SC3D   | SC5    |
|--------------------------------|--------|--------|--------|--------|--------|--------|--------|--------|
| SiO <sub>2</sub>               | 38.72  | 37.30  | 38.45  | 38.24  | 37.08  | 38.08  | 38.25  | 38.03  |
| Al <sub>2</sub> O <sub>3</sub> | 21.93  | 21.26  | 21.77  | 21.35  | 21.08  | 21.57  | 21.98  | 21.78  |
| FeO                            | 34.59  | 30.68  | 32.42  | 30.49  | 27.82  | 30.93  | 34.12  | 35.96  |
| MgO                            | 4.74   | 2.68   | 3.76   | 2.66   | 2.35   | 4.10   | 5.40   | 4.05   |
| MnO                            | 2.02   | 8.78   | 5.50   | 7.35   | 7.00   | 6.01   | 1.37   | 1.90   |
| CaO                            | 0.95   | 1.13   | 1.15   | 2.98   | 4.87   | 1.40   | 0.97   | 0.84   |
| Total                          | 102.95 | 101.83 | 103.05 | 103.07 | 100.20 | 102.09 | 102.09 | 102.56 |

## Normalized moles based on 8 total cations

|                  |        |        |        |        |        |        |        |        |
|------------------|--------|--------|--------|--------|--------|--------|--------|--------|
| Si               | 2.999  | 2.965  | 2.995  | 2.988  | 2.969  | 2.985  | 2.973  | 2.973  |
| Al <sup>IV</sup> | 0.001  | 0.035  | 0.005  | 0.012  | 0.031  | 0.015  | 0.027  | 0.027  |
| Al <sup>VI</sup> | 2.001  | 1.956  | 1.993  | 1.955  | 1.957  | 1.977  | 1.986  | 1.980  |
| Fe <sup>+3</sup> | 0.000  | 0.079  | 0.012  | 0.071  | 0.088  | 0.038  | 0.041  | 0.046  |
| Fe <sup>+2</sup> | 2.240  | 1.960  | 2.099  | 1.921  | 1.774  | 1.989  | 2.176  | 2.305  |
| Mg               | 0.547  | 0.318  | 0.437  | 0.310  | 0.280  | 0.479  | 0.626  | 0.472  |
| Mn               | 0.133  | 0.591  | 0.363  | 0.486  | 0.475  | 0.399  | 0.090  | 0.126  |
| Ca               | 0.079  | 0.096  | 0.096  | 0.250  | 0.418  | 0.118  | 0.081  | 0.070  |
| Total            | 8.000  | 8.000  | 8.000  | 7.993  | 7.992  | 8.000  | 8.000  | 7.999  |
| O                | 12.000 | 12.005 | 12.000 | 12.009 | 12.011 | 12.000 | 12.012 | 12.012 |
| $X_{py}$         | 0.182  | 0.104  | 0.145  | 0.102  | 0.092  | 0.158  | 0.208  | 0.156  |
| $X_{al}$         | 0.747  | 0.670  | 0.702  | 0.656  | 0.614  | 0.671  | 0.736  | 0.779  |
| $X_{gr}$         | 0.026  | 0.032  | 0.032  | 0.082  | 0.138  | 0.390  | 0.027  | 0.023  |
| $X_{sp}$         | 0.044  | 0.194  | 0.121  | 0.160  | 0.156  | 0.132  | 0.030  | 0.042  |

## MICROPROBE ANALYSES

## GARNETS

|                                | SE9A   | S18    | SN2    | STB3B  | STB4B  | STB5A  | STB7A  | SX5D   |
|--------------------------------|--------|--------|--------|--------|--------|--------|--------|--------|
| SiO <sub>2</sub>               | 39.44  | 38.07  | 37.82  | 38.14  | 38.59  | 38.59  | 37.72  | 38.10  |
| Al <sub>2</sub> O <sub>3</sub> | 22.49  | 21.56  | 21.28  | 21.46  | 21.79  | 21.74  | 21.44  | 21.59  |
| FeO                            | 32.77  | 36.48  | 33.30  | 33.00  | 35.07  | 34.07  | 32.38  | 34.05  |
| MgO                            | 6.54   | 3.41   | 4.65   | 4.72   | 4.63   | 4.84   | 4.38   | 5.32   |
| MnO                            | 1.13   | 2.25   | 1.95   | 2.80   | 0.61   | 1.93   | 3.10   | 1.22   |
| CaO                            | 1.10   | 1.05   | 1.09   | 1.46   | 1.29   | 1.22   | 1.98   | 1.03   |
| Total                          | 103.47 | 102.82 | 100.09 | 101.58 | 101.98 | 102.39 | 101.00 | 101.31 |

## Normalized moles based on 8 total cations

|                  |        |        |        |        |        |        |        |        |
|------------------|--------|--------|--------|--------|--------|--------|--------|--------|
| Si               | 2.998  | 2.983  | 3.011  | 2.991  | 3.012  | 3.001  | 2.978  | 2.986  |
| Al <sup>iv</sup> | 0.002  | 0.017  | 0.000  | 0.009  | 0.000  | 0.000  | 0.022  | 0.014  |
| Al <sup>vi</sup> | 2.013  | 1.974  | 1.996  | 1.975  | 2.005  | 1.993  | 1.972  | 1.980  |
| Fe <sup>+3</sup> | 0.000  | 0.043  | 0.000  | 0.034  | 0.000  | 0.005  | 0.050  | 0.035  |
| Fe <sup>+2</sup> | 2.083  | 2.347  | 2.217  | 2.131  | 2.289  | 2.211  | 2.087  | 2.197  |
| Mg               | 0.741  | 0.398  | 0.552  | 0.552  | 0.539  | 0.561  | 0.515  | 0.621  |
| Mn               | 0.073  | 0.149  | 0.131  | 0.186  | 0.040  | 0.127  | 0.207  | 0.081  |
| Ca               | 0.090  | 0.088  | 0.093  | 0.123  | 0.108  | 0.102  | 0.167  | 0.086  |
| Total            | 8.000  | 7.999  | 8.000  | 8.001  | 7.993  | 8.000  | 7.998  | 8.000  |
| O                | 12.018 | 12.000 | 12.009 | 12.008 | 12.020 | 12.014 | 12.000 | 12.000 |
| X <sub>py</sub>  | 0.248  | 0.132  | 0.184  | 0.182  | 0.181  | 0.187  | 0.170  | 0.206  |
| X <sub>al</sub>  | 0.698  | 0.790  | 0.741  | 0.716  | 0.769  | 0.737  | 0.706  | 0.739  |
| X <sub>gr</sub>  | 0.030  | 0.029  | 0.031  | 0.041  | 0.036  | 0.034  | 0.055  | 0.029  |
| X <sub>sp</sub>  | 0.024  | 0.049  | 0.044  | 0.061  | 0.140  | 0.042  | 0.068  | 0.027  |

## MICROPROBE ANALYSES

## GARNETS

|                                | SX9    | SX12  | WLS3B  | WLS11A | WM1C   | WM6A   | WR1    | WR9A   |
|--------------------------------|--------|-------|--------|--------|--------|--------|--------|--------|
| SiO <sub>2</sub>               | 38.34  | 37.35 | 38.39  | 37.76  | 38.74  | 38.08  | 37.07  | 37.97  |
| Al <sub>2</sub> O <sub>3</sub> | 21.56  | 21.09 | 21.94  | 21.28  | 21.58  | 21.90  | 21.32  | 21.87  |
| FeO                            | 33.01  | 32.22 | 34.15  | 31.55  | 34.14  | 33.30  | 33.80  | 32.84  |
| MgO                            | 5.73   | 6.75  | 5.06   | 5.02   | 3.19   | 5.85   | 4.11   | 4.25   |
| MnO                            | 1.64   | 0.99  | 1.61   | 3.30   | 0.26   | 2.19   | 2.62   | 5.65   |
| CaO                            | 1.10   | 1.08  | 1.16   | 2.16   | 4.35   | 1.15   | 1.93   | 1.23   |
| Total                          | 101.38 | 99.48 | 102.31 | 101.07 | 102.26 | 102.47 | 100.85 | 103.81 |

## Normalized moles based on 8 total cations

|                  |        |        |        |        |        |        |        |        |
|------------------|--------|--------|--------|--------|--------|--------|--------|--------|
| Si               | 2.993  | 2.952  | 2.981  | 2.965  | 3.026  | 2.942  | 2.935  | 2.931  |
| Al <sup>IV</sup> | 0.007  | 0.048  | 0.019  | 0.035  | 0.000  | 0.058  | 0.065  | 0.069  |
| Al <sup>VI</sup> | 1.977  | 1.917  | 1.989  | 1.934  | 1.987  | 1.936  | 1.925  | 1.920  |
| Fe <sup>+3</sup> | 0.029  | 0.131  | 0.040  | 0.111  | 0.000  | 0.122  | 0.164  | 0.149  |
| Fe <sup>+2</sup> | 2.126  | 1.999  | 2.178  | 1.961  | 2.230  | 2.030  | 2.074  | 1.971  |
| Mg               | 0.667  | 0.795  | 0.586  | 0.588  | 0.371  | 0.674  | 0.485  | 0.489  |
| Mn               | 0.108  | 0.066  | 0.106  | 0.219  | 0.017  | 0.143  | 0.176  | 0.369  |
| Ca               | 0.092  | 0.091  | 0.097  | 0.182  | 0.364  | 0.095  | 0.164  | 0.102  |
| Total            | 7.999  | 7.999  | 7.996  | 7.995  | 7.995  | 8.000  | 7.988  | 8.000  |
| O                | 12.009 | 12.000 | 12.000 | 12.016 | 12.022 | 12.000 | 12.028 | 12.006 |
| <br>             |        |        |        |        |        |        |        |        |
| X <sub>py</sub>  | 0.221  | 0.258  | 0.195  | 0.192  | 0.125  | 0.220  | 0.158  | 0.159  |
| X <sub>al</sub>  | 0.713  | 0.691  | 0.738  | 0.677  | 0.748  | 0.702  | 0.731  | 0.688  |
| X <sub>gr</sub>  | 0.030  | 0.030  | 0.032  | 0.059  | 0.122  | 0.031  | 0.053  | 0.033  |
| X <sub>sp</sub>  | 0.036  | 0.021  | 0.035  | 0.072  | 0.006  | 0.047  | 0.057  | 0.120  |

APPENDIX B II

BIOTITE



## MICROPROBE ANALYSES

## BIOTITES

|                                | BL4B  | BO11A | CH1A  | CH1C  | FB1   | FB2C  | FB5A  | FB10  |
|--------------------------------|-------|-------|-------|-------|-------|-------|-------|-------|
| SiO <sub>2</sub>               | 35.03 | 36.09 | 34.77 | 35.38 | 35.51 | 36.62 | 36.27 | 37.64 |
| Al <sub>2</sub> O <sub>3</sub> | 17.50 | 18.13 | 17.98 | 18.06 | 17.36 | 16.92 | 17.02 | 16.84 |
| TiO <sub>2</sub>               | 3.19  | 3.51  | 2.84  | 2.76  | 2.68  | 3.09  | 4.15  | 4.21  |
| FeO                            | 16.95 | 17.46 | 17.44 | 19.02 | 18.40 | 16.93 | 15.52 | 15.75 |
| MnO                            | 0.00  | 0.00  | 0.00  | 0.11  | 0.00  | 0.00  | 0.00  | 0.00  |
| MgO                            | 11.05 | 10.21 | 10.44 | 10.27 | 10.99 | 12.05 | 11.68 | 12.60 |
| CaO                            | 0.00  | 0.00  | 0.00  | 0.00  | 0.00  | 0.00  | 0.00  | 0.00  |
| Na <sub>2</sub> O              | 0.00  | 0.13  | 0.19  | 0.18  | 0.22  | 0.18  | 0.16  | 0.35  |
| K <sub>2</sub> O               | 9.32  | 8.19  | 9.13  | 9.52  | 7.98  | 8.28  | 8.38  | 9.41  |
| Total                          | 93.05 | 93.72 | 92.79 | 95.30 | 93.14 | 94.07 | 93.18 | 96.80 |

Normalized moles based on (O<sub>10</sub>(OH)<sub>2</sub>)

|                  |        |        |        |        |        |        |        |        |
|------------------|--------|--------|--------|--------|--------|--------|--------|--------|
| Si               | 5.412  | 5.476  | 5.396  | 5.390  | 5.470  | 5.542  | 5.512  | 5.532  |
| Al <sup>IV</sup> | 2.588  | 2.524  | 2.604  | 2.610  | 2.530  | 2.458  | 2.488  | 2.468  |
| Al <sup>VI</sup> | 0.599  | 0.750  | 0.685  | 0.663  | 0.622  | 0.559  | 0.561  | 0.450  |
| Ti               | 0.371  | 0.400  | 0.331  | 0.316  | 0.310  | 0.352  | 0.474  | 0.465  |
| Fe*              | 2.190  | 2.215  | 2.264  | 2.423  | 2.370  | 2.143  | 1.972  | 1.936  |
| Mn               | 0.000  | 0.000  | 0.000  | 0.014  | 0.000  | 0.000  | 0.000  | 0.000  |
| Mg               | 2.545  | 2.309  | 2.415  | 2.333  | 2.524  | 2.718  | 2.646  | 2.761  |
| Ca               | 0.000  | 0.000  | 0.000  | 0.000  | 0.000  | 0.000  | 0.000  | 0.000  |
| Na               | 0.000  | 0.038  | 0.057  | 0.053  | 0.066  | 0.053  | 0.047  | 0.100  |
| K                | 0.000  | 0.000  | 0.000  | 0.000  | 0.000  | 0.000  | 0.000  | 0.000  |
| Total            | 13.705 | 13.712 | 13.752 | 13.802 | 13.892 | 13.825 | 13.700 | 13.712 |
| O                | 21.081 | 21.207 | 21.096 | 21.075 | 21.216 | 21.201 | 21.188 | 21.188 |
| <br>             |        |        |        |        |        |        |        |        |
| X <sub>Mg</sub>  | 0.537  | 0.510  | 0.516  | 0.489  | 0.516  | 0.559  | 0.573  | 0.588  |
| X <sub>Fe</sub>  | 0.463  | 0.490  | 0.484  | 0.508  | 0.484  | 0.441  | 0.427  | 0.412  |
| X <sub>Mn</sub>  | 0.000  | 0.000  | 0.000  | 0.003  | 0.000  | 0.000  | 0.000  | 0.000  |





## MICROPROBE ANALYSES

## BIOTITES

|                                | LSB1A | LSB3A | LSB8B | LSB13A | MB1A  | MB3   | MB6C  | MB12  |
|--------------------------------|-------|-------|-------|--------|-------|-------|-------|-------|
| SiO <sub>2</sub>               | 35.69 | 37.14 | 36.47 | 36.18  | 36.15 | 36.20 | 36.07 | 35.82 |
| Al <sub>2</sub> O <sub>3</sub> | 18.53 | 18.60 | 18.52 | 17.08  | 17.50 | 17.65 | 18.45 | 18.58 |
| TiO <sub>2</sub>               | 3.66  | 3.22  | 3.94  | 2.88   | 3.35  | 3.88  | 3.37  | 1.54  |
| FeO                            | 17.92 | 16.32 | 18.39 | 18.12  | 14.51 | 16.36 | 16.77 | 21.34 |
| MnO                            | 0.00  | 0.00  | 0.15  | 0.00   | 0.00  | 0.00  | 0.00  | 1.50  |
| MgO                            | 9.82  | 11.86 | 10.01 | 11.34  | 12.61 | 11.66 | 11.30 | 9.05  |
| CaO                            | 0.08  | 0.00  | 0.00  | 0.00   | 0.00  | 0.15  | 0.09  | 0.35  |
| Na <sub>2</sub> O              | 0.21  | 0.28  | 0.21  | 0.10   | 0.17  | 0.33  | 0.17  | 0.19  |
| K <sub>2</sub> O               | 7.88  | 9.40  | 9.25  | 8.12   | 8.04  | 9.15  | 9.48  | 7.17  |
| Total                          | 93.79 | 96.82 | 96.94 | 93.82  | 92.33 | 95.38 | 95.70 | 95.54 |

Normalized moles based on (O<sub>10</sub>(OH)<sub>2</sub>)

|                  |        |        |        |        |        |        |        |        |
|------------------|--------|--------|--------|--------|--------|--------|--------|--------|
| Si               | 5.431  | 5.462  | 5.416  | 5.519  | 5.504  | 5.424  | 5.398  | 5.452  |
| Al <sup>IV</sup> | 2.569  | 2.538  | 2.584  | 2.481  | 2.496  | 2.576  | 2.602  | 2.548  |
| Al <sup>VI</sup> | 0.754  | 0.685  | 0.658  | 0.590  | 0.644  | 0.541  | 0.652  | 0.785  |
| Ti               | 0.419  | 0.365  | 0.440  | 0.330  | 0.384  | 0.437  | 0.379  | 0.176  |
| Fe*              | 2.280  | 2.007  | 2.284  | 2.312  | 1.847  | 2.050  | 2.099  | 2.716  |
| Mn               | 0.000  | 0.000  | 0.019  | 0.000  | 0.000  | 0.000  | 0.000  | 0.193  |
| Mg               | 2.228  | 2.600  | 2.216  | 2.579  | 2.862  | 2.605  | 2.521  | 2.053  |
| Ca               | 0.013  | 0.000  | 0.000  | 0.000  | 0.000  | 0.024  | 0.014  | 0.057  |
| Na               | 0.062  | 0.080  | 0.060  | 0.030  | 0.050  | 0.096  | 0.049  | 0.056  |
| K                | 0.000  | 0.000  | 0.000  | 0.000  | 0.000  | 0.000  | 0.000  | 0.000  |
| Total            | 13.756 | 13.737 | 13.677 | 13.841 | 13.787 | 13.753 | 13.714 | 14.036 |
| O                | 21.235 | 21.118 | 21.124 | 21.212 | 21.219 | 21.125 | 21.095 | 21.304 |
| <br>             |        |        |        |        |        |        |        |        |
| X <sub>Mg</sub>  | 0.494  | 0.564  | 0.490  | 0.527  | 0.608  | 0.560  | 0.546  | 0.414  |
| X <sub>Fe</sub>  | 0.506  | 0.436  | 0.505  | 0.473  | 0.392  | 0.440  | 0.454  | 0.547  |
| X <sub>Mn</sub>  | 0.000  | 0.000  | 0.004  | 0.000  | 0.000  | 0.000  | 0.000  | 0.039  |



## MICROPROBE ANALYSES

## BIOTITES

|                                | RB11C | RR3C  | RR5B  | SB1A  | SB3A  | SC2B  | SC3D  | SC5   |
|--------------------------------|-------|-------|-------|-------|-------|-------|-------|-------|
| SiO <sub>2</sub>               | 36.59 | 34.72 | 36.06 | 36.59 | 35.63 | 35.95 | 35.81 | 36.14 |
| Al <sub>2</sub> O <sub>3</sub> | 19.09 | 18.95 | 19.85 | 16.79 | 16.56 | 17.33 | 18.05 | 18.90 |
| TiO <sub>2</sub>               | 2.34  | 1.69  | 2.52  | 2.04  | 2.16  | 2.51  | 3.83  | 3.21  |
| FeO                            | 16.90 | 20.27 | 18.65 | 21.30 | 20.59 | 19.77 | 18.41 | 19.28 |
| MnO                            | 0.00  | 0.29  | 0.20  | 0.00  | 0.12  | 0.24  | 0.17  | 0.00  |
| MgO                            | 11.23 | 8.96  | 9.94  | 9.59  | 9.89  | 10.76 | 10.74 | 9.24  |
| CaO                            | 0.08  | 0.00  | 0.00  | 0.00  | 0.00  | 0.00  | 0.00  | 0.00  |
| Na <sub>2</sub> O              | 0.35  | 0.23  | 0.24  | 0.20  | 0.22  | 0.20  | 0.22  | 0.28  |
| K <sub>2</sub> O               | 8.90  | 9.09  | 9.16  | 8.85  | 8.91  | 8.98  | 9.30  | 8.09  |
| Total                          | 95.48 | 94.20 | 96.62 | 95.36 | 94.08 | 95.74 | 96.08 | 95.14 |

Normalized moles based on (O<sub>10</sub>(OH)<sub>2</sub>)

|                  |        |        |        |        |        |        |        |        |
|------------------|--------|--------|--------|--------|--------|--------|--------|--------|
| Si               | 5.460  | 5.377  | 5.373  | 5.595  | 5.530  | 5.454  | 5.385  | 5.451  |
| Al <sup>IV</sup> | 2.540  | 2.623  | 2.627  | 2.405  | 2.470  | 2.546  | 2.615  | 2.549  |
| Al <sup>VI</sup> | 0.818  | 0.836  | 0.858  | 0.621  | 0.559  | 0.553  | 0.583  | 0.811  |
| Ti               | 0.263  | 0.197  | 0.282  | 0.235  | 0.252  | 0.286  | 0.382  | 0.364  |
| Fe*              | 2.109  | 2.625  | 2.324  | 2.724  | 2.673  | 2.508  | 2.315  | 2.432  |
| Mn               | 0.000  | 0.038  | 0.025  | 0.000  | 0.016  | 0.031  | 0.022  | 0.000  |
| Mg               | 2.498  | 2.069  | 2.208  | 2.186  | 2.288  | 2.434  | 2.407  | 2.078  |
| Ca               | 0.013  | 0.000  | 0.000  | 0.000  | 0.000  | 0.000  | 0.000  | 0.000  |
| Na               | 0.101  | 0.069  | 0.069  | 0.059  | 0.066  | 0.059  | 0.064  | 0.082  |
| K                | 0.000  | 0.000  | 0.000  | 0.000  | 0.000  | 0.000  | 0.000  | 0.000  |
| Total            | 13.802 | 13.834 | 13.766 | 13.825 | 13.854 | 13.871 | 13.773 | 13.767 |
| O                | 21.153 | 21.102 | 21.129 | 21.137 | 21.118 | 21.131 | 21.108 | 21.222 |
| <br>             |        |        |        |        |        |        |        |        |
| X <sub>Mg</sub>  | 0.542  | 0.437  | 0.485  | 0.445  | 0.460  | 0.489  | 0.507  | 0.461  |
| X <sub>Fe</sub>  | 0.458  | 0.555  | 0.510  | 0.555  | 0.537  | 0.504  | 0.488  | 0.539  |
| X <sub>Mn</sub>  | 0.000  | 0.008  | 0.006  | 0.000  | 0.003  | 0.006  | 0.005  | 0.000  |

## MICROPROBE ANALYSES

## BIOTITES

|                                | SE9A  | SI8   | SN2   | STB3B | STB4B | STB5A | STB7B | SX5D  |
|--------------------------------|-------|-------|-------|-------|-------|-------|-------|-------|
| SiO <sub>2</sub>               | 37.16 | 35.62 | 36.10 | 35.75 | 36.26 | 36.07 | 36.08 | 35.80 |
| Al <sub>2</sub> O <sub>3</sub> | 17.76 | 18.72 | 17.86 | 17.97 | 17.72 | 18.36 | 17.54 | 17.73 |
| TiO <sub>2</sub>               | 3.35  | 2.29  | 2.51  | 2.73  | 2.75  | 2.84  | 3.21  | 3.42  |
| FeO                            | 16.17 | 20.90 | 18.48 | 17.52 | 17.10 | 19.06 | 18.31 | 16.70 |
| MnO                            | 0.00  | 0.10  | 0.10  | 0.00  | 0.00  | 0.00  | 0.00  | 0.10  |
| MgO                            | 12.39 | 9.12  | 11.11 | 11.00 | 11.38 | 10.28 | 10.75 | 11.48 |
| CaO                            | 0.00  | 0.00  | 0.12  | 0.11  | 0.00  | 0.00  | 0.00  | 0.06  |
| Na <sub>2</sub> O              | 0.30  | 0.32  | 0.00  | 0.25  | 0.26  | 0.19  | 0.00  | 0.22  |
| K <sub>2</sub> O               | 8.18  | 9.10  | 9.67  | 9.07  | 9.17  | 8.04  | 7.84  | 9.52  |
| Total                          | 95.31 | 96.17 | 95.95 | 94.40 | 94.64 | 94.84 | 93.73 | 95.03 |

Normalized moles based on (O<sub>10</sub>(OH)<sub>2</sub>)

|                  |        |        |        |        |        |        |        |        |
|------------------|--------|--------|--------|--------|--------|--------|--------|--------|
| Si               | 5.514  | 5.402  | 5.442  | 5.440  | 5.488  | 5.456  | 5.499  | 5.409  |
| Al <sup>IV</sup> | 2.486  | 2.598  | 2.558  | 2.560  | 2.512  | 2.544  | 2.501  | 2.591  |
| Al <sup>VI</sup> | 0.620  | 0.749  | 0.615  | 0.663  | 0.649  | 0.729  | 0.650  | 0.567  |
| Ti               | 0.374  | 0.261  | 0.285  | 0.312  | 0.313  | 0.323  | 0.368  | 0.389  |
| Fe*              | 2.007  | 2.651  | 2.330  | 2.230  | 2.165  | 2.411  | 2.334  | 2.110  |
| Mn               | 0.000  | 0.013  | 0.013  | 0.000  | 0.000  | 0.000  | 0.000  | 0.013  |
| Mg               | 2.741  | 2.062  | 2.497  | 2.495  | 2.568  | 2.318  | 2.443  | 2.586  |
| Ca               | 0.000  | 0.000  | 0.019  | 0.018  | 0.000  | 0.000  | 0.000  | 0.010  |
| Na               | 0.086  | 0.094  | 0.000  | 0.074  | 0.076  | 0.056  | 0.000  | 0.064  |
| K                | 0.000  | 0.000  | 0.000  | 0.000  | 0.000  | 0.000  | 0.000  | 0.000  |
| Total            | 13.828 | 13.830 | 13.759 | 13.792 | 13.771 | 13.837 | 13.795 | 13.739 |
| O                | 21.226 | 21.120 | 21.070 | 21.120 | 21.115 | 21.224 | 21.238 | 21.082 |
| <br>             |        |        |        |        |        |        |        |        |
| X <sub>Mg</sub>  | 0.577  | 0.436  | 0.516  | 0.528  | 0.543  | 0.490  | 0.511  | 0.549  |
| X <sub>Fe</sub>  | 0.423  | 0.561  | 0.481  | 0.472  | 0.457  | 0.510  | 0.489  | 0.448  |
| X <sub>Mn</sub>  | 0.000  | 0.003  | 0.003  | 0.000  | 0.000  | 0.000  | 0.000  | 0.003  |



APPENDIX B III

CORDIERITE

## MICROPROBE ANALYSES

## CORDIERITES

|                                | BI12  | BL2A  | BL2B  | BL3A  | BL4B  | BO11A | GO2C  | GO5A  |
|--------------------------------|-------|-------|-------|-------|-------|-------|-------|-------|
| SiO <sub>2</sub>               | 48.68 | 47.95 | 48.77 | 48.55 | 48.24 | 47.55 | 48.09 | 48.38 |
| Al <sub>2</sub> O <sub>3</sub> | 32.44 | 32.52 | 32.43 | 32.27 | 32.52 | 31.93 | 32.42 | 32.27 |
| TiO <sub>2</sub>               | 0.00  | 0.00  | 0.00  | 0.00  | 0.00  | 0.00  | 0.00  | 0.00  |
| FeO                            | 9.77  | 6.41  | 6.63  | 7.46  | 7.28  | 7.15  | 7.40  | 6.83  |
| MnO                            | 0.12  | 0.00  | 0.00  | 0.12  | 0.00  | 0.00  | 0.15  | 0.00  |
| MgO                            | 6.89  | 9.32  | 8.98  | 8.59  | 8.66  | 8.57  | 8.79  | 8.93  |
| CaO                            | 0.00  | 0.00  | 0.04  | 0.00  | 0.00  | 0.00  | 0.00  | 0.00  |
| Na <sub>2</sub> O              | 0.47  | 0.31  | 0.00  | 0.00  | 0.21  | 0.34  | 0.34  | 0.00  |
| K <sub>2</sub> O               | 0.00  | 0.00  | 0.00  | 0.00  | 0.00  | 0.05  | 0.00  | 0.00  |
| Total                          | 98.37 | 96.51 | 96.85 | 96.99 | 96.91 | 95.59 | 97.19 | 96.41 |

Normalized moles based on 11 total cations and 18(O)

|                  |        |        |        |        |        |        |        |        |
|------------------|--------|--------|--------|--------|--------|--------|--------|--------|
| Si               | 5.028  | 4.971  | 5.058  | 5.050  | 5.007  | 4.545  | 4.978  | 5.046  |
| Al <sup>IV</sup> | 0.972  | 1.029  | 0.942  | 0.950  | 0.993  | 1.455  | 1.022  | 0.955  |
| Al <sup>VI</sup> | 2.982  | 2.945  | 3.032  | 3.012  | 2.985  | 3.135  | 2.931  | 3.018  |
| Ti               | 0.000  | 0.000  | 0.000  | 0.000  | 0.000  | 0.000  | 0.000  | 0.000  |
| Fe <sup>+3</sup> | 0.092  | 0.146  | 0.000  | 0.000  | 0.052  | 0.390  | 0.152  | 0.000  |
| Mn               | 0.012  | 0.000  | 0.000  | 0.006  | 0.000  | 0.000  | 0.102  | 0.000  |
| Fe <sup>+2</sup> | 0.752  | 0.408  | 0.573  | 0.650  | 0.578  | 0.184  | 0.488  | 0.595  |
| Mg               | 1.061  | 1.439  | 1.389  | 1.331  | 1.341  | 1.222  | 1.355  | 1.385  |
| Ca               | 0.000  | 0.000  | 0.006  | 0.000  | 0.000  | 0.000  | 0.000  | 0.000  |
| Na               | 0.099  | 0.062  | 0.000  | 0.000  | 0.044  | 0.069  | 0.062  | 0.000  |
| K                | 0.000  | 0.000  | 0.000  | 0.000  | 0.000  | 0.000  | 0.000  | 0.000  |
| Total            | 10.998 | 11.000 | 11.000 | 10.999 | 10.999 | 11.000 | 11.000 | 11.000 |
| <br>             |        |        |        |        |        |        |        |        |
| X <sub>Mg</sub>  | 0.557  | 0.722  | 0.708  | 0.672  | 0.680  | 0.680  | 0.679  | 0.699  |
| X <sub>Fe</sub>  | 0.443  | 0.278  | 0.292  | 0.328  | 0.320  | 0.320  | 0.321  | 0.301  |

## MICROPROBE ANALYSES

## CORDIERITES

|                                | LSB1A | LSB8B | MB3   | MK1B  | NLS5C | SC3D  | SN2   | STB4B |
|--------------------------------|-------|-------|-------|-------|-------|-------|-------|-------|
| SiO <sub>2</sub>               | 48.84 | 47.77 | 47.65 | 45.71 | 48.87 | 48.66 | 48.77 | 47.88 |
| Al <sub>2</sub> O <sub>3</sub> | 32.62 | 32.08 | 31.98 | 38.77 | 32.95 | 32.81 | 32.86 | 32.32 |
| TiO <sub>2</sub>               | 0.00  | 0.00  | 0.00  | 0.00  | 0.00  | 0.00  | 0.00  | 0.00  |
| FeO                            | 6.95  | 7.12  | 6.75  | 6.63  | 7.59  | 6.74  | 6.57  | 7.18  |
| MnO                            | 0.09  | 0.19  | 0.00  | 0.17  | 0.00  | 0.13  | 0.09  | 0.00  |
| MgO                            | 8.92  | 8.78  | 8.83  | 6.24  | 8.75  | 9.02  | 9.18  | 8.38  |
| CaO                            | 0.00  | 0.00  | 0.00  | 0.00  | 0.00  | 0.00  | 0.00  | 0.00  |
| Na <sub>2</sub> O              | 0.00  | 0.29  | 0.26  | 0.17  | 0.24  | 0.36  | 0.30  | 0.52  |
| K <sub>2</sub> O               | 0.10  | 0.00  | 0.00  | 0.00  | 0.00  | 0.00  | 0.00  | 0.00  |
| Total                          | 97.52 | 96.23 | 95.47 | 97.69 | 98.40 | 97.72 | 97.77 | 96.28 |

## Normalized moles based on 11 total cations and 18(O)

|                  |        |        |        |        |        |        |        |        |
|------------------|--------|--------|--------|--------|--------|--------|--------|--------|
| Si               | 5.044  | 4.983  | 5.001  | 4.708  | 4.990  | 4.989  | 4.995  | 5.016  |
| Al <sup>IV</sup> | 0.956  | 1.017  | 0.999  | 1.292  | 1.010  | 1.011  | 1.005  | 0.984  |
| Al <sup>VI</sup> | 3.015  | 2.093  | 2.962  | 3.422  | 2.967  | 2.956  | 2.969  | 3.012  |
| Ti               | 0.000  | 0.000  | 0.000  | 0.000  | 0.000  | 0.000  | 0.000  | 0.000  |
| Fe <sup>+3</sup> | 0.000  | 0.147  | 0.152  | 0.000  | 0.095  | 0.179  | 0.100  | 0.021  |
| Mn               | 0.006  | 0.019  | 0.000  | 0.012  | 0.000  | 0.012  | 0.006  | 0.000  |
| Fe <sup>+2</sup> | 0.620  | 0.474  | 0.492  | 0.569  | 0.556  | 0.400  | 0.460  | 0.608  |
| Mg               | 1.371  | 1.366  | 1.381  | 0.959  | 1.332  | 1.380  | 1.403  | 1.309  |
| Ca               | 0.000  | 0.000  | 0.000  | 0.000  | 0.000  | 0.000  | 0.000  | 0.000  |
| Na               | 0.000  | 0.063  | 0.063  | 0.037  | 0.049  | 0.074  | 0.061  | 0.050  |
| K                | 0.006  | 0.000  | 0.000  | 0.000  | 0.000  | 0.000  | 0.000  | 0.000  |
| Total            | 11.001 | 11.001 | 10.999 | 10.999 | 10.999 | 11.000 | 10.999 | 11.000 |
| $X_{Mg}$         | 0.689  | 0.687  | 0.682  | 0.628  | 0.672  | 0.704  | 0.715  | 0.675  |
| $X_{Fe}$         | 0.311  | 0.313  | 0.318  | 0.372  | 0.328  | 0.296  | 0.285  | 0.325  |



## APPENDIX B IV

## PLAGIOCLASE

$$X_{an} = Ca/Ca+Na+K$$

$$X_{ab} = Na/Ca+Na+K$$

$$X_{or} = K/Ca+Na+K$$

## MICROPROBE ANALYSES

## PLAGIOCLASE

|                                | BI12   | BL2A   | BL2B  | BL3A   | BL4B   | BO11A  | GO2C  | GO5A  |
|--------------------------------|--------|--------|-------|--------|--------|--------|-------|-------|
| SiO <sub>2</sub>               | 61.33  | 61.39  | 61.02 | 62.81  | 61.02  | 61.22  | 60.78 | 61.06 |
| Al <sub>2</sub> O <sub>3</sub> | 24.35  | 24.59  | 24.23 | 25.15  | 24.97  | 24.48  | 24.15 | 24.34 |
| Fe <sub>2</sub> O <sub>3</sub> | 0.16   | 0.00   | 0.00  | 0.25   | 0.13   | 0.00   | 0.09  | 0.00  |
| CaO                            | 5.70   | 5.90   | 5.73  | 5.94   | 6.93   | 5.88   | 5.80  | 5.81  |
| Na <sub>2</sub> O              | 8.68   | 8.35   | 8.41  | 8.62   | 8.07   | 8.42   | 8.36  | 8.37  |
| K <sub>2</sub> O               | 0.00   | 0.20   | 0.29  | 0.02   | 0.21   | 0.26   | 0.26  | 0.23  |
| Total                          | 100.22 | 100.43 | 99.68 | 102.79 | 101.33 | 100.26 | 99.44 | 99.81 |

## Normalized moles based on 5 total cations

|                  |       |       |       |       |       |       |       |       |
|------------------|-------|-------|-------|-------|-------|-------|-------|-------|
| Si               | 2.711 | 2.713 | 2.712 | 2.713 | 2.678 | 2.202 | 2.710 | 2.714 |
| Al               | 1.269 | 1.280 | 1.272 | 1.280 | 1.293 | 1.275 | 1.271 | 1.277 |
| Fe <sup>+3</sup> | 0.005 | 0.000 | 0.000 | 0.010 | 0.005 | 0.000 | 0.003 | 0.000 |
| Ca               | 0.271 | 0.279 | 0.273 | 0.275 | 0.327 | 0.279 | 0.276 | 0.278 |
| Na               | 0.743 | 0.717 | 0.727 | 0.722 | 0.686 | 0.723 | 0.724 | 0.721 |
| K                | 0.000 | 0.011 | 0.016 | 0.001 | 0.010 | 0.016 | 0.016 | 0.011 |
| Total            | 4.999 | 5.000 | 5.000 | 5.001 | 4.999 | 4.495 | 5.000 | 5.001 |

|                 |       |       |       |       |       |       |       |       |
|-----------------|-------|-------|-------|-------|-------|-------|-------|-------|
| X <sub>an</sub> | 0.267 | 0.277 | 0.269 | 0.276 | 0.320 | 0.272 | 0.272 | 0.275 |
| X <sub>ab</sub> | 0.733 | 0.712 | 0.716 | 0.723 | 0.671 | 0.710 | 0.712 | 0.714 |
| X <sub>or</sub> | 0.000 | 0.011 | 0.016 | 0.001 | 0.010 | 0.016 | 0.016 | 0.110 |

## MICROPROBE ANALYSES

## PLAGIOCLASE

|                                | LPC9A  | LSB1A  | LSB8B  | MB3    | MK1B  | NLS5C | SC3D  | SC5   |
|--------------------------------|--------|--------|--------|--------|-------|-------|-------|-------|
| SiO <sub>2</sub>               | 62.49  | 63.11  | 61.92  | 62.23  | 61.71 | 61.27 | 60.94 | 62.29 |
| Al <sub>2</sub> O <sub>3</sub> | 24.16  | 23.95  | 24.15  | 23.95  | 24.08 | 24.00 | 24.09 | 23.46 |
| Fe <sub>2</sub> O <sub>3</sub> | 0.00   | 0.00   | 0.14   | 0.00   | 0.00  | 0.00  | 0.00  | 0.10  |
| CaO                            | 5.16   | 4.77   | 5.22   | 5.26   | 5.37  | 5.53  | 5.49  | 4.60  |
| Na <sub>2</sub> O              | 9.00   | 9.32   | 8.76   | 8.77   | 8.74  | 8.60  | 8.67  | 9.21  |
| K <sub>2</sub> O               | 0.12   | 0.22   | 0.30   | 0.31   | 0.03  | 0.16  | 0.18  | 0.08  |
| Total                          | 100.93 | 101.37 | 100.49 | 100.52 | 99.93 | 99.56 | 99.37 | 99.74 |

## Normalized moles based on 5 total cations

|                  |       |       |       |       |       |       |       |       |
|------------------|-------|-------|-------|-------|-------|-------|-------|-------|
| Si               | 2.739 | 2.731 | 2.730 | 2.745 | 2.734 | 2.725 | 2.714 | 2.758 |
| Al               | 1.249 | 1.241 | 1.256 | 1.246 | 1.256 | 1.256 | 1.263 | 1.224 |
| Fe <sup>+3</sup> | 0.000 | 0.000 | 0.005 | 0.000 | 0.000 | 0.000 | 0.000 | 0.003 |
| Ca               | 0.242 | 0.224 | 0.246 | 0.249 | 0.255 | 0.265 | 0.262 | 0.218 |
| Na               | 0.764 | 0.792 | 0.747 | 0.747 | 0.751 | 0.743 | 0.750 | 0.793 |
| K                | 0.005 | 0.011 | 0.016 | 0.016 | 0.003 | 0.011 | 0.011 | 0.005 |
| Total            | 4.999 | 4.999 | 5.000 | 5.003 | 4.999 | 5.000 | 5.000 | 5.001 |

|                 |       |       |       |       |       |       |       |       |
|-----------------|-------|-------|-------|-------|-------|-------|-------|-------|
| X <sub>an</sub> | 0.239 | 0.218 | 0.244 | 0.246 | 0.253 | 0.260 | 0.256 | 0.214 |
| X <sub>ab</sub> | 0.756 | 0.771 | 0.740 | 0.738 | 0.744 | 0.729 | 0.733 | 0.781 |
| X <sub>or</sub> | 0.005 | 0.011 | 0.016 | 0.016 | 0.003 | 0.110 | 0.011 | 0.005 |

## MICROPROBE ANALYSES

## PLAGIOCLASE

|                                | SN2    | STB4  |
|--------------------------------|--------|-------|
| SiO <sub>2</sub>               | 61.27  | 59.64 |
| Al <sub>2</sub> O <sub>3</sub> | 24.97  | 25.24 |
| Fe <sub>2</sub> O <sub>3</sub> | 0.10   | 0.12  |
| CaO                            | 6.06   | 6.87  |
| Na <sub>2</sub> O              | 8.51   | 7.98  |
| K <sub>2</sub> O               | 0.18   | 0.12  |
| Total                          | 101.09 | 99.97 |

## Normalized moles based on 5 total cations

|                  |       |       |
|------------------|-------|-------|
| Si               | 2.694 | 2.653 |
| Al               | 1.294 | 1.320 |
| Fe <sup>+3</sup> | 0.003 | 0.005 |
| Ca               | 0.275 | 0.326 |
| Na               | 0.724 | 0.689 |
| K                | 0.011 | 0.005 |
| Total            | 4.999 | 4.999 |

|                 |       |       |
|-----------------|-------|-------|
| X <sub>an</sub> | 0.272 | 0.320 |
| X <sub>ab</sub> | 0.717 | 0.675 |
| X <sub>or</sub> | 0.011 | 0.005 |

APPENDIX C  
GRAVITY RESULTS

## APPENDIX C

## GRAVITY RESULTS

- I Northwest profile - Manitoba
- II Southwest profile - Manitoba
- III South profile - Manitoba
- IV Northeast profile - Manitoba
- V Southeast profile - Manitoba
- VI Ontario profile

APPENDIX C I  
NORTHWEST PROFILE - MANITOBA

## NORTHWEST PROFILE

| Station Number | Distance (km) | Bouguer Gravity (mgal) | Degrees | Latitude Minutes | Seconds |
|----------------|---------------|------------------------|---------|------------------|---------|
| MN28           | 0             | -19.87                 | 50      | 53               | 54      |
| MN29           | 0.286         | -20.50                 | 50      | 54               | 4       |
| MN30           | 0.956         | -22.56                 | 50      | 54               | 27      |
| MN31           | 1.68          | -23.94                 | 50      | 54               | 52      |
| MN32           | 2.387         | -24.19                 | 50      | 55               | 16      |
| MN33           | 3.057         | -24.50                 | 50      | 55               | 39      |
| MN34           | 3.808         | -23.87                 | 50      | 56               | 5       |
| MN35           | 4.595         | -25.44                 | 50      | 56               | 32      |
| MN36           | 5.507         | -25.25                 | 50      | 57               | 3       |
| MN37           | 6.24          | -25.31                 | 50      | 57               | 28      |
| MN38           | 6.901         | -24.37                 | 50      | 57               | 51      |
| MN39           | 7.76          | -26.31                 | 50      | 58               | 20      |
| MN40           | 8.859         | -27.25                 | 50      | 58               | 58      |
| MN41           | 9.244         | -27.44                 | 50      | 59               | 11      |
| MN42           | 9.914         | -29.62                 | 50      | 59               | 34      |
| MN43           | 10.665        | -29.06                 | 51      | 0                | 0       |
| MN44           | 11.076        | -29.06                 | 51      | 0                | 14      |
| MN45           | 11.845        | -29.37                 | 51      | 0                | 40      |
| MN46           | 12.444        | -27.12                 | 51      | 1                | 11      |
| MN47           | 13.204        | -26.12                 | 51      | 1                | 27      |
| MN48           | 13.901        | -27.50                 | 51      | 1                | 51      |
| MN49           | 14.545        | -27.19                 | 51      | 2                | 13      |
| MN50           | 15.108        | -26.62                 | 51      | 2                | 32      |
| MN51           | 15.653        | -25.44                 | 51      | 2                | 51      |
| MN52           | 16.154        | -25.25                 | 51      | 3                | 8       |
| MN53           | 16.825        | -24.31                 | 51      | 3                | 31      |
| MN54           | 17.584        | -26.44                 | 51      | 3                | 37      |
| MN55           | 18.344        | -27.06                 | 51      | 4                | 23      |
| MN56           | 19.068        | -25.94                 | 51      | 4                | 48      |
| MN57           | 19.685        | -24.75                 | 51      | 5                | 9       |
| MN58           | 20.463        | -18.81                 | 51      | 5                | 36      |
| MN59           | 21.348        | -18.25                 | 51      | 6                | 6       |
| MN60           | 21.956        | -17.87                 | 51      | 6                | 27      |
| MN61           | 22.6          | -19.06                 | 51      | 6                | 49      |
| MN62           | 23.351        | -20.62                 | 51      | 7                | 15      |
| MN63           | 24.092        | -17.25                 | 51      | 7                | 40      |



## NORTHWEST PROFILE (CONT.)

| Station Number | Distance (km) | Bouguer Gravity (mgal) | Latitude Degrees | Minutes | Seconds |
|----------------|---------------|------------------------|------------------|---------|---------|
| MN64           | 24.986        | -15.25                 | 51               | 8       | 11      |
| MN65           | 25.63         | -14.19                 | 51               | 8       | 33      |
| MN66           | 26.444        | -13.31                 | 51               | 9       | 1       |
| MN67           | 27.23         | -13.75                 | 51               | 9       | 28      |
| MN68           | 27.874        | -12.50                 | 51               | 9       | 50      |
| MN69           | 28.348        | -15.94                 | 51               | 10      | 6       |
| MN70           | 29.018        | -17.69                 | 51               | 10      | 29      |
| MN71           | 29.68         | -17.06                 | 51               | 10      | 52      |

APPENDIX C II  
SOUTHWEST PROFILE - MANITOBA

## SOUTHWEST PROFILE

| Station Number | Distance (km) | Bouguer Gravity (mgal) | Latitude |         |         |
|----------------|---------------|------------------------|----------|---------|---------|
|                |               |                        | Degrees  | Minutes | Seconds |
| P20            | .0            | -15.31                 | 50       | 34      | 20      |
| P19            | 1.291         | -14.87                 | 50       | 35      | 2       |
| P18            | 2.871         | -14.56                 | 50       | 35      | 54      |
| P17            | 4.356         | -17.12                 | 50       | 36      | 42      |
| P16            | 4.742         | -17.50                 | 50       | 36      | 55      |
| P15            | 6.247         | -19.50                 | 50       | 37      | 44      |
| P14            | 6.831         | -19.37                 | 50       | 38      | 3       |
| P13            | 8.395         | -21.75                 | 50       | 38      | 54      |
| P12            | 8.831         | -23.31                 | 50       | 39      | 8       |
| P11            | 9.563         | -21.31                 | 50       | 39      | 32      |
| P10            | 10.266        | -24.19                 | 50       | 39      | 55      |
| P9             | 10.989        | -22.56                 | 50       | 40      | 19      |
| P8             | 11.742        | -22.56                 | 50       | 40      | 43      |
| P7             | 12.593        | -22.37                 | 50       | 41      | 11      |
| P6             | 13.237        | -21.56                 | 50       | 41      | 32      |
| P5             | 13.92         | -20.81                 | 50       | 41      | 54      |
| P4             | 14.157        | -20.44                 | 50       | 42      | 2       |
| P3             | 14.771        | -21.37                 | 50       | 42      | 22      |
| P2             | 15.414        | -20.06                 | 50       | 42      | 43      |
| P1             | 16.019        | -20.31                 | 50       | 43      | 3       |
| P0             | 16.642        | -20.25                 | 50       | 43      | 23      |
| MN1            | 17.256        | -21.44                 | 50       | 43      | 43      |
| MN2            | 18.108        | -21.25                 | 50       | 44      | 11      |
| MN3            | 18.791        | -16.94                 | 50       | 44      | 33      |
| MN4            | 19.612        | -17.06                 | 50       | 45      | 0       |
| MN5            | 20.187        | -16.31                 | 50       | 45      | 19      |
| MN6            | 20.929        | -15.62                 | 50       | 45      | 43      |
| MN7            | 21.365        | -14.69                 | 50       | 45      | 57      |
| MN8            | 21.85         | -13.12                 | 50       | 46      | 13      |
| MN9            | 22.404        | -11.69                 | 50       | 46      | 31      |
| MN10           | 23.008        | -11.62                 | 50       | 46      | 51      |
| MN11           | 23.533        | -11.19                 | 50       | 47      | 8       |
| MN12           | 24.147        | -11.94                 | 50       | 47      | 28      |
| MN13           | 24.572        | -11.37                 | 50       | 47      | 42      |
| MN14           | 25.186        | -11.12                 | 50       | 48      | 2       |
| MN15           | 25.949        | -9.81                  | 50       | 48      | 27      |
| MN16           | 26.781        | -10.06                 | 50       | 48      | 54      |
| MN17           | 27.641        | -12.25                 | 50       | 49      | 22      |
| MN18           | 28.473        | -14.87                 | 50       | 49      | 49      |
| MN19           | 29.235        | -14.75                 | 50       | 50      | 14      |

## SOUTHWEST PROFILE (CONT.)

| Station Number | Distance (km) | Bouguer Gravity (mgal) | Latitude Degrees | Minutes | Seconds |
|----------------|---------------|------------------------|------------------|---------|---------|
| MN20           | 30.057        | -14.69                 | 50               | 50      | 41      |
| MN21           | 30.76         | -15.56                 | 50               | 51      | 4       |
| MN22           | 31.473        | -16.31                 | 50               | 51      | 27      |
| MN23           | 31.958        | -15.06                 | 50               | 51      | 43      |
| MN24           | 32.79         | -15.81                 | 50               | 52      | 10      |
| MN25           | 33.582        | -16.37                 | 50               | 52      | 36      |
| MN26           | 34.294        | -17.81                 | 50               | 52      | 59      |
| MN27           | 35.086        | -17.69                 | 50               | 53      | 25      |
| MN28           | 35.987        | -19.87                 | 50               | 53      | 54      |

APPENDIX C III  
SOUTH PROFILE - MANITOBA

## SOUTH PROFILE

| Station Number | Distance (km) | Bouguer Gravity (mgal) | Latitude |         |         |
|----------------|---------------|------------------------|----------|---------|---------|
|                |               |                        | Degrees  | Minutes | Seconds |
| LDB74          | 0             | -65.00                 | 49       | 37      | 31      |
| LDB73          | 0.977         | -65.44                 | 49       | 38      | 5       |
| LDB72          | 2.477         | -60.00                 | 49       | 38      | 57      |
| LDB71          | 3.995         | -56.50                 | 49       | 39      | 50      |
| LDB70          | 5.382         | -53.50                 | 49       | 40      | 38      |
| LDB69          | 6.97          | -52.19                 | 49       | 41      | 33      |
| LDB68          | 8.619         | -49.44                 | 49       | 42      | 30      |
| LDB67          | 10.189        | -48.81                 | 49       | 43      | 25      |
| LDB66          | 11.69         | -47.44                 | 49       | 44      | 17      |
| LDB65          | 12.553        | -46.75                 | 49       | 44      | 47      |
| LDB64          | 13.966        | -44.69                 | 49       | 45      | 36      |
| LDB63          | 15.502        | -42.37                 | 49       | 46      | 29      |
| LDB62          | 16.278        | -41.50                 | 49       | 46      | 56      |
| LDB61          | 17.84         | -40.44                 | 49       | 47      | 49      |
| LDB60          | 19.375        | -36.94                 | 49       | 48      | 44      |
| LDB59          | 20.858        | -36.62                 | 49       | 49      | 35      |
| LDB58          | 22.376        | -37.25                 | 49       | 50      | 28      |
| LDB57          | 23.911        | -33.87                 | 49       | 51      | 21      |
| LDB56          | 25.429        | -35.69                 | 49       | 52      | 14      |
| LDB55          | 25.953        | -34.50                 | 49       | 52      | 32      |
| LDB54          | 27.366        | -35.50                 | 49       | 53      | 21      |
| LDB53          | 28.639        | -35.94                 | 49       | 54      | 5       |
| LDB52          | 30.131        | -36.06                 | 49       | 54      | 57      |
| LDB51          | 31.597        | -37.81                 | 49       | 55      | 48      |
| LDB50          | 32.399        | -37.81                 | 49       | 56      | 16      |
| LDB49          | 33.586        | -34.50                 | 49       | 56      | 57      |
| LDB48          | 34.912        | -35.56                 | 49       | 57      | 43      |
| LDB47          | 36.211        | -36.06                 | 49       | 58      | 28      |
| LDB46          | 37.703        | -36.75                 | 49       | 59      | 20      |
| LDB45          | 39.256        | -37.37                 | 50       | 0       | 14      |
| LDB44          | 40.722        | -38.19                 | 50       | 1       | 5       |
| LDB43          | 42.257        | -37.94                 | 50       | 1       | 58      |
| LDB42          | 43.609        | -40.12                 | 50       | 2       | 45      |
| LDB41          | 45.048        | -40.62                 | 50       | 3       | 35      |
| LDB40          | 46.723        | -41.75                 | 50       | 4       | 33      |
| LDB39          | 47.787        | -43.12                 | 50       | 5       | 10      |
| LDB38          | 48.974        | -44.56                 | 50       | 5       | 51      |
| LDB37          | 49.689        | -44.12                 | 50       | 6       | 16      |
| LDB36          | 51.19         | -44.87                 | 50       | 7       | 8       |
| LDB35          | 52.742        | -45.06                 | 50       | 8       | 2       |

## SOUTH PROFILE (CONT.)

| Station Number | Distance (km) | Bouguer Gravity (mgal) | Latitude |         |         |
|----------------|---------------|------------------------|----------|---------|---------|
|                |               |                        | Degrees  | Minutes | Seconds |
| LDB34          | 54.191        | -43.87                 | 50       | 8       | 52      |
| LDB33          | 55.77         | -43.87                 | 50       | 9       | 47      |
| LDB32          | 57.322        | -44.06                 | 50       | 10      | 41      |
| LDB31          | 58.762        | -44.37                 | 50       | 11      | 31      |
| LDB30          | 60.289        | -42.44                 | 50       | 12      | 24      |
| LDB29          | 61.85         | -40.56                 | 50       | 13      | 18      |
| LDB28          | 63.481        | -39.56                 | 50       | 14      | 15      |
| LDB27          | 64.066        | -39.12                 | 50       | 14      | 35      |
| LDB26          | 65.444        | -38.44                 | 50       | 15      | 23      |
| LDB25          | 66.482        | -37.06                 | 50       | 15      | 59      |
| LDB24          | 68.07         | -34.00                 | 50       | 16      | 18      |
| LDB23          | 69.57         | -36.69                 | 50       | 16      | 45      |
| LDB22          | 70.8          | -32.37                 | 50       | 18      | 29      |
| LDB21          | 71.725        | -31.81                 | 50       | 19      | 1       |
| LDB20          | 73.112        | -31.69                 | 50       | 19      | 49      |
| LDB19          | 73.862        | -31.69                 | 50       | 20      | 15      |
| LDB18          | 75.415        | -31.19                 | 50       | 21      | 9       |
| LDB17          | 76.741        | -33.25                 | 50       | 21      | 55      |
| LDB16          | 78.529        | -34.06                 | 50       | 22      | 57      |
| LDB15          | 79.811        | -33.25                 | 50       | 23      | 42      |
| LDB14          | 80.204        | -32.75                 | 50       | 23      | 55      |
| LDB13          | 81.958        | -31.69                 | 50       | 24      | 56      |
| LDB12          | 83.162        | -30.50                 | 50       | 25      | 38      |
| LDB11          | 84.61         | -28.69                 | 50       | 26      | 28      |
| LDB10          | 86.311        | -30.56                 | 50       | 27      | 27      |
| LDB9           | 87.515        | -24.62                 | 50       | 28      | 9       |
| LDB8           | 88.125        | -24.37                 | 50       | 28      | 30      |
| LDB7           | 89.006        | -24.87                 | 50       | 29      | 1       |
| LDB6           | 90.568        | -22.94                 | 50       | 29      | 55      |
| LDB5           | 91.772        | -22.87                 | 50       | 30      | 37      |
| LDB4           | 92.958        | -19.19                 | 50       | 31      | 18      |
| LDB3           | 94.11         | -18.00                 | 50       | 31      | 58      |
| LDB2           | 95.601        | -17.75                 | 50       | 32      | 50      |
| LDB1           | 97.05         | -14.19                 | 50       | 33      | 40      |
| P20            | 98.201        | -15.31                 | 50       | 34      | 20      |

APPENDIX C IV  
NORTHEAST PROFILE - MANITOBA



## NORTHEAST PROFILE

| Station Number | Distance (km) | Bouguer Gravity (mgal) | Latitude |         |         |
|----------------|---------------|------------------------|----------|---------|---------|
|                |               |                        | Degrees  | Minutes | Seconds |
| NP100          | 0             | -71.75                 | 50       | 32      | 57      |
| NP99           | 0.524         | -70.50                 | 50       | 33      | 18      |
| NP98           | 0.949         | -72.38                 | 50       | 33      | 35      |
| NP97           | 1.649         | -69.19                 | 50       | 34      | 3       |
| NP96           | 2.022         | -71.81                 | 50       | 34      | 18      |
| NP95           | 2.192         | -71.50                 | 50       | 34      | 25      |
| NP94           | 2.539         | -71.06                 | 50       | 34      | 39      |
| NP93           | 2.768         | -67.56                 | 50       | 34      | 48      |
| NP92           | 3.364         | -54.69                 | 50       | 35      | 12      |
| NP91           | 3.914         | -58.81                 | 50       | 35      | 34      |
| NP90           | 4.562         | -57.12                 | 50       | 36      | 0       |
| NP89           | 4.882         | -61.50                 | 50       | 36      | 13      |
| NP86           | 5.655         | -58.00                 | 50       | 36      | 44      |
| NP85           | 6.034         | -57.69                 | 50       | 36      | 59      |
| NP84           | 6.656         | -64.37                 | 50       | 37      | 24      |
| NP83           | 7.232         | -71.06                 | 50       | 37      | 47      |
| NP82           | 7.808         | -76.75                 | 50       | 38      | 10      |
| NP81           | 8.011         | -72.38                 | 50       | 38      | 18      |
| NP80           | 8.43          | -70.75                 | 50       | 38      | 35      |
| NP76           | 9.3           | -73.31                 | 50       | 39      | 10      |
| NP75           | 9.726         | -75.88                 | 50       | 39      | 27      |
| NP74           | 10.321        | -74.94                 | 50       | 39      | 51      |
| NP73           | 10.596        | -76.00                 | 50       | 40      | 2       |
| NP65           | 11.493        | -78.38                 | 50       | 40      | 38      |
| NP64           | 11.898        | -74.63                 | 50       | 40      | 54      |
| NP63           | 12.121        | -80.00                 | 50       | 41      | 3       |
| NP62           | 12.298        | -81.94                 | 50       | 41      | 10      |
| NP61           | 12.344        | -79.31                 | 50       | 41      | 12      |
| NP60           | 12.671        | -81.25                 | 50       | 41      | 25      |
| NP59           | 12.946        | -82.56                 | 50       | 41      | 36      |
| NP58           | 13.22         | -76.81                 | 50       | 41      | 47      |
| NP57           | 14.117        | -80.81                 | 50       | 42      | 23      |
| NP56           | 14.693        | -77.88                 | 50       | 42      | 46      |
| NP55           | 15.014        | -79.69                 | 50       | 42      | 59      |
| NP54           | 15.91         | -81.06                 | 50       | 43      | 35      |
| NP53           | 16.329        | -81.56                 | 50       | 43      | 52      |
| NP52           | 16.656        | -78.50                 | 50       | 44      | 5       |
| NP51           | 17.311        | -76.69                 | 50       | 44      | 31      |
| NP50           | 18.005        | -80.75                 | 50       | 44      | 59      |
| NP49           | 18.404        | -76.56                 | 50       | 45      | 15      |

## NORTHEAST PROFILE (CONT.)

| Station Number | Distance (km) | Bouguer Gravity (mgal) | Latitude |         |         |
|----------------|---------------|------------------------|----------|---------|---------|
|                |               |                        | Degrees  | Minutes | Seconds |
| NP48           | 19            | -74.38                 | 50       | 45      | 39      |
| NP47           | 19.353        | -74.63                 | 50       | 45      | 53      |
| NP46           | 19.706        | -77.00                 | 50       | 46      | 7       |
| NP45           | 20.027        | -73.69                 | 50       | 46      | 20      |
| NP44           | 20.675        | -74.38                 | 50       | 46      | 46      |
| NP43           | 21.323        | -71.56                 | 50       | 47      | 12      |
| NP42           | 21.722        | -72.06                 | 50       | 47      | 28      |
| NP41           | 22.095        | -73.25                 | 50       | 47      | 43      |
| NP40           | 22.521        | -70.56                 | 50       | 48      | 0       |
| NP39           | 23.214        | -73.13                 | 50       | 48      | 28      |
| NP38           | 23.79         | -71.06                 | 50       | 48      | 51      |
| NP37           | 24.445        | -64.37                 | 50       | 49      | 17      |
| NP36           | 25.067        | -64.25                 | 50       | 49      | 42      |
| NP35           | 25.669        | -56.31                 | 50       | 50      | 6       |
| NP34           | 25.97         | -63.75                 | 50       | 50      | 18      |
| NP32           | 26.408        | -66.56                 | 50       | 50      | 36      |
| NP30           | 27.056        | -56.56                 | 50       | 51      | 2       |
| NP29           | 27.462        | -55.87                 | 50       | 51      | 18      |
| NP28           | 27.861        | -60.56                 | 50       | 51      | 34      |
| NP27           | 28.28         | -55.37                 | 50       | 51      | 51      |
| NP26           | 28.954        | -54.00                 | 50       | 52      | 18      |
| NP23           | 29.726        | -55.31                 | 50       | 52      | 49      |
| NP22           | 30.604        | -59.75                 | 50       | 53      | 24      |
| NP21           | 31.173        | -59.56                 | 50       | 53      | 47      |
| NP20           | 31.546        | -63.25                 | 50       | 54      | 2       |
| NP19           | 32.024        | -64.19                 | 50       | 54      | 21      |
| NP18           | 32.6          | -62.56                 | 50       | 54      | 44      |
| NP17           | 33.149        | -61.06                 | 50       | 55      | 6       |
| NP16           | 33.843        | -56.00                 | 50       | 55      | 34      |
| NP15           | 34.4          | -57.69                 | 50       | 55      | 56      |
| NP14           | 34.995        | -53.56                 | 50       | 56      | 20      |
| NP13           | 35.388        | -56.62                 | 50       | 56      | 36      |
| NP12           | 35.964        | -59.37                 | 50       | 56      | 59      |
| NP11           | 36.494        | -57.19                 | 50       | 57      | 20      |
| NP10           | 36.841        | -60.00                 | 50       | 57      | 34      |
| NP9            | 37.26         | -59.06                 | 50       | 57      | 51      |
| NP8            | 37.914        | -61.44                 | 50       | 58      | 17      |
| NP7            | 38.333        | -64.62                 | 50       | 58      | 34      |
| NP6            | 38.837        | -65.25                 | 50       | 58      | 54      |

## NORTHEAST PROFILE (CONT.)

| Station Number | Distance (km) | Bouguer Gravity (mgal) | Latitude Degrees | Minutes | Seconds |
|----------------|---------------|------------------------|------------------|---------|---------|
| NP5            | 39.079        | -64.56                 | 50               | 59      | 4       |
| NP4            | 39.655        | -65.50                 | 50               | 59      | 27      |
| NP3            | 40.231        | -68.00                 | 50               | 59      | 50      |
| NP2            | 40.63         | -67.94                 | 51               | 0       | 6       |

APPENDIX C V  
SOUTHEAST PROFILE - MANITOBA

## SOUTHEAST PROFILE

| Station Number | Distance (km) | Bouguer Gravity (mgal) | Latitude |         |         |
|----------------|---------------|------------------------|----------|---------|---------|
|                |               |                        | Degrees  | Minutes | Seconds |
| NP141          | .0            | -46.37                 | 50       | 16      | 18      |
| NP140          | 0.806         | -46.44                 | 50       | 16      | 45      |
| NP139          | 1.404         | -50.56                 | 50       | 17      | 5       |
| NP138          | 2.248         | -49.19                 | 50       | 17      | 33      |
| NP137          | 3.112         | -50.94                 | 50       | 18      | 2       |
| NP136          | 3.766         | -48.69                 | 50       | 18      | 24      |
| NP135          | 4.525         | -50.25                 | 50       | 18      | 49      |
| NP134          | 5.275         | -47.94                 | 50       | 19      | 14      |
| NP133          | 6.299         | -48.50                 | 50       | 19      | 48      |
| NP132          | 7.077         | -51.94                 | 50       | 20      | 14      |
| NP131          | 7.827         | -49.19                 | 50       | 20      | 39      |
| NP130          | 8.728         | -46.56                 | 50       | 21      | 9       |
| NP129          | 9.42          | -45.50                 | 50       | 21      | 32      |
| NP128          | 10.227        | -46.31                 | 50       | 21      | 59      |
| NP127          | 10.976        | -48.06                 | 50       | 22      | 24      |
| NP126          | 11.667        | -51.06                 | 50       | 22      | 47      |
| NP125          | 12.342        | -42.00                 | 50       | 23      | 10      |
| NP124          | 13.414        | -37.44                 | 50       | 23      | 45      |
| NP123          | 14.249        | -37.00                 | 50       | 24      | 13      |
| NP121          | 15.273        | -37.69                 | 50       | 24      | 47      |
| NP120          | 15.776        | -41.56                 | 50       | 25      | 4       |
| NP119          | 16.383        | -42.87                 | 50       | 25      | 24      |
| NP118          | 17.284        | -44.94                 | 50       | 25      | 54      |
| NP117          | 18.063        | -44.81                 | 50       | 26      | 20      |
| NP116          | 18.936        | -41.00                 | 50       | 26      | 49      |
| NP115          | 19.834        | -42.87                 | 50       | 27      | 19      |
| NP114          | 20.7          | -47.69                 | 50       | 27      | 48      |
| NP113          | 21.279        | -49.25                 | 50       | 28      | 7       |
| NP112          | 21.971        | -46.50                 | 50       | 28      | 30      |
| NP111          | 22.616        | -45.50                 | 50       | 28      | 52      |
| NP110          | 23.1          | -48.25                 | 50       | 29      | 8       |
| NP109          | 23.669        | -52.00                 | 50       | 29      | 27      |
| NP108          | 24.362        | -58.44                 | 50       | 29      | 50      |
| NP107          | 25.235        | -59.56                 | 50       | 30      | 19      |
| NP106          | 25.481        | -62.37                 | 50       | 30      | 27      |
| NP105          | 26.288        | -68.13                 | 50       | 30      | 54      |

## SOUTHEAST PROFILE (CONT.)

| Station Number | Distance (km) | Bouguer Gravity (mgal) | Latitude Degrees | Latitude Minutes | Latitude Seconds |
|----------------|---------------|------------------------|------------------|------------------|------------------|
| NP104          | 27.037        | -67.25                 | 50               | 31               | 19               |
| NP103          | 27.815        | -70.94                 | 50               | 31               | 45               |
| NP102          | 28.536        | -69.94                 | 50               | 32               | 9                |
| NP101          | 29.314        | -69.63                 | 50               | 32               | 35               |
| NP100          | 29.978        | -71.75                 | 50               | 32               | 57               |

APPENDIX C VI  
ONTARIO PROFILE

## ONTARIO PROFILE

| Station Number | Distance (km) | Bouguer Gravity (mgal) | Latitude |         |
|----------------|---------------|------------------------|----------|---------|
|                |               |                        | Degrees  | Minutes |
| 161            | 0             | -48.36                 | 49       | 51.20   |
| 160            | 1.3           | -46.08                 | 49       | 51.90   |
| 159            | 3.15          | -41.48                 | 49       | 52.90   |
| 158            | 4.07          | -41.34                 | 49       | 53.40   |
| 157            | 5.74          | -41.79                 | 49       | 54.30   |
| 156            | 7.03          | -43.32                 | 49       | 55.00   |
| 155            | 8.14          | -43.74                 | 49       | 55.60   |
| 154            | 10.18         | -41.74                 | 49       | 56.70   |
| 153            | 12.03         | -40.06                 | 49       | 57.70   |
| 152            | 13.14         | -39.75                 | 49       | 58.30   |
| 151            | 13.69         | -39.17                 | 49       | 58.60   |
| 150            | 14.06         | -38.73                 | 49       | 58.80   |
| 149            | 15.91         | -37.77                 | 49       | 59.80   |
| 148            | 16.47         | -36.64                 | 50       | 0.10    |
| 147            | 17.02         | -36.80                 | 50       | 0.40    |
| 146            | 17.95         | -36.17                 | 50       | 0.90    |
| 145            | 18.87         | -34.81                 | 50       | 1.40    |
| 144            | 19.98         | -33.40                 | 50       | 2.00    |
| 143            | 20.91         | -33.86                 | 50       | 2.50    |
| 142            | 21.28         | -33.17                 | 50       | 2.70    |
| 141            | 22.39         | -33.21                 | 50       | 3.30    |
| 140            | 22.76         | -33.49                 | 50       | 3.50    |
| 139            | 24.05         | -33.39                 | 50       | 4.20    |
| 138            | 25.35         | -32.31                 | 50       | 4.90    |
| 137            | 26.46         | -31.46                 | 50       | 5.50    |
| 136            | 28.12         | -31.41                 | 50       | 6.40    |
| 135            | 29.05         | -30.25                 | 50       | 6.90    |
| 134            | 31.45         | -32.05                 | 50       | 8.20    |
| 133            | 32.75         | -30.67                 | 50       | 8.90    |
| 132            | 33.86         | -30.40                 | 50       | 9.50    |
| 131            | 34.97         | -32.77                 | 50       | 10.10   |
| 130            | 35.52         | -34.80                 | 50       | 10.40   |
| 129            | 35.71         | -34.67                 | 50       | 10.50   |
| 128            | 36.82         | -34.24                 | 50       | 11.10   |
| 127            | 37.93         | -34.30                 | 50       | 11.70   |
| 126            | 39.22         | -33.80                 | 50       | 12.40   |
| 125            | 39.96         | -33.15                 | 50       | 12.80   |
| 124            | 40.33         | -34.84                 | 50       | 13.00   |
| 123            | 42.18         | -33.53                 | 50       | 14.00   |
| 122            | 43.48         | -34.07                 | 50       | 14.70   |



## ONTARIO PROFILE (CONT.)

| Station Number | Distance (km) | Bouguer Gravity (mgal) | Latitude |         |
|----------------|---------------|------------------------|----------|---------|
|                |               |                        | Degrees  | Minutes |
| 121            | 44.59         | -35.80                 | 50       | 15.30   |
| 120            | 45.33         | -33.95                 | 50       | 15.70   |
| 119            | 46.81         | -34.14                 | 50       | 16.50   |
| 118            | 48.47         | -35.16                 | 50       | 17.40   |
| 117            | 49.21         | -36.19                 | 50       | 17.80   |
| 116            | 49.77         | -35.73                 | 50       | 18.10   |
| 115            | 50.32         | -35.82                 | 50       | 18.40   |
| 114            | 52.73         | -35.59                 | 50       | 19.70   |
| 113            | 54.21         | -34.99                 | 50       | 20.50   |
| 112            | 54.76         | -35.32                 | 50       | 20.80   |
| 111            | 55.32         | -35.82                 | 50       | 21.10   |
| 110            | 56.61         | -35.26                 | 50       | 21.80   |
| 109            | 58.09         | -34.61                 | 50       | 22.60   |
| 108            | 59.57         | -36.54                 | 50       | 23.40   |
| 107            | 61.42         | -38.20                 | 50       | 24.40   |
| 106            | 61.79         | -34.88                 | 50       | 24.60   |
| 105            | 63.46         | -31.54                 | 50       | 25.50   |
| 104            | 64.94         | -31.44                 | 50       | 26.30   |
| 103            | 67.16         | -30.98                 | 50       | 27.50   |
| 102            | 68.64         | -31.51                 | 50       | 28.30   |
| 101            | 69.93         | -28.64                 | 50       | 29.00   |
| 100            | 71.23         | -26.26                 | 50       | 29.70   |
| 99             | 72.52         | -26.96                 | 50       | 30.40   |
| 98             | 72.71         | -25.15                 | 50       | 30.50   |
| 97             | 74            | -24.77                 | 50       | 31.20   |
| 96             | 76.04         | -24.43                 | 50       | 32.30   |
| 95             | 77.89         | -25.69                 | 50       | 33.30   |
| 94             | 79.92         | -27.62                 | 50       | 34.40   |
| 93             | 81.77         | -29.60                 | 50       | 35.40   |
| 92             | 82.14         | -29.40                 | 50       | 35.60   |
| 91             | 83.25         | -30.29                 | 50       | 36.20   |
| 90             | 84.73         | -31.97                 | 50       | 37.00   |
| 89             | 87.14         | -32.23                 | 50       | 38.30   |
| 88             | 87.32         | -33.36                 | 50       | 38.40   |
| 87             | 90.71         | -39.14                 | 50       | 40.23   |
| 86             | 91.34         | -39.30                 | 50       | 40.57   |
| 85             | 91.5          | -40.15                 | 50       | 40.66   |
| 84             | 92.34         | -40.42                 | 50       | 41.11   |
| 83             | 92.61         | -41.16                 | 50       | 41.26   |
| 82             | 93.15         | -41.61                 | 50       | 41.55   |

## ONTARIO PROFILE (CONT.)

| Station Number | Distance (km) | Bouguer Gravity (mgal) | Latitude |         |
|----------------|---------------|------------------------|----------|---------|
|                |               |                        | Degrees  | Minutes |
| 81             | 93.85         | -44.89                 | 50       | 41.93   |
| 80             | 94.07         | -43.89                 | 50       | 42.05   |
| 79             | 94.41         | -44.87                 | 50       | 42.23   |
| 78             | 94.76         | -45.45                 | 50       | 42.42   |
| 77             | 95.65         | -46.87                 | 50       | 42.90   |
| 76             | 96.19         | -47.08                 | 50       | 43.19   |
| 75             | 96.66         | -46.60                 | 50       | 43.45   |
| 74             | 97.31         | -46.86                 | 50       | 43.80   |
| 73             | 97.88         | -47.44                 | 50       | 44.11   |
| 72             | 98.5          | -47.57                 | 50       | 44.44   |
| 71             | 98.66         | -47.60                 | 50       | 44.53   |
| 70             | 99.09         | -48.24                 | 50       | 44.76   |
| 69             | 99.59         | -48.18                 | 50       | 45.03   |
| 68             | 100.25        | -48.18                 | 50       | 45.39   |
| 67             | 100.9         | -48.71                 | 50       | 45.74   |
| 66             | 101.44        | -47.78                 | 50       | 46.03   |
| 65             | 102.23        | -46.72                 | 50       | 46.46   |
| 64             | 102.86        | -44.60                 | 50       | 46.80   |
| 63             | 103.47        | -40.03                 | 50       | 47.13   |
| 62             | 103.99        | -40.52                 | 50       | 47.41   |
| 61             | 104.75        | -40.97                 | 50       | 47.82   |
| 60             | 105.27        | -40.16                 | 50       | 48.10   |
| 59             | 105.42        | -43.20                 | 50       | 48.18   |
| 58             | 105.93        | -45.08                 | 50       | 48.46   |
| 57             | 106.16        | -42.31                 | 50       | 48.58   |
| 56             | 106.53        | -46.45                 | 50       | 48.78   |
| 55             | 107.26        | -47.94                 | 50       | 49.18   |
| 54             | 107.9         | -48.44                 | 50       | 49.52   |
| 53             | 108.26        | -48.28                 | 50       | 49.72   |
| 52             | 109.01        | -49.47                 | 50       | 50.12   |
| 51             | 109.56        | -50.41                 | 50       | 50.42   |
| 50             | 110.3         | -56.64                 | 50       | 50.82   |
| 49             | 110.65        | -53.71                 | 50       | 51.01   |
| 48             | 111.06        | -53.47                 | 50       | 51.23   |
| 47             | 111.48        | -54.75                 | 50       | 51.46   |
| 46             | 111.82        | -55.29                 | 50       | 51.64   |
| 45             | 112.22        | -55.22                 | 50       | 51.86   |
| 44             | 112.54        | -55.81                 | 50       | 52.03   |
| 43             | 112.94        | -55.90                 | 50       | 52.25   |
| 42             | 113.31        | -56.45                 | 50       | 52.45   |

## ONTARIO PROFILE (CONT.)

| Station Number | Distance (km) | Bouguer Gravity (mgal) | Latitude |         |
|----------------|---------------|------------------------|----------|---------|
|                |               |                        | Degrees  | Minutes |
| 41             | 113.63        | -57.04                 | 50       | 52.62   |
| 40             | 113.96        | -56.45                 | 50       | 52.80   |
| 39             | 114.26        | -59.79                 | 50       | 52.96   |
| 38             | 114.52        | -56.71                 | 50       | 53.10   |
| 37             | 114.59        | -58.49                 | 50       | 53.14   |
| 36             | 114.81        | -57.83                 | 50       | 53.26   |
| 35             | 115.11        | -58.47                 | 50       | 53.42   |
| 34             | 115.39        | -58.99                 | 50       | 53.57   |
| 33             | 115.63        | -59.48                 | 50       | 53.70   |
| 32             | 115.89        | -59.19                 | 50       | 53.84   |
| 31             | 116.16        | -59.19                 | 50       | 53.99   |
| 30             | 116.53        | -60.30                 | 50       | 54.19   |
| 29             | 117.27        | -60.52                 | 50       | 54.59   |
| 28             | 118           | -59.45                 | 50       | 54.98   |
| 27             | 118.59        | -58.19                 | 50       | 55.30   |
| 26             | 118.92        | -55.07                 | 50       | 55.48   |
| 25             | 119.23        | -55.05                 | 50       | 55.65   |
| 24             | 119.51        | -52.45                 | 50       | 55.80   |
| 23             | 119.87        | -51.43                 | 50       | 55.99   |
| 22             | 120.29        | -51.05                 | 50       | 56.22   |
| 21             | 120.64        | -51.11                 | 50       | 56.41   |
| 20             | 121.03        | -52.46                 | 50       | 56.62   |
| 19             | 121.23        | -52.54                 | 50       | 56.73   |
| 18             | 121.34        | -51.93                 | 50       | 56.79   |
| 17             | 121.49        | -51.09                 | 50       | 56.87   |
| 16             | 121.7         | -51.13                 | 50       | 56.98   |
| 15             | 121.9         | -50.51                 | 50       | 57.09   |
| 14             | 122.1         | -50.96                 | 50       | 57.20   |
| 13             | 122.25        | -50.92                 | 50       | 57.28   |
| 12             | 122.46        | -50.40                 | 50       | 57.39   |
| 11             | 122.49        | -50.37                 | 50       | 57.41   |
| 10             | 122.66        | -51.06                 | 50       | 57.50   |
| 9              | 122.95        | -52.06                 | 50       | 57.66   |
| 8              | 123.32        | -53.63                 | 50       | 57.86   |
| 7              | 123.68        | -55.73                 | 50       | 58.05   |

## ONTARIO PROFILE (CONT.)

| Station Number | Distance (km) | Bouguer Gravity (mgal) | Latitude |         |
|----------------|---------------|------------------------|----------|---------|
|                |               |                        | Degrees  | Minutes |
| 6              | 123.92        | -56.54                 | 50       | 58.18   |
| 5              | 124.21        | -57.42                 | 50       | 58.34   |
| 4              | 124.29        | -57.86                 | 50       | 58.38   |
| 3              | 124.53        | -60.09                 | 50       | 58.51   |
| 2              | 124.71        | -59.52                 | 50       | 58.61   |
| 1              | 126.35        | -63.82                 | 50       | 59.50   |

## REFERENCES

## REFERENCES

- Anglin, C.D. and Franklin, J.M., 1989, Preliminary lead isotope studies of base metal and gold mineralization in the eastern Wabigoon Subprovince, northwestern Ontario: In Curr. Res. Part C, Geol. Sur. Can., v. 89-1C, p.385-292.
- Arculus, R.J., and Ruff, L.J., 1990, Genesis of continental crust: evidence from island arcs, granulites, and exospheric processes: In Vielzeuf, D., and Vidal, Ph., Eds., Granulites and crustal evolution, Kluwer Academic Publishers, p. 7-23.
- Ayres, L.D., and Thurston, P.C., 1985, Archean supracrustal sequences in the Canadian shield: an overview: In Ayres, L.D., Thurston, P.C., Card, K.D., and Weber, W., Eds., Evolution of Archean Supracrustal Sequences, Geological Association of Canada Special Paper 28, p. 343-380.
- Bartlett, J.A., 1978, Metamorphic trends in the metasedimentary rocks North of Eagle Lake Ontario: unpublished B. Sci. thesis, University of Western Ontario, 73p.
- Baumann, R.M., 1985, Metamorphism and migmatization of metasediments in the Precambrian English River Subprovince, western Ontario: unpub. M.Sci. thesis, Univ. of North Dakota.
- Beakhouse, G.P., 1977, A subdivision of the western English River subprovince: Can J Earth Sci., v. 14, p.1481-1489.
- Beakhouse, G.P., 1985, The relationship of supracrustal sequences to a basement complex in the western English River Subprovince: In Ayres, L.D., Thurston, P.C., Card, K.D., Weber., W., Eds., Evolution of Archean Supracrustal Sequences, Geological Association of Canada Special Paper 28, p. 169-178.
- Beakhouse, G.P., McNutt, R.H. and Krogh, T.E., 1988, Comparative Rb-Sr and U-Pb zircon geochronology of late- to post-tectonic plutons in the Winnipeg River belt, northwestern Ontario, Canada: Chem Geol., v. 72, p.337-351.
- Beakhouse, G.P., and McNutt, R.H., 1991, Contrasting types of Late Archean plutonic rocks in northwestern Ontario: implications for crustal evolution in the Superior Province: Precambrian Research, v. 49, p. 141-65.

- Blackburn, C.E., 1980, Towards a mobilist tectonic model for part of the Archean of northwestern Ontario: *Geoscience Canada*, v. 7, no. 2, p. 64-72.
- Blackburn, C.E., Bond, W.D., Breaks, F.W., Davis, D.W., Edwards, G.R., Poulsen, K.H., Trowell, N.F. and Wood, J., 1985, Evolution of Archean volcanic-sedimentary sequences of the western Wabigoon Subprovince and its margins: a review: In Ayres, L.D., Thurston, P.C., Card, K.D., Weber, W., Eds., *Evolution of Archean Supercrustals Sequences*, Geological Association of Canada Special Paper 28, p.89-116.
- Bohlen, S.R., 1987, Pressure-temperature-time paths and a tectonic model for the evolution of granulites: *J Geology*, v. 95, p. 617-632.
- Bohlen, S.R., Boettcher, A.L., Wall, V.J. and Clemens, J.D., 1983, Stability of Phlogopite-Quartz and Sanidine-Quartz: A model for melting in the lower crust: *Contrib Mineral Petrol.*, v. 83, p. 270-277.
- Braile, L.W., Hinze, W.J., von Frese, R.R.B., and Keller, G.R., 1989, Seismic properties of the crust and uppermost mantle of the conterminous United States and adjacent Canada: In Pakiser, L.C., and Mooney, W.D., Eds., *Geophysical of the Continental United States*, Geological Society of America Memoir 172, p. 655-680.
- Breaks, F.W. and Bond, W.D., 1977, English River Subprovince (Marchington Lake Area); p.18-28 in *Summary of Field Work, 1977* by the Geological Branch, edited by V.G. Milne, White, O.L. Barlow, R.B. and J.A. Robertson, Ontario Geological Survey Misc. Paper 75, 208p.
- Breaks, F.W., Bond, W.D., Desnoyers, D.W., Stone, D. and Harris, N., 1976a, Operation Kenora-Ear Falls, Bruce-Bluffy Lakes Sheet, District of Kenora; Ont. Div. Mines, Prelim. Map P. 1199, Geol. Ser., Scale 1:63 360 or 1 inch to 1 mile, Geology 1975.
- Breaks, F.W., Bond, W.D., Desnoyers, D.W., Stone, D. and Harris, N., 1976b, Operation Kenora-Ear Falls, Papaonga-Wapesi Lakes Sheet, District of Kenora; Ont. Div. Mines, Prelim. Map P. 1200, Geol. Ser., Scale 1:63 360 or 1 inch to 1 mile, Geology 1975.
- Breaks, F.W., Bond, W.D., Harris, N., and Desnoyers, D.W., 1976, Operation Kenora-Ear Falls, Lac Seul Sheet, District of Kenora; Ont. Div. Mines, Prelim. Map P. 1202, Geol. Ser., Scale 1:63 360 or 1 inch to 1 mile. Geology 1975.

- Breaks, F.W., Bond, W.D., Westerman, C.J., and Desnoyers, D.W., 1976, Operation Kenora-Ear Falls, Perrault Lake Sheet, District of Kenora; Ont. Div. Mines, Prelim. Map P. 1201, Geol. Ser., Scale 1:63 360 or 1 inch to 1 mile. Geology 1975.
- Breaks, F.W., Bond, W.D., and Stone, D., 1978, Preliminary geological synthesis of the English River Subprovince, northwestern Ontario and its bearing upon mineral exploration: Ont Geol Surv Misc Pap 72, 55p.
- Card, K.D., 1990, A review of the Superior Province of the Canadian Shield, a product of Archean accretion: Precambrian Research, v. 48, p. 99-156.
- Card, K.D., and Ciesielsky, A., 1986, DNAG No. 1 Subdivisions of the Superior Province of the Canadian Shield: Geoscience Canada, v. 13, p.5-13.
- Chipera, S.J., 1985, Metamorphism in the eastern Lac Seul region of the English River Subprovince, Ontario: unpub. M.Sci. thesis, Univ. of North Dakota.
- Chipera, S.J. and Perkins, D., 1988, Evaluation of biotite-garnet geothermometers: application to the English River subprovince, Ontario: Contrib Mineral Petrol., v.98, p.40-48.
- Clemens, J.D., 1990, The granulite-granite connexion: In Vielzeuf, D., and Vidal, Ph., Eds., Granulites and Crustal Evolution, Kluwer Academic Publishers, p. 25-36.
- Corfu, F., 1988, Differential response of U-Pb systems in coexisting accessory minerals, Winnipeg River Subprovince, Canadian Shield: implications for Archean crustal growth and stabilization: Contrib Mineral Petrol., v. 98, p. 312-325.
- Corfu, F. and Andrews, A.J., 1987, Geological Constraints on the timing of magnetism, deformation and gold mineralization in the Red Lake greenstone belt, northwestern Ontario: Can J Earth Sci., v. 24, p.1302-1320.
- Davis, D.W., Blackburn, C.E. and Krogh, T.E., 1982, Zircon U-Pb ages from the Wabigoon-Manitou Lakes region, Wabigoon Subprovince, northwest Ontario: Can J Earth Sci., v. 19, p.254-266.



- Davis, D.W., Suctliffe, R.H. and Trowell, N.F., 1988, Geochronological constraints on the tectonic evolution of a Late Archean greenstone belt, Wabigoon subprovince, northwest Ontario, Canada: *Precambrian Res.*, v. 39, p. 171-191.
- Ellis, D.J., 1987, Origin and evolution of granulites in normal and thickened crusts: *Geology*, v. 15, p. 167-170.
- England, P.C. and Thompson, A.B., 1984, Pressure-temperature- time paths of regional metamorphism I. Heat transfer during the evolution of regions of thickened continental crust: *J of Petrol.*, v. 25, pt. 4, p. 894-928.
- Ferry, J.M., and Spear, F.S., 1978, Experimental calibration of the partitioning of Fe and Mg between biotite and garnet: *Contrib Mineral Petrol.*, v. 66, p. 113-117.
- Fountain, D.M., 1989, Growth and modification of lower continental crust in extended terrains: the role of extension and magmatic underplating: In Mereu, R.F., Mueller, S., and Fountain, D.M., Eds., *Properties and Processes of Earth's Lower Crust*, Geophysical Monograph: 51, IUGG v. 6, p. 287- 300.
- Fountain, D.M., and Christensen, N.I., 1989, Composition of the continental crust and upper mantle; a review: In Pakiser, L.C., and Mooney, W.D., Eds., *Geophysical Framework of the Continental United States*, Geological Society of America Memoir 172, p. 711-742.
- Fountain, D.M., Percival, J., and Salisbury, M.H., 1990, Exposed cross sections of the continental crust-- synopsis: In Salisbury, M.H., and Fountain, D.M., Eds., *Exposed Cross- Sections of the Continental Crust*, Kluwer Academic Publishers, p. 653-662.
- Fountain, D.M., and Salisbury, M.H., 1981, Exposed cross-sections through the continental crust: implications for crustal structure, petrology, and evolution: *Earth and Planetary Science Letters*, v. 56, p. 263-277.
- Fyfe, W.S., 1973, The generation of batholiths: *Tectonophysics*, v. 17, p. 273-283.
- Ganguly, J., and Saxena, S.K., 1984, Mixing properties of aluminosilicate garnets: constraints from natural and experimental data, and applications to geothermobarometry: *Am Mineral.*, v. 69, p. 88-97.

- Ghent, E.D., 1976, Plagioclase-garnet- $\text{Al}_2\text{SiO}_5$ -quartz: a potential geobarometer-geothermometer: *Am Mineral.*, v. 61, p. 710-714.
- Gibb, R.A., 1968, The densities of Precambrian rocks from northern Manitoba: *Can J Earth Sci.*, v. 5, p. 433-438.
- Gibbs, A.K., Payne, B., Setzer, T., Brown, L.D., Oliver, J.E., Kaufman, S., 1984, Seismic-reflection study of the Precambrian crust of central Minnesota: *Geol Soc of Am Bull.*, v. 95, p. 280-294.
- Grant, J.A., 1973, Phase equilibria in high-grade metamorphism and partial melting of pelitic rocks: *Am J Sci.*, v. 273, p. 289-317.
- Grant, J.A., 1985, Phase equilibria in partial melting of pelitic rocks: In Ashworth, J.R., Ed., *Migmatites*, Blackie and Son Ltd, p. 86-144.
- Green, A., Milkereit, B., Percival, J., Davidson, A., Parrish, R., Cook, F., Geis, W., Cannon, W., Hutchinson, D., West, G., and Clowes, R., 1990, Origin of deep crustal reflections: seismic profiling across high-grade metamorphic terranes in Canada: *Tectonophysics*, v. 173, p. 627-638.
- Gravity and Geodynamics Division, Earth Physics Branch, Energy, Mines and Resources Canada, 1981: Manuscript Map no. 48090 for Gravity Map of Canada 1980, Ottawa, Canada.
- Gravity and Geodynamics Division, Earth Physics Branch, Energy, Mines and Resources Canada, 1981: Manuscript Map no. 48096 for Gravity Map of Canada 1980, Ottawa, Canada.
- Hall, D.H., and Hajnal, Z., 1969, Crustal structure of Northwestern Ontario: refraction seismology: *Can J Earth Sci.*, v. 6, p. 81-99.
- Hall, D.H., and Brisbin, W.C., 1982, Overview of regional geophysical studies in Manitoba and northwestern Ontario: *Can J Earth Sci.*, v. 19, p. 2049-2059.
- Hamilton, W.B., 1989, Crustal geologic processes of the United States: In Pakiser, L.C., and Mooney, W.D., Eds., *Geophysical Framework of the Continental United States*, Geological Society of America Memoir 172, p. 743-782.

- Harris, N.B.W., 1976, The significance of garnet and cordierite from the Sioux Lookout Region of the English River Gneiss Belt, northern Ontario: *Contrib Mineral Petrol.*, v. 55, p. 91-104.
- Harris, N.B.W., and Goodwin, A.M., 1976, Archean rocks from the eastern Lac Seul region of the English River Gneiss Belt, northwestern Ontario, part 1. Petrology, chemistry, and metamorphism: *Can J Earth Sci.*, v. 13, p. 1201-1211.
- Harrison, T.N., Brown, P.E., Dempster, T.J., and Becker, S.M., 1990, Granite magmatism and extensional tectonics in Southern Greenland: *Geological Journal*, v. 25, p. 287-293.
- Henke, K.R., 1984, Archean metamorphism in northwestern Ontario and southeastern Manitoba: unpub. M.Sci. thesis, Univ. of North Dakota.
- Hess, P.C., 1969, The metamorphic paragenesis of cordierite in pelitic rocks: *Contrib Mineral Petrol.*, v. 24, p. 191-207.
- Hoffer, E., 1976, The reaction sillimanite + biotite + quartz = cordierite + K-feldspar + H<sub>2</sub>O and partial melting in the system K<sub>2</sub>O-FeO-MgO-Al<sub>2</sub>O<sub>3</sub>-SiO<sub>2</sub>-H<sub>2</sub>O: *Contrib Mineral Petrol.*, v. 55, p. 127-130.
- Holdaway, M.J., 1971, Stability of Andalusite and the aluminum silicate phase diagram: *Am J Sci.*, v. 271, p. 97-131.
- Holdaway, M.J., and Lee, S.M., 1977, Fe-Mg Cordierite stability in high-grade pelitic rocks based on experimental, theoretical, and natural observations: *Contrib Mineral Petrol.*, v. 63, p. 175-198.
- Hyndman, D.W., 1981, Controls on source and depth of emplacement of granitic magma: *Geology*, v. 9, p. 244-249.
- Indares, A., and Martignole, J., 1985, Biotite-garnet geothermometry in the granulite facies: the influence of Ti and Al in biotite: *Am Mineral.*, v. 70, p. 272-278.
- Krogh, T.E., Harris, N.B.W., and Davis, G.L., 1976, Archean rocks from the eastern Lac Seul region of the English River Gneiss Belt, northwestern Ontario, part 2. Geochronology: *Can J Earth Sci.*, v. 13, p. 1212-1215.

- Langford, F.F., and Morin, J.A., 1976, The development of the Superior Province of northwestern Ontario by merging island arcs: *Am J Sci.*, v. 276, p.1023-1034.
- Malinconico, L.L. and Larson, T., 1985, Gravity--an interactive modeling program: Environmental Simulations Laboratory, Southern Illinois University, Carbondale, Illinois.
- Manitoba Mineral Resources Division, 1979, Geological Map of Manitoba, Scale 1:1,000,000, Map 79-2.
- McRitchie, W.D., and Weber, W., Eds., 1971, Geology and Geophysics of the Rice Lake region, southeastern Manitoba (Pioneer Project): Manitoba Department of Mines and Natural Resources, Mines Branch, Publication 71-1, 430 p.88.
- Newton, R.C., 1988, Fluids and melting in the Archean deep crust of southern India: In Ashworth, J.R. and Brown, M., Eds., High temperature metamorphism and crustal anatexis, Unwin Hyman Ltd, p. 149-179.
- Newton, R.C., and Haselton, H.T., 1981, Thermodynamics of the garnet-plagioclase- $Al_2SiO_5$ -quartz geobarometer: In Newton, R.C., Navrotsky, A., and Wood, B.J., Eds., Thermodynamics of Minerals and Melts, Springer, p. 131-148.
- Nunes, P.D., and Thurston, P.C., 1980, Two hundred and twenty million years of Archean evolution: a zircon U-Pb age stratigraphic study of the Uchi-Confederation Lakes greenstone belt, northwestern Ontario: *Can J Earth Sci.*, v. 17, p. 710- 721.
- Ontario Geological Survey, 1980: Geological Highway Map, northern Ontario; Ontario Geological Survey, Map 2440.
- Perchuk, L.L., and Lavrent'eva, I.V., 1983, Experimental investigation of exchange equilibria in the system cordierite-garnet-biotite: In Saxena, S.K., Ed., Kinetics and Equilibrium in Mineral Reaction, Springer-Verlag, p. 199-239.
- Perchuk, L.L., Podlesskii, K.K., and Aranovic, L.Ya., 1981, Calculation of thermodynamic properties of end-member minerals from natural parageneses: In Newton, R.C., Navrotsky, A., and Wood, B.J., Eds., Thermodynamics of Minerals and Melts, Springer, p. 125-131.
- Percival, J.A., 1990, Archean tectonic setting of granulite terrains of the Superior Province, Canada: A view

- from the bottom: In Vielzeuf, D., and Vidal, Ph., Eds., *Granulites and Crustal Evolution*, Kluwer Academic Publishers, p. 171-193.
- Percival, J.A., 1989, Granulite terranes and the lower crust of the Superior Province: In Mereu, R.F., Mueller, S., and Fountain, D.M., Eds., *Properties and Processes of Earth's Lower Crust*, Geophysical Monograph: 51, IUGG v. 6, p. 301-310.
- Percival, J.A., and Card, K.D., 1985, Structure and evolution of Archean crust in central Superior Province, Canada: In Ayres, L.D., Thurston, P.C., Card, K.D., and Weber, W., Eds., *Evolution of Archean Supracrustal Sequences*, Geological Association of Canada Special Paper 28, p. 179-192.
- Percival, J.A., Green, A.G., Milkereit, B., Cook, F.A., Geis, W., and West, G.F., 1989, Seismic reflection profiles across deep continental crust exposed in the Kapuskasing uplift structure: *Nature*, v. 342, p. 416-420.
- Percival, J.A., and McGrath, P.H., 1986, Deep crustal structure and tectonic history of the northern Kapuskasing uplift of Ontario: an integrated petrological-geophysical study: *Tectonics*, v. 5, no. 4, p. 553-572.
- Roob, C.K., 1987, *Metamorphism in the Wabigoon Subprovince in the vicinity of Vermilion Bay and Sioux Lookout, Ontario*: unpub. M.Sci. thesis, Univ. of North Dakota.
- Schreyer, W. and Seifert, F., 1969, Compatibility relations of the aluminum silicates in the systems  $MgO-Al_2O_3-SiO_2-H_2O$  at high pressures: *Am J Sci.*, v. 267, p. 371-388.
- Schumacher, R., Schenk, V., Raase, P., and Vitanage, P.W., 1990, Granulite facies metamorphism of metabasic and intermediate rocks in the Highland Series of Sri Lanka: In Ashworth, J.R., and Brown, M., Eds., *High temperature metamorphism and crustal anatexis*, Unwin Hyman Ltd, p. 235- 271.
- Schwerdtner, W.M., Morgan, J., and Stott, G.M., 1985, Contacts between greenstone and gneiss complexes within the Wabigoon Subprovince, northwestern Ontario: In Ayres, L.D., Thurston, P.C., Card, K.D., and Weber, W., Eds., *Evolution of Archean Supracrustal Sequences*, Geological Association of Canada Special Paper 28, p. 117-123.

- Simpson, R.W., and Jachens, R.C., 1989, Gravity methods in regional studies: In Pakiser, L.C., and Mooney, W.D., Eds., Geophysical Framework of the Continental United States, Geological Society of America Memoir 172, p.35-44.
- Smithson, S.B., 1989, Contrasting types of lower crust: In Mereu, R.F., Mueller, S., and Fountain, D.M., Eds., Properties and processes of Earth's Lower Crust, Geophysical Monograph: 51, IUGG v. 6, p. 53-64.
- Smithson, S.B., and Brown, S.K., 1977, A model for lower continental crust: Earth and Planetary Science Letters, v. 35, p. 134-144.
- Speer, J.A., 1982, Metamorphism of the pelitic rocks of the Snyder Group in the contact aureole of the Kiglapait layered intrusion, Labrador: effects of buffering partial pressures of water: Can J Earth Sci., v. 19, p. 1888-1909.
- Telford, W.M., Geldart, L.P., Sheriff, R.E., and Keys, D.A., 1976, Applied Geophysics: Cambridge University Press, 860p.
- Thompson, A.B., 1976, Mineral reactions in pelitic rocks: 1. Prediction of P-T-X (Fe-Mg) phase relations: Am J of Sci., v. 276, p. 401-424.
- Thompson, A.B., 1983, Fluid-absent metamorphism: J Geol Soc London, v. 140, p. 533-547.
- Thompson, A.B., 1990, Heat, fluids, and melting in the granulite facies: In Vielzeuf, D., and Vidal, Ph., Eds., Granulites and Crustal Evolution, Kluwer Academic Publishers, p. 37-57.
- Thompson, A.B., and England, P.C., 1984, Pressure-temperature-time paths of regional metamorphism II. Their inference and interpretation using mineral assemblages in metamorphic rocks: J of Petrol., v. 25, pt. 4, p. 929-955.
- Turcotte, D.L., 1989, Geophysical processes influencing the lower continental crust: In Mereu, R.F., Mueller, S., and Fountain, D.M., Eds., Properties and Processes of Earth's Lower Crust, Geophysical Monograph: 51, IUGG v. 6, p. 321- 330.
- Turcotte, D.L., and Schubert, G., 1982, Geodynamics - Applications of Continuum Physics to Geological Problems: John Wiley and Sons, Inc., 450 p.

- Vielzeuf, D., Clemens, J.D., Pin, C., and Moinet, E., 1990, Granites, granulites and crustal differentiation: In Vielzeuf, D., and Vidal, Ph., Eds., Granulites and Crustal Evolution, Kluwer Academic Publishers, p. 59-85.
- Weber, W., and Mezger, K., 1990, An oblique cross section of Archean continental crust at the northwestern margin of Superior Province, Manitoba, Canada: In Salisbury, M.H., and Fountain, D.M., Eds., Exposed Cross-Sections of the Continental Crust, Kluwer Academic Publishers, p. 327-341.
- Wells, P.R.A., 1979, Chemical and thermal evolution of Archaean sialic crust, southern west Greenland: J of Petrol., v. 20, pt. 2, p. 187-226.
- Wells, P.R.A., 1980, Thermal models for the magmatic accretion and subsequent metamorphism of continental crust: Earth and Planetary Science Letters, v. 46, p. 253-265.
- Winkler, H.G.F., 1979, Petrogenesis of metamorphic rocks, (5th ed.): Springer-Verlag, New York, 348 p.